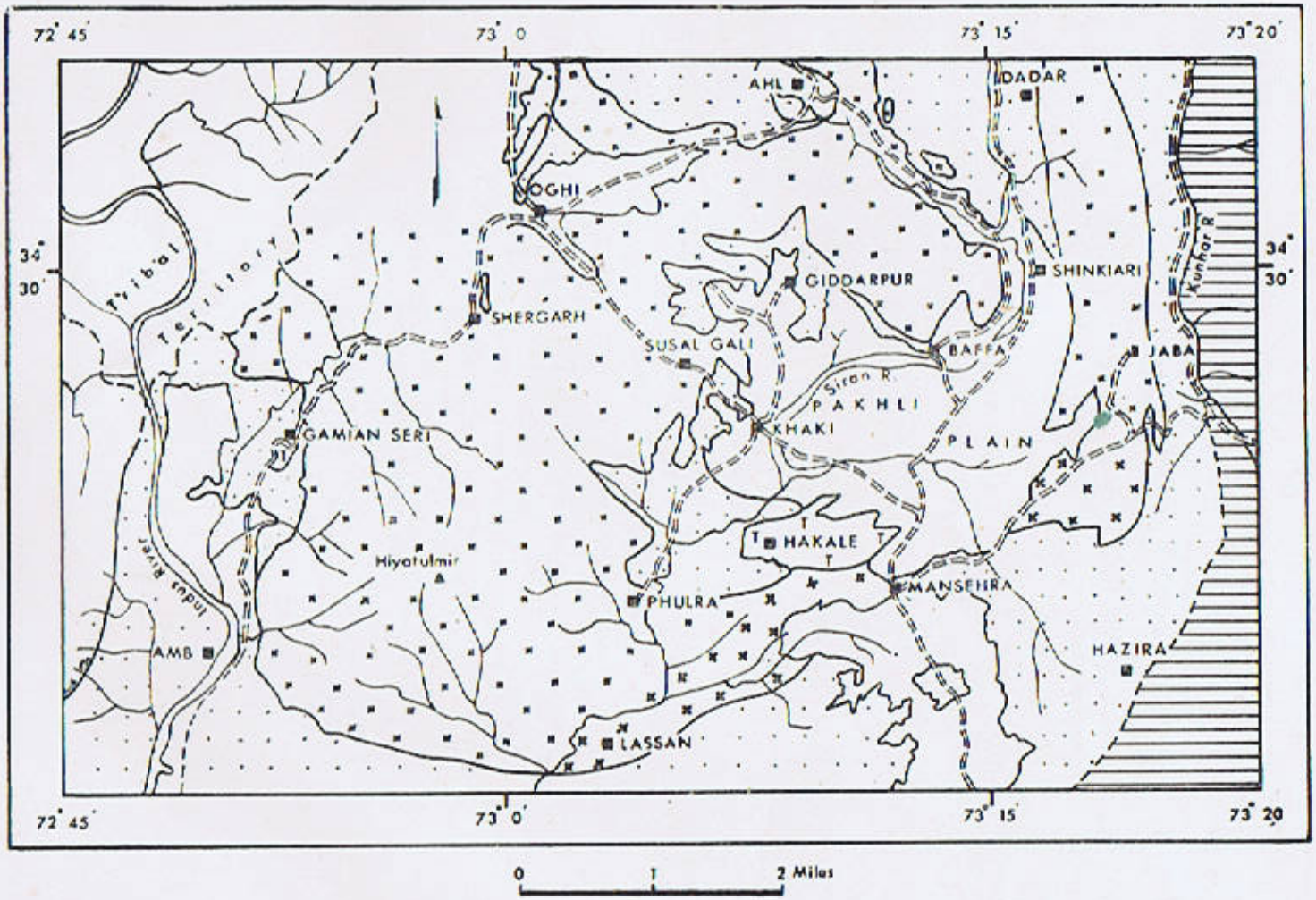

Fig. 1. The Geological Map of the Mansehra and Amb State Area.

GEOLOGY OF THE MANSEHRA-AMB STATE AREA, NORTHERN WEST PAKISTAN

BY

F.A. SHAMS

Department of Geology, Punjab University, Lahore, Pakistan

Abstract : *About 600 square miles of area, covering large part of Mansehra sub-division of the Hazara District and the adjoining Amb State, in northern part of the West Pakistan, has been mapped and an original geological map, on the scale of 1 inch to mile has been prepared.*

The area constitutes the hard crystalline core of a major syntaxial loop of the northwest Himalayas and is composed of semi-pelitic to psammitic schists and quartzites that have suffered regional metamorphism upto kyanite grade of the Barrovian type. These schists bound a large granitic complex composed of an older group of gneissic (the Susalgali gneiss) to granitoid rocks (The Mansehra granite and the andalusite-bearing granites), ranging from granite to granodiorite, and a younger group of sodaclase granites (The Hakale granite, Karkala granite etc.). In addition, there are a large number of aplites and pegmatites, and a few porphyry dykes are met with. Dolerites cut the entire plutonic complex and are met with as ophitic dolerites, epidiorites and amphibolites, depending upon their age of emplacement.

Details of fields observations and laboratory studies are given as far as the general geological aspects of the area are concerned.

INTRODUCTION

The Mansehra-Amb State area, about 600 sq. miles in extent, constitutes a large part of the Mansehra subdivision of the Hazara District and the adjoining Amb State (Long. 72° 45′ E to 73°20′ E ; Lat. 34° 15′ N to 34° 45′ N)

Lithologically, the area is composed of semi-pelitic to psammitic schists and quartzites that are associated with a plutonic complex of granitic rocks of varying types and of different ages. A large number of doleritic sills and dykes cut both the granitic as well as the metamorphic terrains.

Structurally, the area constitutes hard crystalline core of a major syntaxial loop of the northwest Himalayas (Wadia, 1931). The general strike of this structure swings in an arcuate fashion. From Balakot south to Batrasi, the strike is almost north-south and then bends sharply to become east-northeast to west-southwest. With local variations, it continues in this direction until near Lassan when it adopts a west-northwest to east-southeast trend that persists upto Darband. Thereafter, it again bends sharply to become essentially north-south. There is the famous Balakot re-entrant in the east and the Indus re-entrant in the west. In the entire area, the strata dip inwards at different inclinations but becoming less and less steeply inclined in the northern direction. The regional structure, thus, is a gignatic synform with a nearly northeast-southwest axis, the plunge of which decreases in magnitude in the north-easterly direction.

The area is characterised by contrasted topography. The steep ridges follow the arcuate structure of the area and enclose a large alluvial filled intermontane basin (The Pakhli Plain) in the heart of the area. In general, the altitude rises in all outward directions, especially in the northern area where it rises more than 7000 feet above sea level.

The alluvial filled valleys, including the Pakhli plain, show succession of two or more terraces of

erosion. Besides these, there are many patches of high level older alluvial that is found perched at 6000 feet or more above sea level. This alluvial is either relict of an ancient peneplain, like the one suggested by Hayden (1913) or partly represents aeolian deposits, much of which had been washed down to fill the Pakhli plain etc.

MAPPABLE LITHOLOGICAL UNITS

Due to its geographical location and passing through it of many important roads, the Mansehra-Amb State area must had been visited by large number of geologists of the older Geological Survey of India. However, the first serious note on the geology of the area was published by Wynne (1877). He elaborated his observations in a supplementary note (1879) in which he presented a geological map of Hazara on the scale of 1" to 8 miles and also produced the first stratigraphical subdivision of the area. Relevant part of his scheme is reproduced below :—

	Tanol Series
	I Attock Slate Series
Probably Palaeozoic	B Intrusive traps, in Attock State and Tanols also in metamorphic rocks
	A Hazara Gneiss and the most crystalline altered beds.

The area was re-mapped by Middlemiss (1890-1893) on the scale of 1 inch to a mile. He did not delineate boundaries of granitic and metamorphic formations and showed them togather (Middlemiss 1896). Middlemiss (*op. cit.* p. 9) drew up a slightly different scheme and the corresponding part of his table is reproduced below.

II Infra-Triassic—Carboniferous or Carbo-Permian.

I Slate series—Age unknown

Crystalline and Metamorphic Rocks

	b "Tanol"—Infratriassic in main.
Palaeozoic or older	a Crystalline rocks—Equivalent of I and II above.
	x Intrusive gneissic granite
	y Intrusive dyke rocks.

In the text of his publication (*op. cit.*, p. 64), Middlemiss subdivided the granitic rocks on the basis of their structure as, (A) foliated, (B) semi-foliated and (C) non-foliated. Although it was a pioneer attempt, yet it lacked appreciation of their mutual relationship with respect to the nature of origin and age of formation.

On the basis of field experience and for the sake of mapping and description, the present writer has subdivided the granitic and metamorphic formations as follows :—

3. Dolerites and meta-dolerites :

   Intrusive in all the older formations

2. Hazara Granitic Complex

   (*a*) Older Granites and Gneiss :

   Susalgali granitic gneiss
   Mansehra granite
   Andalusite granites
   Associated acid minor bodies.

   (*b*) Younger tourmaline granites :

   Hakale granite
   Karkala granite
   Sukal granite
   Associated acid minor bodies.

1. Pre-granite Metamorphic Rocks.

   Hazara Schistose Group

   Pelitic schists to quartzites with meta-conglomerate bands.

This scheme has been followed for preparing the general map (Fig. 1) and for description of the lithological units, as will follow.

THE REGIONAL STRUCTURE OF THE AREA

As already mentioned, the area is characterised by a spectacular regional flexure (orogenic syntaxis) whose effects extend even outside the Mansehra-Amb State area. As a result of this tectonic phase (s), the area shows regional swinging on an arcuate fashion of strike of every type of rock formation ; the latter were so powerfully involved that the whole area evolved as a "structural unit". This fact stands out excellantly on a structural map of the area (Fig. 2) in which are shown the generalized strike trend lines alongwith their dip directions, disregarding minor discordances.

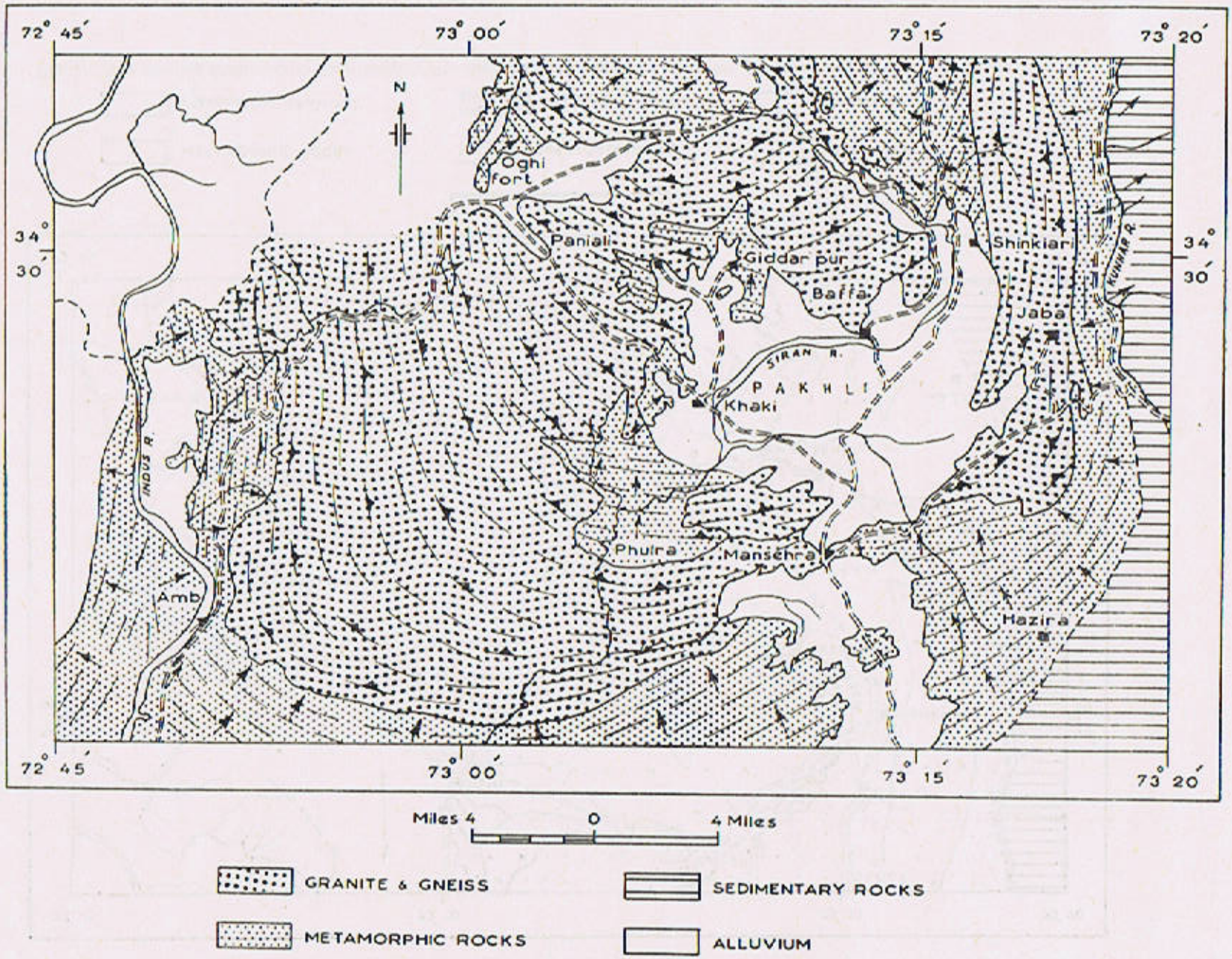

Fig. 2. Generalized structural map of the Mansehra-Amb State area.

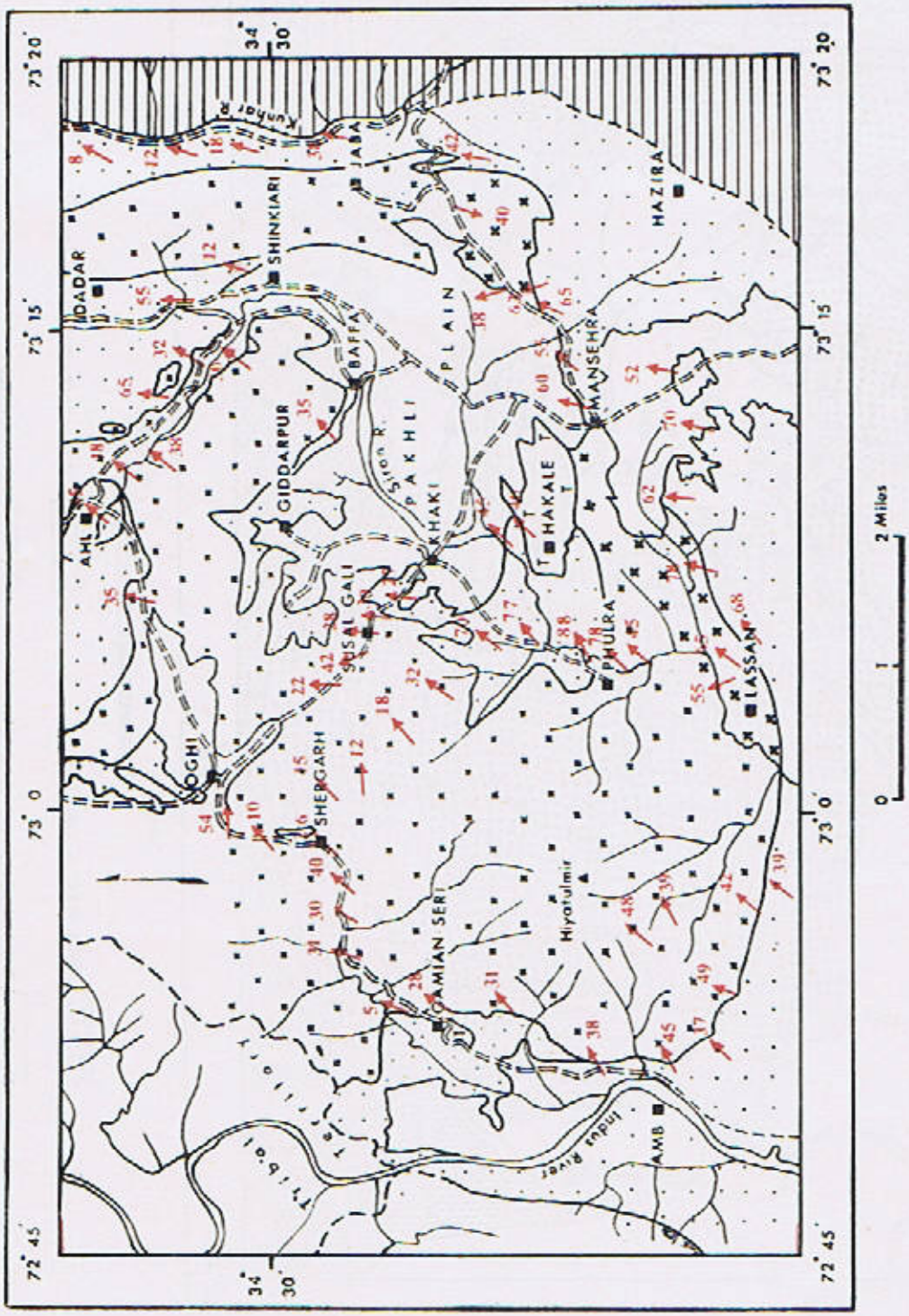

Fig. 3. Map showing orientation of the slickenside lineations imprinted upon rocks of the granite-metamorphic contact zones.

The Mesozoic and younger sedimentary rocks, extensions of which once blanketed the entire crystalline region, are now met with only in the eastern and south-eastern parts of the area, where metamorphic rocks are in contact with them. This contact marks a stratigraphic-cum-tectonic break, which is one of the major "boundary faults" of the north-west Himalayas. All along their contact, the rocks are sheared and fractured and *nalas* and streams have carved their courses along them.

The Garhi Habibullah Khan-Balakot section is very instructive. Although the actual contact zone is covered under the bed of river Kunhar, yet rocks on both sides of the river—sedimentary beds on the eastern side and metamorphic rocks on the western side—bear excellent proof of this powerful trust-faulting ; they are folded, sheared and frequently mylonitized. The surfaces of these rocks carry slickenside lineation, with a plunge towards the north and strong tension gashes developed across the strike of the beds.

The most important structural feature of the metamorphic rocks is their schistosity (S_1). Due to dominant control of the phyllonitic minerals, the S_1 is best developed in the rocks of pelitic composition and becomes weaker as the composition becomes psammitic. Everywhere, the S_1 planes are parallel to the bedding planes of sedimentation origin. There is plenty of evidence that S_1 planes acted as planes of tectonic gliding during orogenic evolution of the area. In addition to mineral-smearing on the S_1 planes, the above impression is supported by the observation that certain minerals of metamorphic origin, such as garnet and staurolite etc., had suffered rotation within these planes.

Superimposed on S_1 is a younger schistosity (S_2) which is inclined to the former at variable angles. The S_2 is marked by reorientation of minerals of older generation and neo-crystallization of minerals within these planes. On opening the rocks along S_1, the S_2 can be apprehended as traces of mineral streakiness (marking a lineation) and micro-crenulation. On larger scale, the younger structural phase is thought to be responsible for widespread folding (or refolding) of the metamorphic rocks ; the intensity of folding increasing towards their contact with granitic bodies and sometime acquiring the form of fold mullions at the immediate contacts. Furthermore, sets of closely spaced puckers are frequently seen that are inclined to S_2 at variable angles and hint towards the tectonic influence of the granitic bodies.

Like S_1 of the metamorphic rocks the most prominent structure in the granitic rocks is marked by the planes of gneissosity in the gneissic rocks and the planes of easy splitting in the granitoid rocks. There is such a close genetic relationship between these two types of structures that the one type can be continued into the other without break or angular discordancy, except for their close spacing and relatively stronger development in the gneissic rocks. It appears that either the development of net-work texture in the granitoid facies had weakened the intensity of the gneissic structure or that the net-work texture had been obliterated on the imposition of gneissosity as a result of tectonic evolution of the area.

Everywhere jointing is fairly well developed in the granitic rocks. Local folding and faulting is occasionally noticed in the gneissic rocks and rarely ptygmatically folded aplite veins are seen. Some of the very closely folded facies of the gneissic rocks sometime turn out to be granitized fragments of schists that inhereted structures from pre-granitic period.

Frequently joints in the granitic bodies have been filled by basic injections that are now met with as dolerites and amphibolites, depending upon their ages of emplacement. It is interesting to note that the basic bodies, of earlier periods of emplacement, had suffered folding and shearing along definite joint systems in the marginal zones of the granitic bodies ; such joints are oriented mostly in diagonal fashion to the nearby contact plane against the metamorphic strata. Thin aplitic, pegmatitic and quartz bodies are also generally emplaced along joint openings and movements along these joints had affected them as well. It appears that a strong stress component once acted along directions that were everywhere normal to the plane of contact of the granitic bodies and the metamorphic strata. The field observations show that simultaneous with or under the influence of this stress, the granitic bodies suffered regional expansion. This is thought to be reason for intense shearing and upthrusting of marginal zones of granitic bodies. The structural evidence for this phenomenon is excellently brought out in Fig. 3, in which are plotted slickenside lineations imprinted upon the marginal zones of the granitic bodies and the schists at their contacts. It is noteworthy that everywhere these linear structures are independent of the regional strike and that their generalized regional orientation is intimately linked with the direction of extension of the granitic complex.

FORM AND SHAPE OF GRANITIC BODIES

(*i*) Sheet-like from :

This term is applied to refer to the plutons of tabular nature that are structurally conformable to

the bedding and/or schistosity of the country rocks irrespective of the nature of origin of the granitic rocks. In the Mansehra-Amb State area, this form is shown by the granitic bodies of the eastern half of the area, wherein two gigantic sheets are present i.e. the Masar Ridge sheet and the Baffa-Oghi sheet (see Fig. 1). In addition there are a number of minor sheets in the Giddarpur-Khaki area so that this appears to be the most important and fundamental form of the granitic bodies.

(*ii*) **Mushroom-Like Form :**

This unique form is exhibited by the Hiyatulmir massif in the Amb State. Its southern and western edges dip concordantly underneath the metamorphic strata while the schists of the Khaki area abut against it discordantly. It appears that this form had been acquired by the granitic body by way of up-thrusting and mushroom-like expansion. The steep gradient of the topography and the radial pattern of drainage in the area of Hiyatulmir massif is noteworthy.

(*iii*) **Sills and Laccolith :**

These forms are especially exhibited by bodies of younger tourmaline granites. The Karkala granite is a typical example of a sill-like intrusion while the Hakale granite makes a small laccolith.

The presumed forms of the granitic bodies, as described above, have been supported by gravity survey data as well (Aziz, 1961).

THE PRE-GRANITIC METAMORPHIC ROCKS

General

Less than half of the Mansehra-Amb State area is occupied by crystalline rocks that represent metamorphosed equivalents of oldest clastic sediments that were laid in the Himalayan geosyncline (Tethys sea). The presence of graded bedding, cross-bedding, non-diastrophic structures of sedimentary origin and lithological banding etc. prove their sedimentary origin.

The least metamorphosed equivalents of these rocks are met with in the form of Hazara Slate Formation which make enormous thickness outside the Mansehra-Amb State area, in the eastern and south-eastern directions. Such a correlation has been supported by previous workers in the Hazara District.

The Lithological Facies

The various lithological facies of sediments, that were involved in the regional metamorphism and other plutonic processes, are briefly described below :—

(*a*) *The Psephitic Facies.*

Psephitic or conglomeratic bands have so far been found to occur at two levels only ; both are of different type and are described below :—

One of the bands is composed of nodules of a carbonate rock that are set in a psammitic matrix. It occurs about 1 mile east of Chitta Batta, in the Shahkhel Garhi area northeast of Mansehra. It is only a few feet wide and the largest size of the pebbles so far seen, is about $3'' \times 1''$ in cross-section. The carbonate material had mostly reacted with the silicate matrix with the production of calc-silicate minerals, as has been described elsewhere in detail (Shams, 1963). It is probable that this band is genetically related to the mildly calcareous schist horizon that is present towards the south-west at more or less the same stratigraphical level.

The second occurrence of psephitic material is seen near Chorgali, along the Khaki-Oghi road section. It is composed of quartzitic pebbles set in a finely schistose matrix of psammitic nature ; the pebbles are of variable size that reach 4"x2" dimensions or so. This band grades laterally into somewhat gritty material that has been found as far as Amb State in the south-west direction.

(*b*) *Psammitic Facies.*

This is the predominent lithological material of the area, under investigation, and makes considerable thicknesses that persist over long distances along the regional strike. Commonly across but rarely along the strike, the psammitic strata grades gradually or abruptly into pure quartzitic material. This change occurs due to decrease in the mica content and increase in the grain size of the psammitic material. The quartzitic rocks, sometime contain feldspar minerals and may approach arkosic composition. At places, ferruginous varieties of quartzites are seen such as at Rihar, Bilal Jan Kari and Khabbal etc.

(*c*) *Pelitic—Psammtic Banded Facies.*

These rocks are characterised by an impressive alternation of pelitic and psammitic bands ; the constituent bands vary in thickness from half an inch to six inches or so while banding on microscopic scale is also present. The thickness of individual zones of banded rocks commonly reaches few hundred feet and sometime abruptly passes into thick beds of psammitic composition. Beautiful

exposures are seen on the hillock east of Mansehra Rest House, along Chorgali, Gamian Seri and Chitta Batta sections etc. Almost everywhere these rocks show structures of seimentation origin such as troughs and grading etc. which are useful for finding geographical orientation of the beds. Two features are very common in these rocks ; firstly, the psammitic bands, whenever

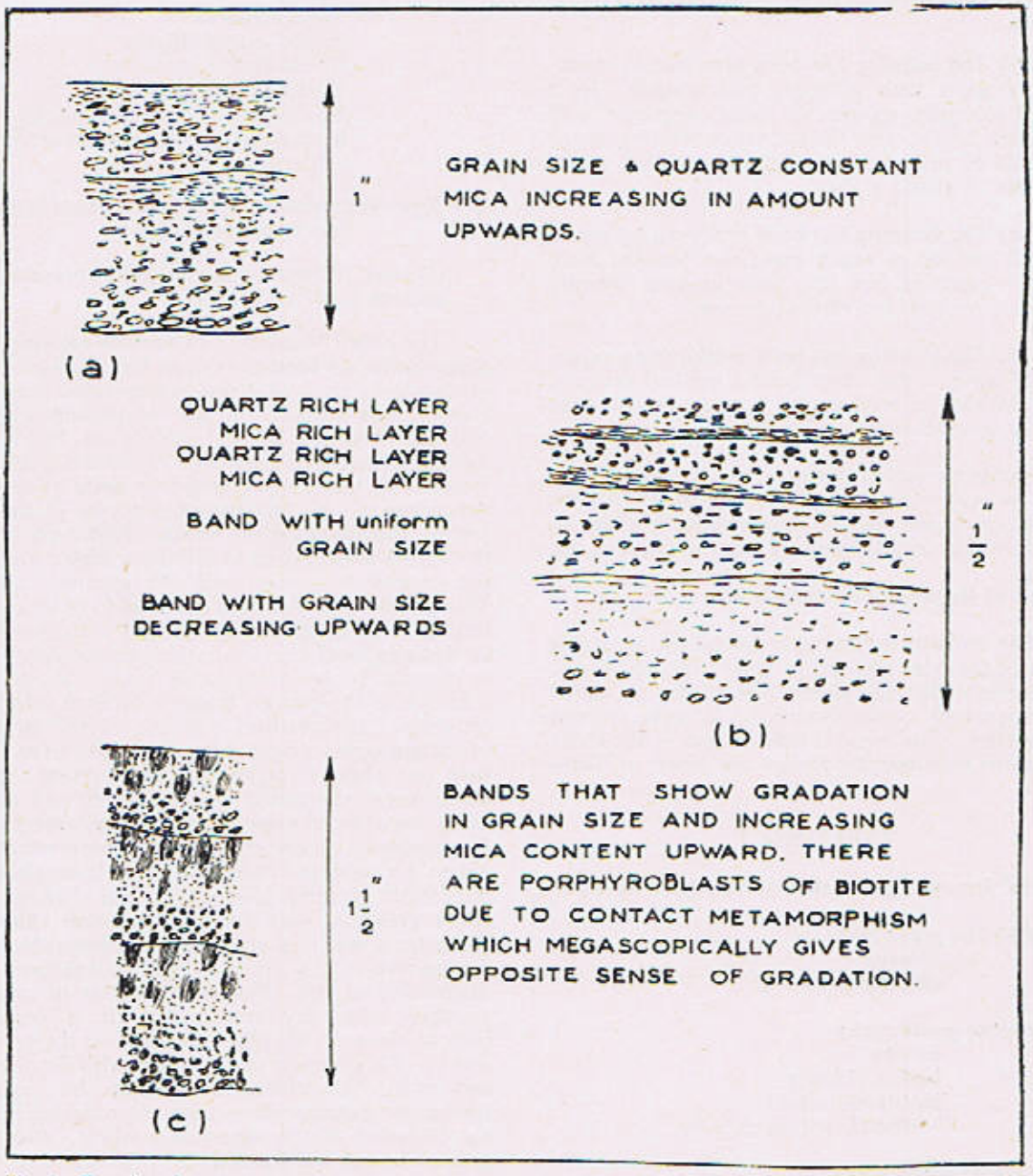

Fig. 4. Drawings from rock sections to illustrate various types of sedimentation banding. Biotite of (c) developed due to thermal effects.

reach thickness of a few inches, show traces of current bedding and secondly, there is ubiquitous grading of grain size within individual bands ; these two features frequently combine togather. On the whole, these rocks show three types of banding :—

(*i*) The banding has been produced by repitition of units with different mineralogies. In a typical example, quartz-rich bands alternate with mica-rich bands, with the former containing minor amounts of mica and the latter containing minor amounts of quartz grains.

(*ii*) The banding has been produced by repitition of laminae in which grain size remains more or less constant but the mica content steadily increases towards top of the laminae.

(*iii*) The banding has been produced by repitition of laminae that show both a gradual decrease in grain size as well as an increase in the mica content towards top of individual bands.

Sometime various types of banding are present close to each other in a single specimen. All the above cases are shown diagramatically (Fig. 4) based on thin section study of representative rocks.

Nature of Regional Metamorphism

The mineral assemblages in the metamorphic rocks of the Mansehra-Amb-State area, show that the regional metamorphism was of the so called Barrovian type ; upto kyanite grade rocks are met in the area. The mineral assemblages in the rocks of various metamorphic grades are given in Table No. 1.

TABLE NO. 1

Mineral Assemblages of the Metamorphic Rocks

(*i*) Chlorite grade rocks :
chlorite
chlorite-chloritoid

(*ii*) Biotite grade rocks :
biotite
biotite-chlorite
biotite-chloritoid
biotite-chloritoid-chlorite

(*iii*) Garnet grade rocks :
biotite
biotite-chlorite
biotite-garnet
biotite-garnet-chlorite
biotite-garnet-chloritoid-chlorite
biotite-chloritoid-chlorite

(*iv*) Staurolite grade rocks :
biotite
biotite-chlorite
biotite-garnet-chlorite
biotite-garnet-staurolite
biotite-staurolite-chlorite
biotite-garnet-staurolite-chlorite
biotite-garnet-chloritoid-staurolite-chlorite

(*v*) Kyanite grade rocks : (schist fragment in gneiss)
biotite-garnet-kyanite

(Quartz, feldspars and muscovite are commonly present in all associations).

The exact boundaries of various metamorphic grades have not been marked so far. However field observations show that the metamorphic grade increases with increase in the stratigraphical level and the isograds show tendency to follow the arcuate structure of the area. It is noteworthy that location of the granitic bodies is more or less independent of the metamorphic grades of the adjoining metasedimentary strata. However, locally the schists always tend to acquire a higher grade at the immediate contact with the granitic bodies. This phenomenon has been observed to be intimately linked with the effects of thermal metamorphism so that any local increase in the metamorphic grade is thought to have happened under the thermal influence of the granitic bodies combined with local tectonics. The textural relations of the minerals of metamorphic origin show that there were more than one phase of regional metamorphism ; systematic work is required to characterize and distinguish between various phases of metamorphism. Superimposed on the progressive regional metamorphism (or metamorphisms) was a later phase of phyllonitic metamorphism that had affected the entire area and gave rise to ubiquitous chlorite ; the latter is met in every type of metamorphic rock irrespective of the grade of metamorphism. The orientation of this chlorite is such as to mark a younger schistosity/lineation which is common both to the metamorphic as well as to the granitic rocks and is generally in agreement with the orientation of S_2. Therefore, it is felt that this regional retrograde metamorphism took place during orogenic evolution of the region as a whole, after the granitic bodies had formed.

THE HAZARA GRANITIC COMPLEX

More than half of the Mansehra-Amb State area is occupied by granitic* rocks of varying

*The term is used to cover coarse-grained quartzofeldspathic rocks varying in composition from pure granite to quartz diorite.

types and of different ages of formation. They have been grouped together into the Hazara Granitic Complex ; their sub-division has been given already while detailed description is given below :—

A. Older Granites and Gneiss

This group includes the Susalgali granitic gneiss, the Mansehra granite, the andalustie-bearing granites and the associated acid minor intrusives. Structurally, there are all gradations between massive, semi and true gneissic types, while the intensity and frequency of foliated material generally increases northwards. Catacalstic facies are also present and are met as narrow marginal portions of the complex and as faulted and sheared zones. The structural and mineralogical investigations have shown that various members of the older group are genetically related and differ from each other simply in their location and level in the stratigraphical order.

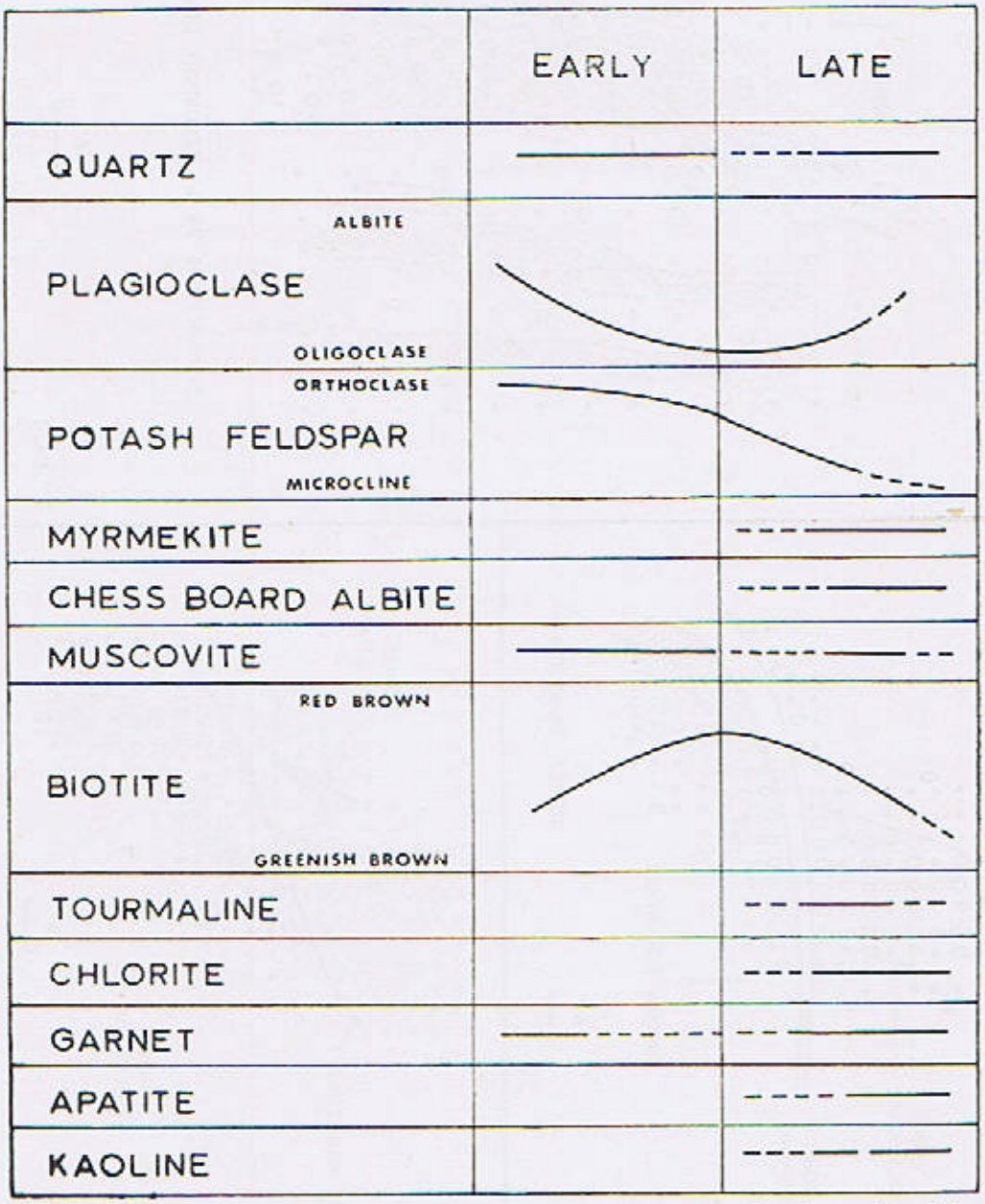

Fig. 5. Showing nature and range of minerals present in the older granite and gneiss members of the Hazara Granite Complex.

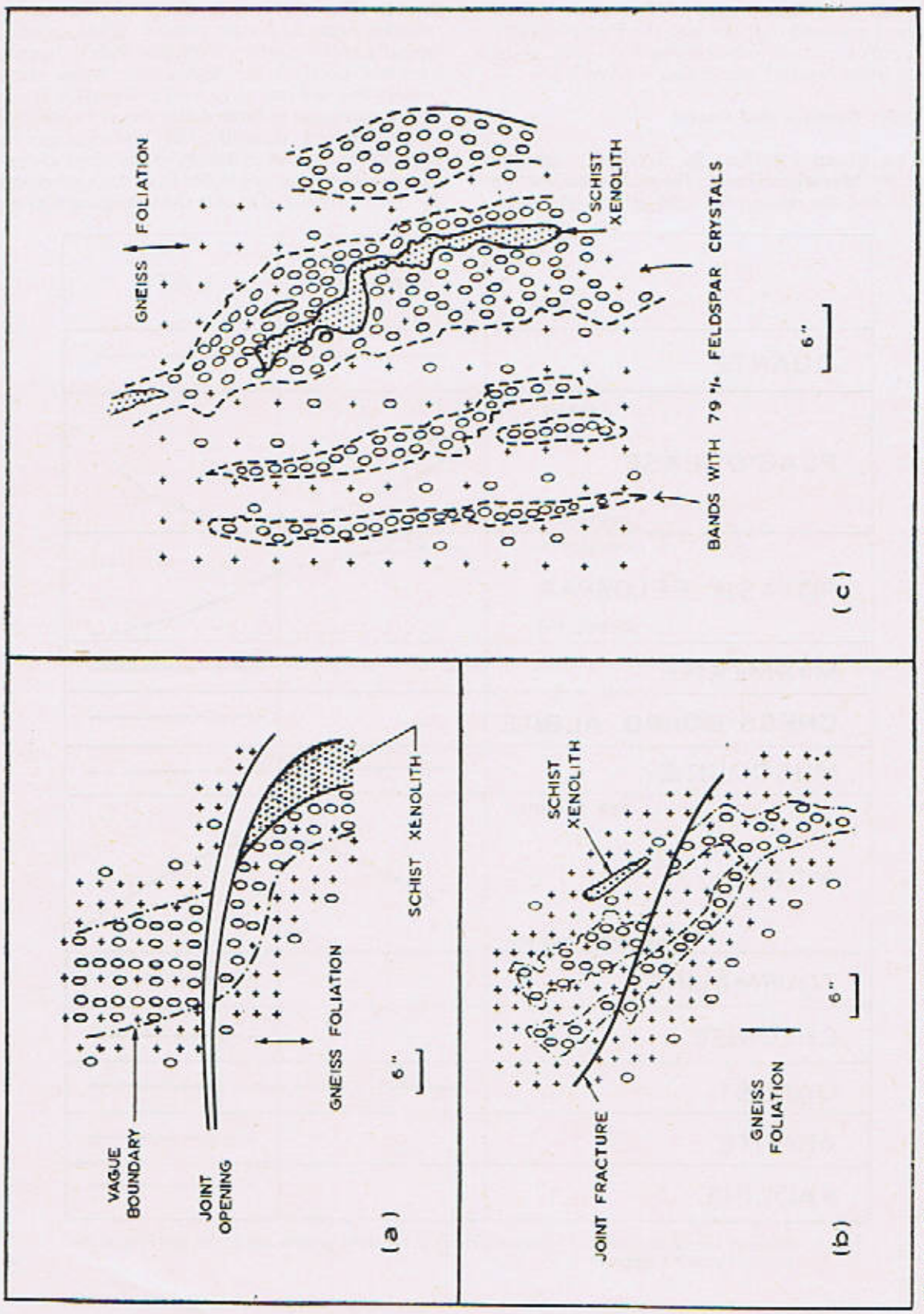

Fig. 6. Sketch drawings to illustrate feldspar seggregation in the Susaigali granitic gneiss on the Khaki—Oghi road section.

This conclusion is justified by the following facts :—

(*i*) The foliated structure shows an essential continuity over the entire area and there is no recognisable break as one follows it from one member of the complex to the other.

(*ii*) There are no chilled contacts between various members so that no sharp boundaries can be drawn on the map.

(*iii*) The essential mineral species are fundamentally the same throughout the group and differ only in their relative proportion ; their physical nature and textural relationship (Fig. 5).

The various members of the complex are described in detail below.

1. The Susalgali Granitic Gneiss

Named after the locality of Susalgali, on the Khaki-Oghi road, this is the most important member of the older group and constitutes about 80% of the entire outcrop of the granitic bodies. These rocks vary in colour from greyish white to whitish grey and are almost always foliated. In regions north of Khaki and Baffa villages, these rocks are thoroughly gneissic while south of this arbitrary limit, the gneissic structure is weakly developed (semi-gneissic) and locally even somewhat massive portions are also met. The latter phenomenon shows up vividly in the field sothat big rounded blocks of granitoid material are seen projecting from or having rolled out of thoroughly gnessic rock. Generally speaking, the proportion of material with granitoid structure increases southwards till the marginal belt of the distinctly massive Mansehra granite is met with in the southeast. Locally, small pods and lens-like masses of another granitoid rock, the andalusite-bearing granites, are met with in certain localities in the north. Seggregations of feldspar megacrysts are locally seen (Fig. 6).

On close field observation, two distinct types of rocks (Fig. No. 7) can be apprehended that may locally grade into each other :—

(*i*) Relatively finer grained, strongly gneissose or almost schistose rocks (Fig. No. 7, *a*) ; the typical member being composed of rather small streaks and eyes of quartz and feldspar minerals separated by micaceous folia. These types of rocks always contain a high content of quartz (75% of total mineral content) so that the feldspathic constituents are subordinate. The feldspar minerals occur as small to medium-sized porphyroblastic augens that are mostly of plagioclase ; the potash feldspar is generally a strongly twinned, fine-grained, tabular microcline which is younger than and replaces plagioclase and quartz of the matrix.

(*ii*) Relatively coarse-grained, gneissose to granitoid rocks, characterized by giant feldspar porphyroblasts of potash feldspar (Fig. 7, *b*). The typical rocks either show an augen structure in which micaceous folia wind and swirl around augen-like areas of quartzofeldspathic material, or a network texture in which micaceous minerals as well as quartzofeldspathic minerals are generally dispersed and are oriented in different directions. The latter texture type, by a gerneral increase in the grain size, grades into granitoid rocks ; the Mansehra granite is the most striking result of this phenomenon.

The two texture types are reminiscent of the "metablastic" texture of Scheumann (1937, p. 406) and the "ophthalmatic" texture of Niggli (1948, p. 109) and compare well with those described by Flinn (1954) in the case of the permeated gneisses of Delting, Shetland.

Mineralogically, these rocks are poorer in quartz (upto 1/3rd of the total mineral content) and richer in feldspar, as compared with rocks of the first type. The accessory minerals are same in the two types. The mineralogy of the Susalgali granitic gneis is described in detail below :

Quartz : It is generally present as small to medium-sized grains of anhedral form. Arranged in an interlocking arrangement, these anhedra form continuous bands, sometime locally swelling into small porphyroblastic aggregates. Frequently, they show intricate boundaries against feldspar minerals but, unlike the cases described by Harry (1953), Read (1931) and Cheng (1944), quartz had suffered replacement by feldspar minerals rather than itself being of replacement origin.

Potash Feldspar : It is present as orthoclase and microcline and as all sorts of phases intermediate between them, so that the familiar gridiron twinning of microcline may be almost absent, patchy to strongly developed. There does not seem to be any direct relationship between perfection of the gneissic texture and the physical state of the potash feldspar. For instance, it has been observed that orthoclase may be present even in a strongly sheared rock, while a weakly foliated rock may have strongly twinned microcline. In general, microcline of high obliquity is the more common variety of potash feldspar.

The potash feldspar occurs in two distinct sizes; as Carlsbad twinned megacrysts or porphyroblasts (upto $5'' \times 2'' \times 1''$) and as smaller anhedral material, constituting penetrative stringers in the rock and filling intergranular spaces.

The megacrystic fraction of potash feldspar is

generally drawn out into augen-like form, is frequently rolled and is occasionally fractured, especially when the megacrysts are discordant to the foliation planes. In most of the cases, it is perthitic with either a twinned or an untwinned plagioclase phase. On the other hand, the anhedral fraction of potash feldspar in only rarely perthitic.

The feldspar megacrysts generally contain inclusions of small rectangular tablets or laths of plagioclase, flakes of muscovite and biotite, that are sometime zonally arranged. Some of the enclosed plagioclase crystals contain dust-like inclusions in the interior and thus differ from the independent plagioclase of the groundmass (Fig. 8). In addition, megacrysts of potash feldspar may contain remnants of partially digested quartz or muscovite.

Plagioclase Feldspar : It is present as many varieties and as fractions of different periods of formation, while the overall composition varies

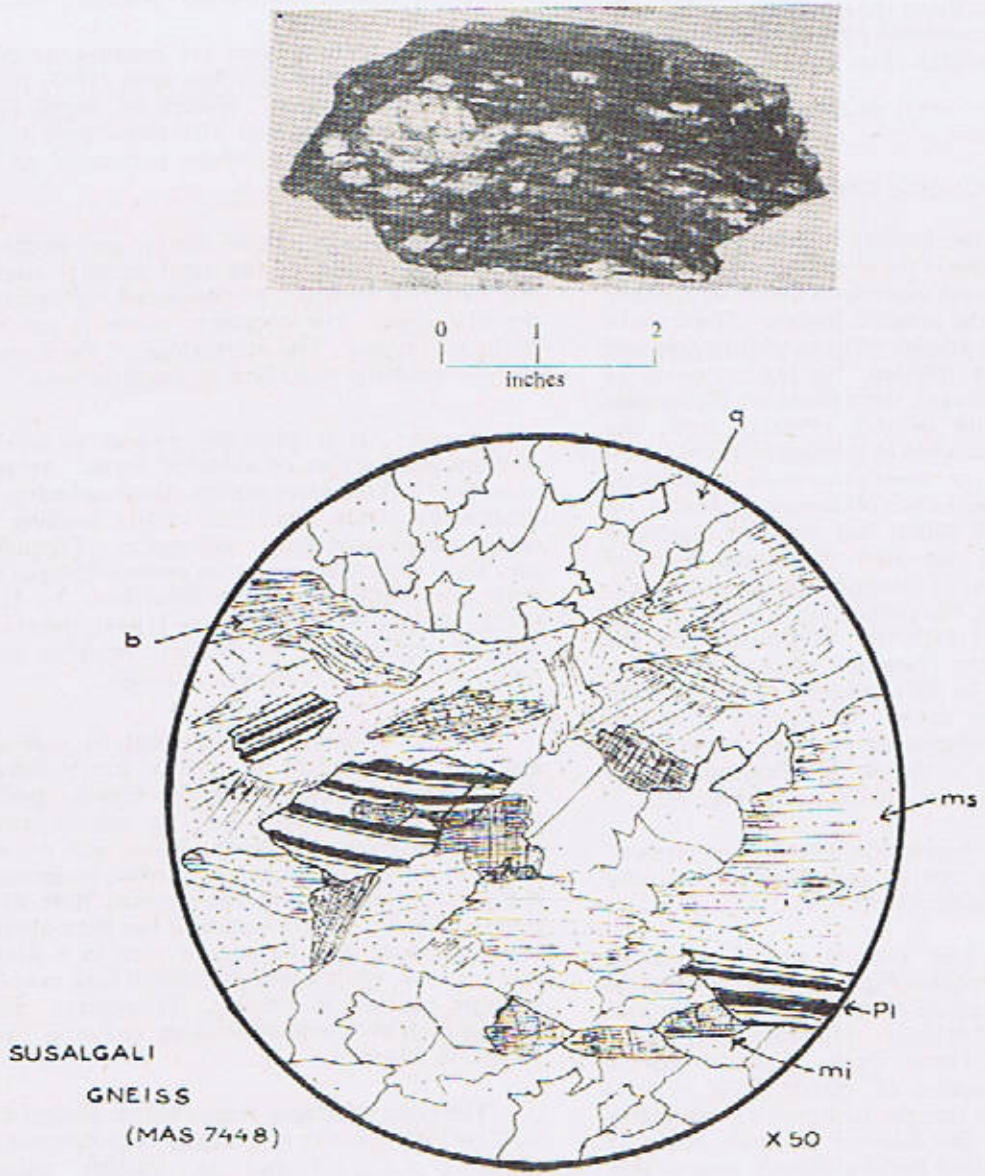

Fig. 7, a. Illustrating one type of the Susalgali granitic gneiss, showing hand specimen and drawing of its thin section. q=quartz b=biotite ms=muscovite pl=plagioclase mi=microcline.

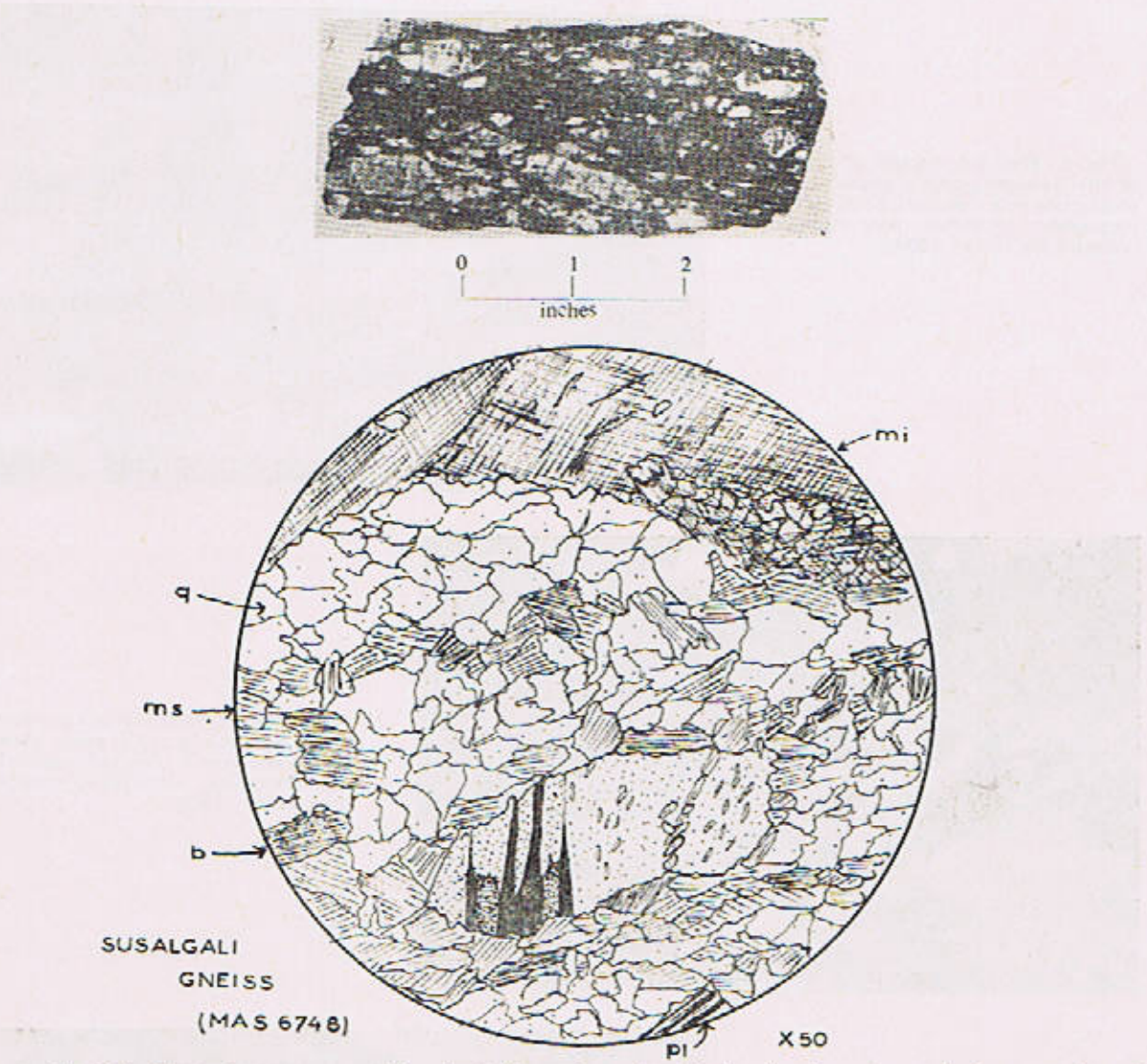

Fig. 7, b. Illustrating one type of the Susalgali granite gneiss, showing hand specimen and drawing of its thin section (symbols same as in Fig. 6).

from pure albite to acid andesine. Following are the probable modes of occurrence of these plagioclase feldspars :—

(*i*) As small, rectangular tablets, mostly enclosed in the potash feldspar megacrysts, in which, they are sometime zonally arranged. These appear to be among the earliest formed generation and perhaps that is why they are frequently full of dust-like inclusions. They show simple twinning, are rarely zoned and their composition does not vary very much. In appearance, their crystals compare well with those formed in the feldspathized fragments of the metamorphic rocks. A small proportion of plagioclase, of similar granularity, has clear interior and is mostly associated with granular microcline of high obliquity.

(*ii*) Plagioclase that is characterized by its growth over micaceous folia of the rocks, in such a way that the latter remain more or less undisturbed (helicytic textures). Sometime, however, the mica folia are dispersed in them in such a manner as to suggest that dispersal was controlled by the crystallographic structure of the feldspar lattice (Fig. 9). These plagioclase crystals almost always shown simple twinning on the albite law and are rarely zoned. This generation of plagioclase is most common and clearly it had suffered from the corrosive and replacive action of microcline ;

Fig. 8. Photomicrograph of a section of the Susalgali granitic gneiss showing plagioclase with dust inclusions, included by younger microcline; note myrmekite replacing the latter (×200).

Fig. 9. Photomicrograph of a section of the Susalgali granitic gneiss showing plagioclase grown over micaceous folia and including structurally controlled mica flakes (×200).

Fig. 10. Photomicrograph of a section of the Susalgali granitic gneiss showing growth of myrmekite that is replacing the potash feldspar (×200).

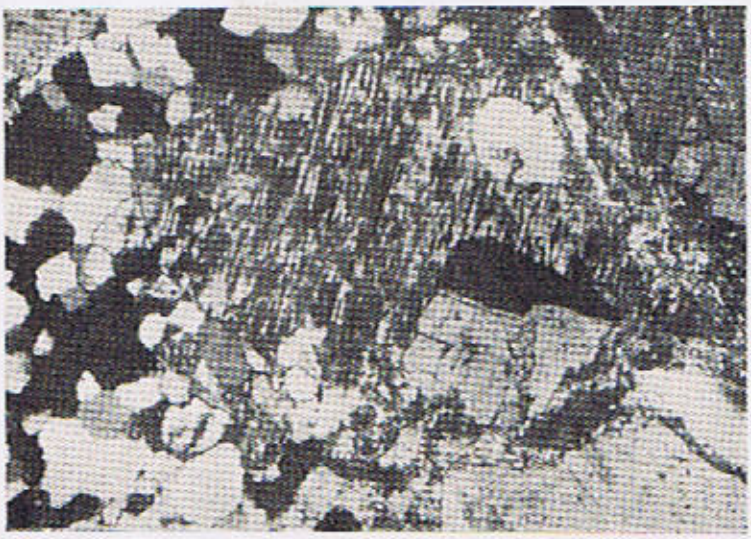

Fig. 11. Photomicrograph of a section of aplite associated with the Susalgali granitic gneiss showing chess-board albite.

sometime this effect had given rise to "antiperthites" of replacement origin, such as described by Cheng (*op. cit.*) and Drescher-Kaaden (1948) from migmatites and injection gneisses.

(*iii*) Of younger age than (*i*) and (*ii*) is the plagioclase of the myrmekite which is ubiquitous in the gneissose rocks. This myrmekite exhibits its peculiar intergrowth of vermicular quartz with albitic plagioclase, forming plug-like intrusions into potassium feldspar and is commonly associated with sheared textures (Fig. 10). Certain of its features are so unique that they are worthy of special investigation. The observations of the writer and the ideas that it gave rise to will be described later on.

(*iv*) Plagioclase, showing chess-board structure. It is restricted to the aplitic bodies that make distinct veins or occur as minor infillings of fractures and joint openings. There is every indication that this plagioclase developed after microcline, from which it inherited the textural base of cross-hatched twinning (Fig. 11), as is described elsewhere (Shams, 1968).

Mica Minerals : Both muscovite and biotite are present and, by making layers of interwoven flakes, contribute to perfection of the gneissic texture.

Biotite is highly variable in colour and in pleochroism. For instance, its colour varies from dark reddish brown to light khaki green, while sometime a gradation into chloritic material is seen. The biotite, of darker colour, occurs in somewhat granitoid portions and is mostly attended by opaque ore grains, rutile and apatite needles, while tourmaline appears, sometime, to have replaced it to variable extent. On the other hand, greenish biotite is present in such portions of rock that, on the basis of modal composition and fabric, are comparable to granitized schist fragments.

Fine flaky mica, especially muscovite, is commonly present as a dispersed material in plagioclase crystals that appeared to have grown over the micaceous layers in the rock ; partial digestion of muscovite is seen in such cases. Biotite is more commonly enclosed by potash feldspar crystals.

Accessory Minerals. Tourmaline (schorlite) is the common accessory, along with ore, apatite, zircon, rutile, monazite etc. Garnet is ubiquitous, in the sense that it is present in every facies of the complex. However, it is always a very minor accessory. Two types of garnets are found ; one occurs as corroded grains, derived from the metamorphic schists and the other as tiny, colourless variety, grown within the rock. The first variety was very unstable and had altered in the same manner as that of the hornfelse rocks.

Epidote is extremely rare and is present only in a few specimens out of those collected by the

writer. It developed as a breakdown product of plagioclase, and does not appear ever to have grown as an independent mineral.

2. The Mansehra Granite

It represents a thoroughly granitoid facies of the older granitic rocks, forming a strip, 2-4 miles wide and about 20 miles long, along the south-eastern margin of the area. Named after the important town of Mansehra, this granite is in contact with the metasedimentary rocks of the Hazara Schistose Group in the east and south-east, merges or passes into the gneissose rocks without sharp contact in the north and north-west while a small part abuts against the Hakale granite. The transitional boundary is difficult to mark on the map and can only be shown approximately.

As one walks from the region of the Susalgali gneiss into the Mansehra granite, three changes can be observed to take place :—

(*i*) Some of the small, drawn-out, micaceous aggregates of the gneiss acquire definite geometrical form and become more and more greenish in colour till they are recognizable as polygonal individuals, composed essentially of muscovite and/or chlorite. These have been called "shimmer aggregates" for the sake of description.

(*ii*) The gneissic structure is generally lost and the texture is distinctly and thoroughly granitoid.

(*iii*) The fragments of metasedimentary rocks are almost always irregular in shape and have rounded edges ; they are not drawn out and sheared as is the case inside the gneiss formation.

These changes can be seen by walking from :—

a—Jaba, through Utter Shisha to Chitta Batta.

b—Phulra, through Garwal to Shahkot.

In the field, the Mansehra granite appears as a whitish grey, massive looking, hard and very prominently porphyritic rock, with megacrysts of potash feldspar (perthitic microcline) which sometime attain a size of $5'' \times 2'' \times 1''$ (Fig. 12). The groundmass consists of a coarse-grained aggregate of whitish and subhedral sodic plagioclase, vitreous and slightly smoky anhedral quartz, dark biotite flakes, occasionally with bronzy lustre, and subordinate muscovite, ore etc. Other essential and characteristic constituents of the granite are the small "shimmer aggregates" that are present almost everywhere in the granite, being particularly abundant in the marginal zones. The leucocratic late members, however, do not have shimmer aggregates.

In this essentially massive rock, weak planes of rift can always be located ; these are made use of by the local population for breaking and trimming blocks for building purposes. The rift-planes are marked by orientation of the microcline megacrysts and this feature stands out vividly in the field. However, this orientation is well-marked only on the surfaces which are cut normal or at very high angle to the plane containing side pinacoids of megacrysts. Furthermore, the orientation is often not followed by individual megacrysts, which may even lie almost at right angle to the general direction. Within the planes, that hold side pinacoids of the megacrysts, the latter lie randomly and therefore this has been taken to mean that the planar structure is not foliated, as one finds in the Susalgali gneiss. This structure may be compared with the "non-layered planar structure" described by Martin (1953) in the case of the Flammanville granite.

Jointing is very prominently developed everywhere and gives rise to splitting of the granite into rectangular blocks, which after having undergone

Fig. 12. Showing megacrysts of feldspar in the Mansehra granite.

exfoliation, acquire somewhat rounded forms. The escarpments are usually covered with such boulders. The joint surfaces are generally rough and hackly, except for those that had undergone slickensiding on local fault planes. Occasionally, joint openings are filled with tourmaline-bearing aplitic material, the plagioclase of which is more albitic than that of the host rock. The detailed mineralogy of the Mansehra granite is described below.

Quartz : It generally occurs in the form of allotriomorphic aggregates or patchy mosaics, with crenulated and interlocking margins.

Replacement by feldspar minerals is predominently exhibited by the presence in them of irregular ramnents of quartz. Sometime, clusters of these inclusions occur in optical continuity and, thus, bear out the fact that they once were part of a larger grain. Sheared, strained and recrystallized quartz is common in the foliated facies of the granite that are present along fault zones or at the margins of the granite body.

Feldspar Minerals :

(*i*) Potash Feldspar : This is almost always found as microperthitic microcline of high obliquity ($\Delta = .95$) that is present as Carlsbad-twinned, euhedral megacrysts and as a patchy fraction showing irregular intrusions into the groundmass. The margins of the megacrysts are generally irregular, especially when in contact with quartz ; the latter then holds lobe-like extensions of the feldspar mineral.

Zonally arranged inclusions of small tabular plagioclase crystals and biotite flakes are common in the megacrysts, while their margins are frequently indented by myrmekite when in contact with plagioclase.

(*ii*) Plagioclase Feldspar : In addition to small tablets, enclosed in the potash feldspar, plagioclase is present as large, subhedral to euhedral crystals. Its composition lies within the basic oligoclase range, while albitic myrmekite is sometime developed in the form of minor extensions. Plagioclase shows complex twinning and is frequently zoned, both in normal and in oscillatory fashion.

Micas : Reddish brown, strongly pleochroic biotite is the prominent mica ; it is generally dispersed in the rock and sometime forms local aggregates. Rutile and ore inclusions are very common and most of the flakes are rich in pleochroic haloes around tiny apatite and zircon crystals.

Minor muscovite is intimately associated with biotie and is rarely transformed into slender fibrolite needles.

Accessory Minerals : Opaque ore, rutile, zircon, apatite, monazite and rare garnet are accessory minerals.

Shimmer Aggregates : These are small polygonal bodies and are the most characteristic constituents of the Mansehra granite, being so abundant that sometimes 10 to 20 individuals can be easily located in a single hand specimen. At the foot of a weathered outcrop of the granite, hundreds of them lie loose on the ground.

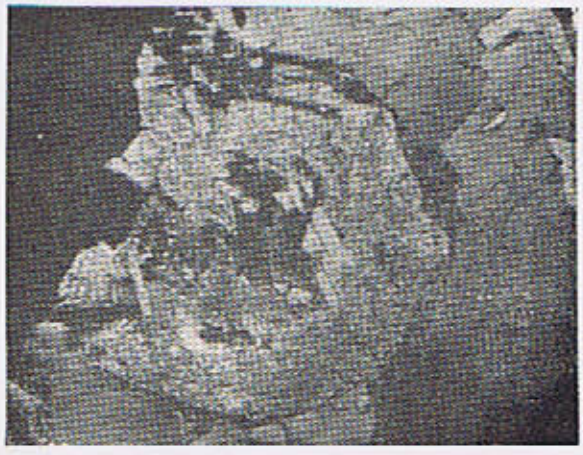

Fig. 13. a. Photomicrograph of a "Shimmer aggregate" in a section of the Mansehra granite, showing outlines as if developed after cordierite.

Fig. 13. b. Photomicrograph of a "Shimmer aggregate" in a section of the Mansehra granite, showing outlines as if developed after andalusite (note cleavage traces).

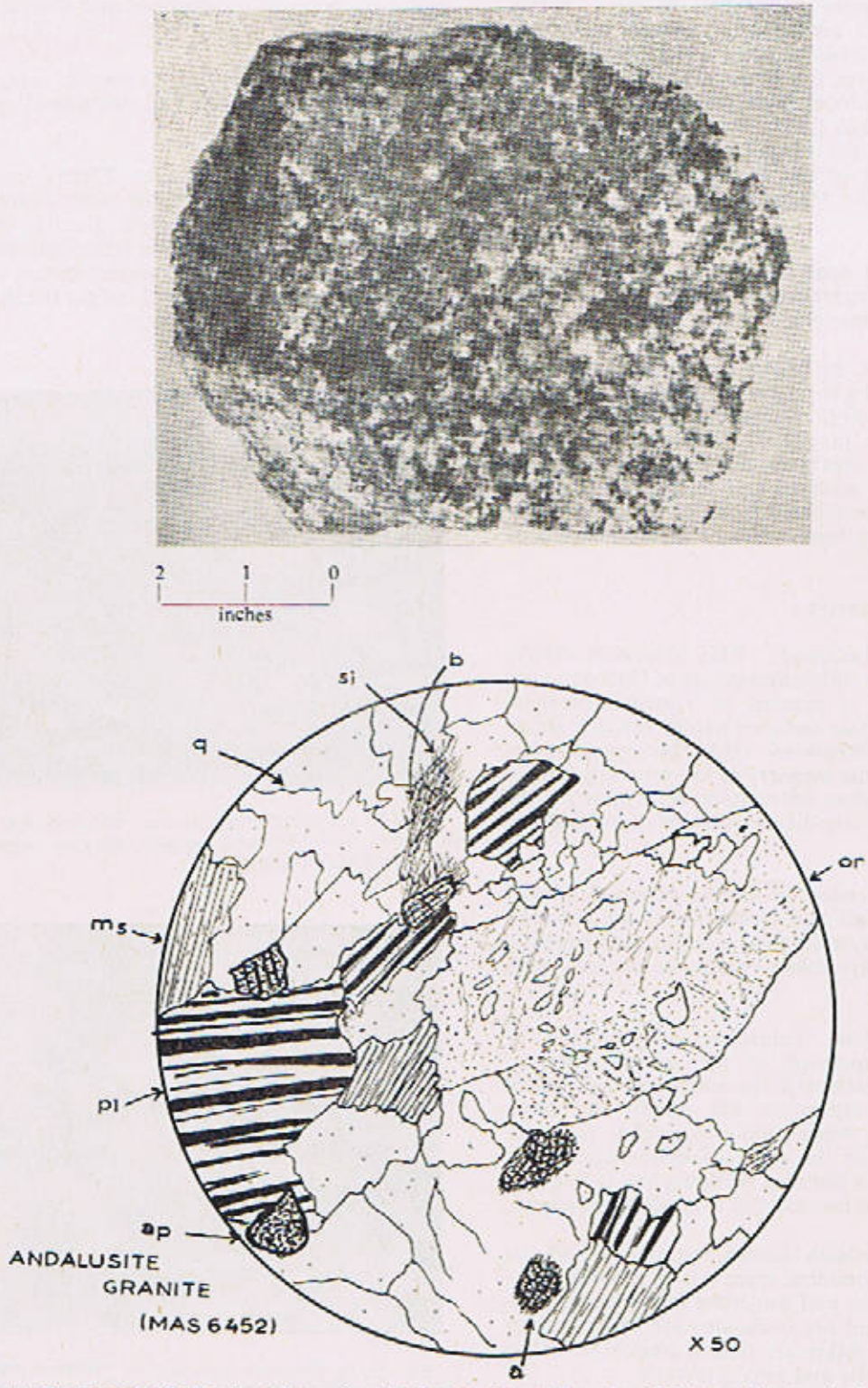

Fig. 14. Photograph of a hand specimen of andalusite granite and drawing of its thin section (symbols same as in Fig. 6).

The "shimmer aggregates" vary in colour from olive green to deep greyish green and have a definite geometrical form. In thin section, they show up as aggregates of chlorite and/or muscovite, sometime with a few biotite flakes in the interior (Fig. 13).

They either are "pinite" pseudomorphs after cordierite or are replacement material after andalusite. It is thought possible that some of these may have developed after staurolite and garnet of the assimilated schist fragments.

3. The Andalusite Granites :

These are minor but important members of the older group of the granitic rocks and occur as small, lens-like or podlike masses within the Susalgali gneiss, in the northern regions of the Mansehra-Amb State area. Typically, these are found within a one mile wide, marginal zone of the gneiss and sometime almost at the contact with the metamorphic rocks. The known occurrences are :—

(*i*) West of Kotli Bala, exposed along road cutting, opposite village Laspata.

(*ii*) North of Karmang Utla and on the road side south of this village.

(*iii*) South of Masjid Danna.

(*iv*) On the Masar Ridge and near Jaba.

In the field, this rock is distinguished from the enclosing gneiss by its finer grain and granitoid texture (Fig. 14), somewhat darker colour and by the presence of small pink specks of andalusite. Furthermore, the size of the feldspar megacrysts is never larger than 1 inch, set in a more or less equidimensional groundmass of minerals. The foliation, marked by orientation of the feldspar crystals (like the Mansehra granite) is generally parallel to the length of the lensioid outcrop and also to the foliation of the enclosing gneiss. The foliation planes of the enclosing gneiss can be followed into and through the andalusite granite, the contacts between the two being transitional over very short distance.

The mode of occurrence and the range of composition of the quartzofeldspathic constituents of this granite are more or less similar to those of the Mansehra granite, except for the smaller average grain size and that the potash feldspar is invariably orthoclase ($\Delta = .05$).

Once again, the mica minerals are also comparable and the essential constituents are similar in nature. The prominent differences in mineralogy from the Mansehra granite are the presence of aluminium silicate minerals such as andalusite and sillimanite and the frequent occurrence of exenocrystic garnet and abundance of apatite and tourmaline.

Aluminium Silicate Minerals : (Fig. 15).

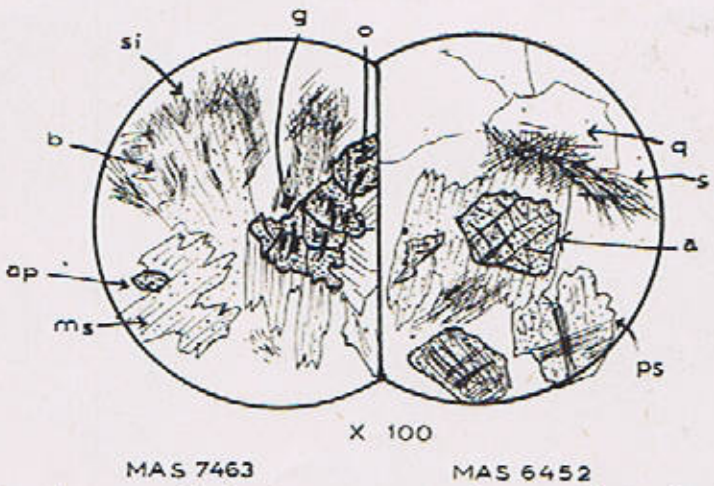

Fig. 15. Drawings from thin sections of andalusite granite showing aluminium silicate minerals and their paragenesis. g=garnet o=ore Si=Sillimanite b=biotite ap=apatite a=andalusite q=quartz ps=pseudomorph of andalusite.

(*i*) Andalusite is the characteristic mineral of the andalusite granites and occurs as clusters of subhedral prismatic grains, with well-developed cleavage. It is pleochroic from very weak pink to nearly colourless and thick sections show colour zoning. It is almost always mantled by muscovite and is sometime completely pseudomorphed.

Very rarely, grains of andalusite are found in other granitoid facies of the complex but never in the gneissose rocks. It appears that it was formed in the initial stages of the genesis of the granitic complex but was later on changed into muscovite, especially where the alteration was helped by shearing, as in the gneissose rocks.

In properties and appearance, this andalusite is very much like that of the hornfelses and may be of similar origin.

(*ii*) Sillimanite, the variety fibrolite, is very common in the andalusite granites and is only rarely seen in other facies of the complex. It seems always to have arisen out of biotite or muscovite and shows tendency to alter to muscovite ; cases of epitaxial growth over mics flakes, such as described by Chinner (1961) do not seem to be present here.

4. The Acid Minor Intrusives :

These are of three types :

(*i*) Pegmatites.

(*ii*) aplites and albitites

and (*iii*) porphyries.

They are described separately below.

The Pegmatites :

These are the coarsest bodies in the area and are found mostly in the northern regions, emplaced in the gneissose rocks. There is hardly any pegmatite in the Mansehra granite and only rare, small patches in the Hakale granite.

The highest concentration of these bodies may be seen in the Khabbal-Oghi region, where they sometime occur as swarms of thin bodies, mostly filling longitudinal joint openings in the gneissose rocks (Fig. 16). They are invariably sheared and occasionally boundinaged and, more rarely, folded along with the foliation of the gneiss (Fig. 17). They have very simple mineralogy, which is similar to

Fig. 16. Swarm of pegmatite bodies inside the Susalgali granite gneiss, Khabbal-Oghi Section.

that of the adjoining gneiss, so that they have quartz, feldspars, micas (muscovite being predominant) large red garnet crystals and long stout prisms of schorl tourmaline. There are reports of some old diggings for beryl in the pegmatites of Paniali but writer could not find a trace of this mineral.

Surface mining for muscovite has been carried out intermittently but this could never develop into an economic proposition due to the sheared nature of most of the muscovite books causing them to break into long, narrow strips of limited industrial utility.

Sometime, the pegmatites show zoning but this is of no particular mineralogical importance. Thus they are the so-called simple pegmatites and compare with Ramberg's replacement pegmatites from Greenland (Rambarg, 1956).

The Aplites and Albitites :

These bodies are the most common of all the minor intrusives and are met with in almost every part of the area, though more concentrated in the contact zones. Petrographically all varieties between strongly sheared to massive types are present. Their thickness varies from less than an inch to many yards as does their length. Mineralogically, they are quartz—two feldspar aplites, albite-quartz aplites and pure albitites. This also is more or less their sequence of formation, not necessarily of their age of formation.

The true aplites are saccharoidal aggregates of granular quartz, potash and plagioclase feldspars and micas with late developing tourmaline. The soda aplites have similar mineralogy, except that their potash feldspar has been metasomatically replaced by albite, with chess-board texture. The albitites seem to have an entirely different and, perhaps, totally independent origin. Their ablite does not show the chess-board pattern and, in thin section, a somewhat aligned aggregation of albite laths is seen ; the feldspar is mostly twinned on the combined albite-carslbad law (Fig. 18).

The albitites are always pure feldspar rocks and at many places these are exploited to provide raw material for the ceramic industry. Those of Utter Shisha and Sandsar are of good quality. Exploited also are those which have suffered hydrothermal alteration into clay material.

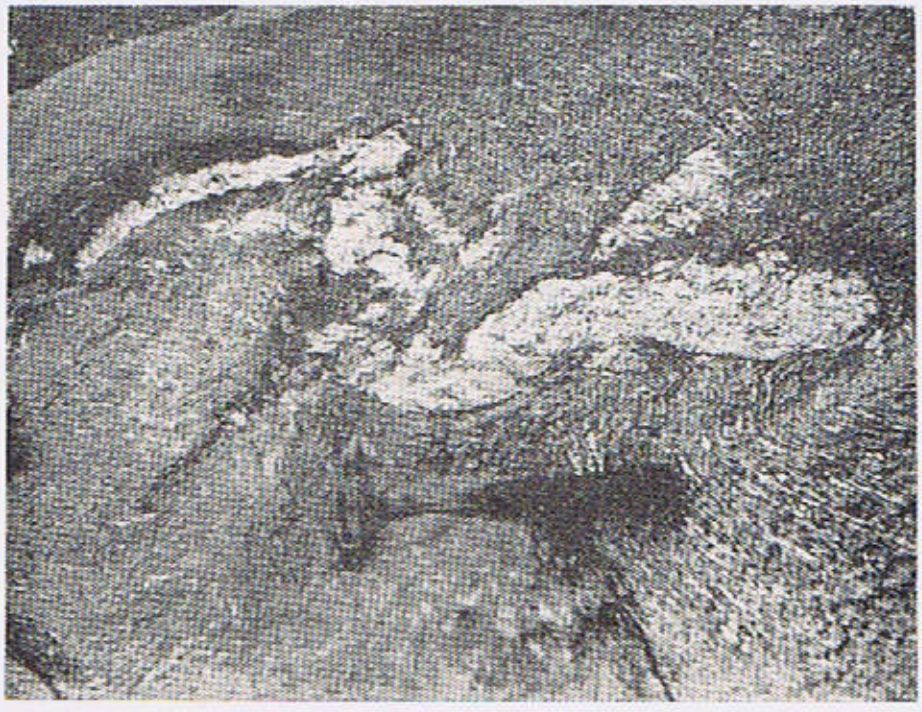

Fig. 17. Pegmatite body showing close structural relationship with the enclosing Susalgali gneiss

Fig. 18. An albitite body near Nelure (a) and photomicrograph of its thin section (b).

Traces of scheelite, developed after wolframite, are present in some tourmaline aplites, located in the Oghi—Khabbal area but they do not appear to be rich enough to be of economic interest (Shams and Fazal, 1967.)

The Porphyries :

These bodies occur rather rarely and, so far, only two localities are known, both related to the Mansehra granite. These are somewhat thick dykes filling joint openings and with feldspar and quartz phenocrysts in a very fine-grained matrix. In both the cases, the rocks are somewhat sheared, to the extent that their potash feldspar has acquired a high obliquity ($\triangle$ = near 0.95).

Their chemical composition is comparable to that of the granite in which they lie, and thus they are thought to represent an accumulation of silicate liquid that was present in the region.

MODAL ANALYSIS OF THE GRANITIC ROCKS.

Thin sections of 18 representative rocks of the major facies of the older group were subjected to modal analysis, using a Swift point-counter. In view of the variable granularity of the rocks, 1 mm traverses were made. The results so obtained are given in the Table No. 2 and are expressed as percentages by volume.

These results have been plotted on two types of diagrams :

(*a*) The modal percentage of the potash feldspar was plotted against the corresponding values of the associated plagioclase feldspar (Fig. 19). A broken line has been drawn to show the probable trend of variation. For comparison, a diagram, modified from that of Tuttle and Bowen (1958)

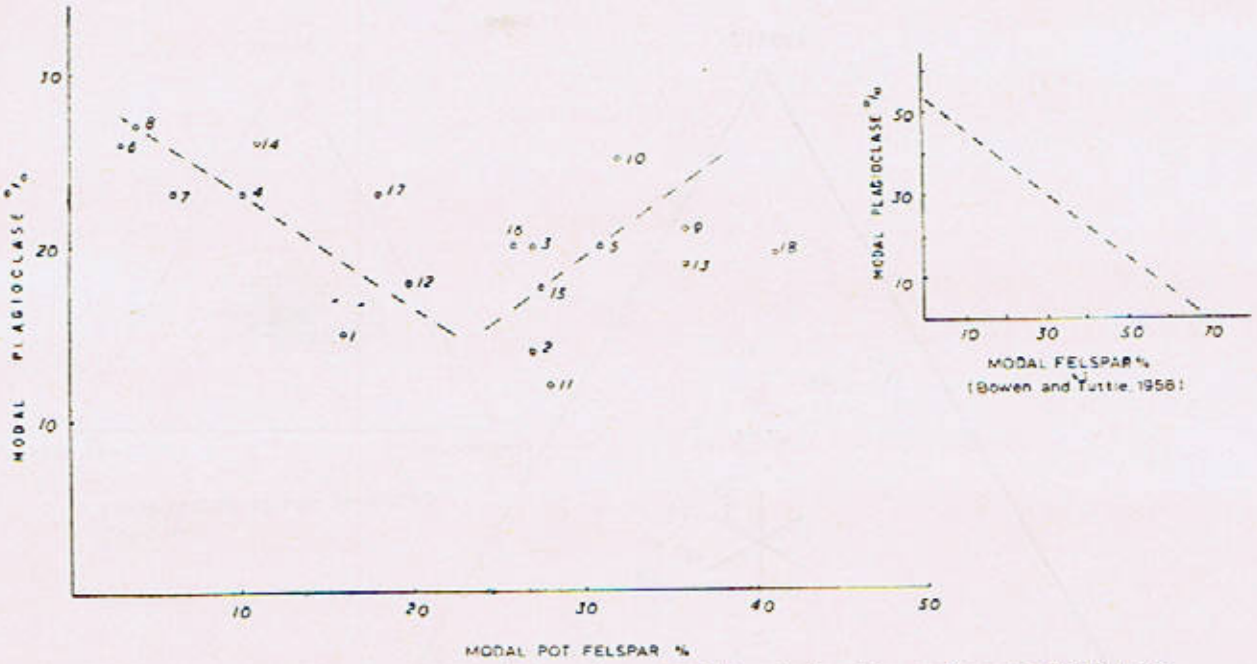

Fig. 19. Showing modal interrelationship of plagioclase and K-feldspar in the older granites and gneiss members.

based on the modal composition of 260 granites, is shown as inset ; the broken line, once again, shows the probable trend of variation.

(*b*) The modal proportions of quartz, potash feldspar and plagioclase have been recalculated to 100 percent and on this basis the position of every rock has been plotted on a triangular diagram (Fig. 20). Given for comparison is a similar diagram by Chayes (1951, p. 41) based on analyses of 260 granites.

The significant points about the granites of the Mansehra-Amb State area are, that these rocks vary from granite to granodiorite, and that :—

(*i*) As shown by Fig. 18, potash feldspar and plagioclase show a reciprocal variation up to a limit of 23—24% of the former, thereafter the modal proportions of both the feldspar constituents increase simultaneously.

(*ii*) Fig. 20 shows that plots of many of the granites of the Mansehra-Amb State area fall somewhat away from the central area. It also shows that the plagioclase content varies within a narrow range, while quartz and potash feldspar show reciprocal variation.

(*iii*) Examination of the remaining mineralogy of the rocks shows that mica minerals, especially muscovite, also show reciprocal variation against potash feldspar, thus showing a decrease in the total contents of quartz and micas.

(*iv*) Fig. 20 shows the inherent mineralogical hetereogeniety in the rocks ; this may be an expression of the two major types of gneissic rocks, as has been described earlier.

THE FRAGMENTS OF METASEDIMENTARY ROCKS INSIDE THE GRANITIC BODIES

The granitic bodies contain such a large number of fragments of the metamorphic rocks that it is one of their field character and has a bearing on their genesis (Fig. 21). Their abundance can be judged from words of Middlemiss (*op. cit.* p. 63) :—

> "So full of included fragments is the rock that they may be found without difficulty every ten yards of the exposed rocks . . . . . and occasionally they are so crowded together as to give almost the appearance of an agglomerate."

The size of the fragments varies from fraction of an inch to many feet while some may run into

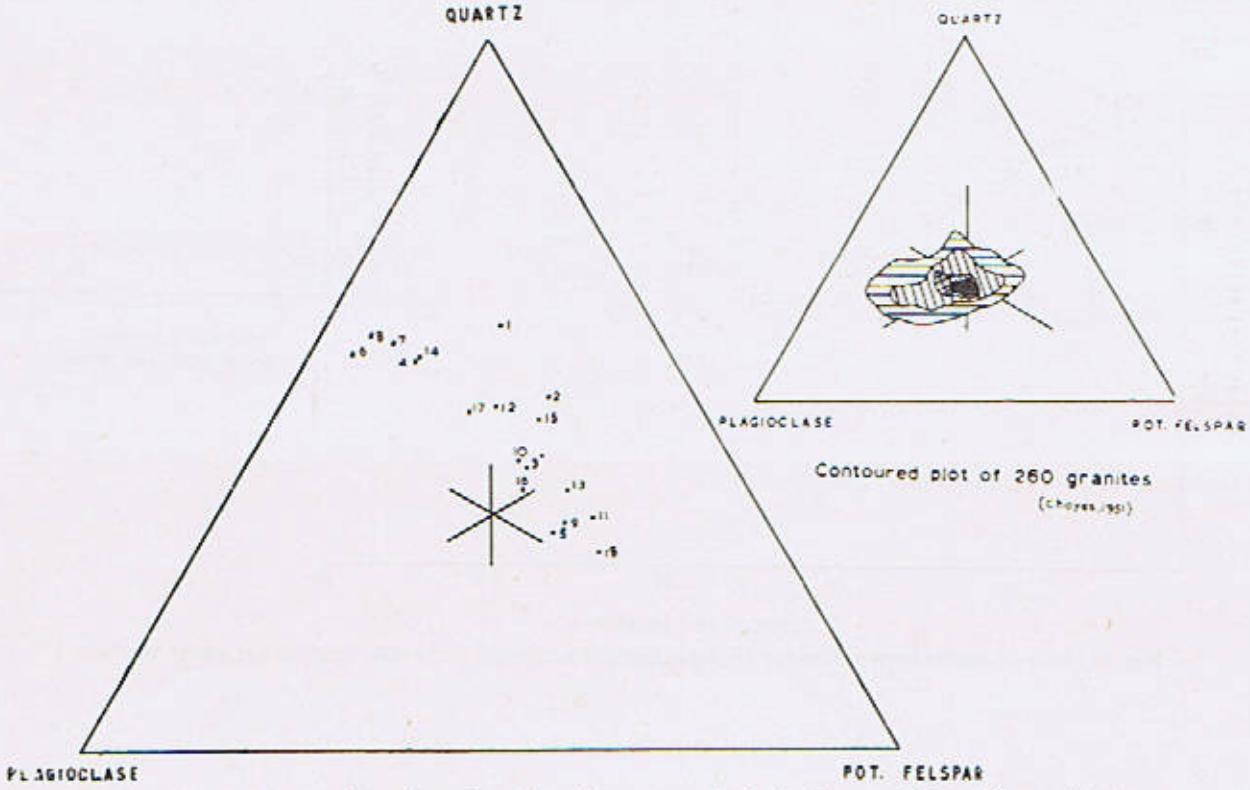

Fig. 20 Showing plots of granitic rocks of the older group on the basis of quartzo-feldspathic constituents.

thousands of yards, such as the Shergarh schist. Lithologically, these bodies belong to the metamorphic formations of the area and fragments of comparable pelitic, psammitic and quartzitic nature are easily recognized (Fig. 22). Frequently even the mineralogical banding, of sedimentation origin, is also present, and is very useful in finding their orientation with respect to the foliation of the granitic host. Observations have shown that banding and / or schistosity and also the dimensional orientation of the fragments are generally conformable to the foliation of the granite. Rarely, however, there are examples where they stand strongly discordant, sometime almost perpandicular to the granite foliation. Most of such fragments are present inside the Mansehra granite ; having had modified inside the gneissose rocks due to shearing.

The ultimate shape of a fragment was controlled by its lithology althogh foliation and jointing controlled their original shape. The pelitic composition appear to have been more favourable for

Fig. 21. Mansehra granite near Mansehra Rest House, showing abundance and alignment of schist fragments.

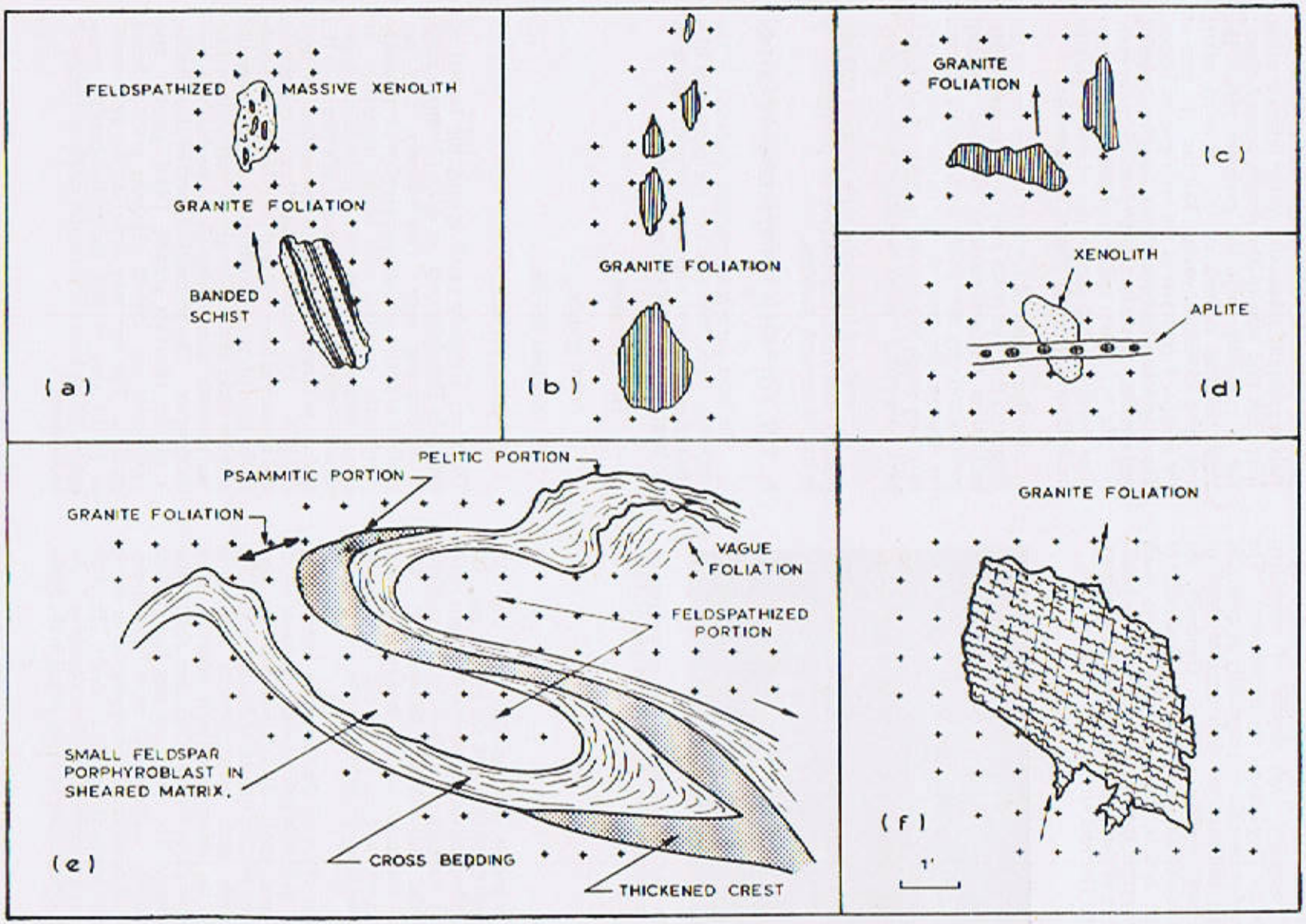

Fig. 22. Drawing of various types of schist fragments inside granitic bodies of the older group.

incorporation so that rock fragments of such composition had acquired high degree of roundness, whether or not they became equidimensional. The fragments of psammitic and especially of quartzitic rocks either had retained their angular shape or had been only weakly modified. Generally, the fragments lie well apart but in the marginal zones of the granitic bodies, they are sometime so much crowded togather that they make beautiful agmatites (Fig. 23), of the type described from Sutherland, Finland and Donegal etc.

Fig. 23. Showing agmatitic aggregate of schist fragments inside the Mansehra granite at marginal zone east of Chitta Batta.

The fragments show various types and different degrees of reaction with the granitic material. It has been observed that quartzitic fragments never reacted very strongly ; were mostly recrystallized, coarsened and only slightly feldspathized. The pelitic and psammitic rocks, however, suffered strong reactions and all variations, from simply baked to completely granitized, can be easily found.

The first effect on the fragments was that of heat so that spotted hornfelses were produced which had developed small, dark greenish-brown local aggregates of biotite, quartz and muscovite. The areas between such porphyroblasts contain, in addition to the above mentioned minerals, large fractions of small, prismatic plagioclase and tabular potash feldspar. The fragments that had suffered further reaction, contain even more feldspar crystals, either as porphyroblastic aggregates or as big euhedral to augen-shaped individuals. Perthitic microcline, of a size similar to those occurring in the main granitic body, can be easily found in the feldspathized material. The orientation of these crystals is generally subparallel to the foliation of the host rock and also to the granite around them ; this is especially so in the gneissose rock. The bigger feldspar crystals contain embayed quartz and mica inclusions, exactly like the type seen in the feldspar megacrysts of the main granitic bodies. The plagioclase feldspar shows complex twinning and generally forms local aggregates of two or more individuals. Minor amounts of sillimanite is sometime developed but due to the advent of granitic fluids it was commonly altered to muscovite.

Further stages of reaction can be seen in the fragments that had fallen prey to the general feldspathization (or granitization) and had acquired composition very near to the host granite. Except for their smaller grain size or darker colour, they look very much like granites in field. Such bodies have been called "ghost xenoliths" by petrologists.

The study of fragments, their reaction with the granites and their contribution to petrogenesis is in itself a research problem.

B. THE YOUNGER TOURMALINE GRANITES

The later periods of plutonic evolution of the Mansehra-Amb State area saw the generation of a number of bodies of tourmaline granite. Some of the larger members of this group are :

1. Hakale granite.
2. Sukal granite.
3. Karkala granite.
4. Dheri granite.

These are relatively small bodies, the biggest of them, the Hakale granite, is only 13 square miles in outcropping area. Petrologically, they are medium to coarse grained non-porphyritic or weakly porphyritic granites, with black tourmaline as one of their essential minerals. In addition plagioclase is almost always in the range of albite while the typical potassium felspar is microcline of high obliquity. The latter is a late-formed constituent and appears to have replaced the other salic minerals of the groundmass. Contrary to the case with the granitic rocks of the older group, muscovite is their characteristic mica, although minor biotite is not uncommon. The geometrical form of these bodies is sill-like (Karkala granite, Dheri granite) and oval-shaped or lensoid (Hakale granite, Sukal granite). The size may sometime be quite small as in the case of thin tourmaline-bearing soda-aplites, which have a comparable origin and mode of occurrence.

Among the tourmaline granites, the Hakale granite which is the largest member of this group will be described in detail.

The Hakale Granite

It is a small, oval-shaped body which occupies a position defined by core of the syntaxial loop of Mansehra-Amb State area. About 13 square miles in extent, it is elongated in the east-north-easterly to west-southwesterly direction. It is in contact with the Mansehra granite in the south and with the metasedimentary rocks in the north ; its eastern extension is covered under alluvium, while it ends as wedge and tongue intrusions into the schist in the western direction. The contact relations show that the Hakale granite is younger than the Mansehra granite, against which it had developed a finer grained (? chilled) edge. (Fig. 24). It is almost a massive body or at the most, a very weak foliation-trace can be seen ; tectonically affected areas, however, have definite foliation. On the weathered surfaces, the foliation shows up much better. The margins of the granite, especially the northern margin are sheared. Compared with the granitic bodies of the older group, this body is much more free of fragments of metamorphic rocks and holds a lesser number of doleritic injections. Jointing is well-developed and in combination with the weathering, gives rise to outcrops that break into somewhat slab-like pieces, in contrast to the sub-rounded boulders of the nearby Mansehra granite.

Petrology :

In thin section, the Hakale granite shows a granoblastic to crystalloblastic aggregate of minerals without any preferred orientation, except for the portions that had suffered shearing due to faulting. The mineralogy of the rock consists of quartz, albitic plagioclase (An_4 to An_{10}), microcline, muscovite, garnet, epidote, tourmaline, biotite and rare ore grains.

The following facts are noteworthy :

(*i*) There is a general crushing of the grains, attended by bending and fracturing. Quartz and feldspar minerals are specially affected and sometime exhibit a mortar-like texture ; even the mica minerals show strain extinction.

(*ii*) The albitic plagioclase was present earlier than microcline, as is shown by the latter's replacement relationship towards the former (Fig. 25).

Fig. 24. Showing contact of Hakale granite with Mansehra granite ; Note fine grained margin of the former.

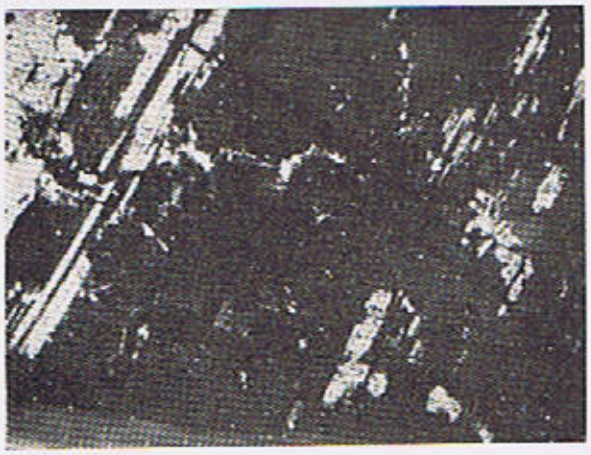

Fig. 25. Photomicrograph of a thin section of Hakale granite showing microline replacing plagioclase : note ramnents of the latter.

BASIC MINOR INTRUSIVES

Minor basic bodies, in the form of dykes and sills, are present almost everywhere in the area cutting both the granitic as well as the metamorphic rocks. Depending upon the age of emplacement, they are met with as all sort of varieties between ophitic dolerites to garnet amphibolites. Detailed investigation has proved that the source magma was of tholeiitic basalt composition. Due to their rather thin dimensions, they suffered somewhat quick cooling so that differentiation effects were not very appreciable except for the development of rare vein-like or patchy pegmatitic concentrations. The older bodies shared regional metamorphism simultaneous with the enclosing schists and closely acquired similar metamorphic status. Therefore, while study of the dolerites of the area reveals the differentiation trend of the parent magma on one hand, investigation of the metadolerites affords knowledge of the effects of metamorphism on the same magma on the other hand. The first aspect of this problem has been studied in detail and is reported elsewhere (Shams, 1968).

ORIGIN OF THE HAZARA GRANITIC COMPLEX

As the aim of this article is to describe geology of the Mansehra-Amb State area in general, details of investigations carried out to understand possible origin of the granitic complex will not be given. It may, however, be useful to report the conclusion that the granitic complex seems to have formed by a process of "magmatic granitization" of the pre-existing metasediments through the agency of hot permeating fluids of ultimate magmatic parentage. Under structural control, only portions of the metamorphic rocks suffered granitization while the tectonic behaviour of the granitized areas was induced after their acquiring mechanical properties different from the non-granitized metamorphic rocks.

The above conclusions are not only supported by the petrological and structural investigations etc. but are also hinted upon by the radiometric data on micas of some of the granitic rocks of the area (Shams, 1967).

The younger tourmaline granites and related minor acidic bodies had close genetic relationship with the major granitic complex.

REFERENCES

Aziz-ur-Rehman 1961 A gravity survey of granites in the Mansehra area. *Geol. Bull. Punjab Univ.* No. 1, 15.

Chayes, F. 1951 Modal composition of granites. *Carnegie Inst. of Washington, Year Book*, No. 50.

Cheng, Y.C. 1944 The migmatite area around Bettyhill, Sutherland *Quart. J. Geol. Soc., London*, **99**, 107.

Chinner, G.A. 1961 The origin of sillimanite in Glen Clova, Angus. *J. Petrology* **2**, 312.

Drescher-Kaden, F.K. 1948 Die Feldspar Quartz Reaktiongefuge der Granite und Gneise. Springer-Verlag, Berlin.

Flinn, D. 1954 On the time relations between regional metamorphism and permeation in Delting, Shetland. *Quart. J. Geol. Soc., London*, **108**, 177.

Harry, W.T. 1954 The composite granitic gneiss of western Ardgour, Argyll. *Quart. J. Geol. Soc., London*, **109**, 285.

Hayden, H.H. 1913 Notes on the relationship of Himalayas to the Indo-Gangetic plains of Indian peninsula. *Rec. Geol. Surv., India*, **43**.

Martin, N.R. 1952 The structure of the granite massif of Flamenville, Manche, N.W. France. *Quart. J. Geol. Soc.*, **108**, 311.

Middlemiss, C.S. 1896 The geology of Hazara and the Black Mountain. *Rec. Geol. Surv., India*, **26**, 1.

Niggli, P. 1948 GESTEINE UND MINERALLAGERSTATTEN., Basel.

Ramberg, H. 1956 Pegmatites in West Greenland. *Bull. Geol. Soc. Amer.*, **67**, 185.

Read, H.H.1931 The geology of Sutherland. *Mem. Geol. Surv. Scotland.*

Scheumann, K.H. 1937 Metatexis and metablastesis. *Min. Pet. Mitt.*, **48**, 402.

Shams, F.A. 1963 The effects of thermal metamorphism upon calcareous nodules in the quartz-mica schists of the Mansehra area, Hazara District, West Pakistan. *Geol. Bull., Punjab. Univ.*, **3**, 25-27.

Shams, F.A. 1967 Chess-board albite in the Mansehra-Amb State area, northern West Pakistan. *Pakistan Journ. Sci. Res.*, **19**, 79-82.

Shams, F.A. and Rahman, F.U. 1966 The petrochemistry of the granitic complex of the Mansehra-Amb State area, northern West Pakistan. *Journ. Sci. Res. Punjab Univ.*, **1**, 47-55.

Shams, F.A. 1967 A note on radiometric ages of micas from some granitic rocks of the Mansehra-Amb State area, northern West Pakistan. *Geol. Bull. Punjab Univ.* **7**, 88-89.

Seams, F.A. and Rehman, F.U. 1967 Tungsten-Molybdenum mineralization north of Oghi, Hazara District, West Pakistan. *Jour. Sci. Res. Punjab Univ.* **2**, 41-46.

Shams, F.A. and Zulfiqar Ahmed 1968 Petrology of the basic minor intrusives of the Mansehra-Amb State Area, Northern West Pakistan Part I. The Dolerites *Geol. Bull. Punjab Univ.* **7**, 45.

Tuttle, O.F. and Bowen, N.L. 1958 Origin of granite in the light of experimental studies in the system—$NaAlSi_3O_8$—$KAlSi_3O_8$—SiO_2—H_2O. *Mem. Geol. Soc. Amer.* No. **74**.

Wadia, D.N. 1931 The syntaxis of the northwest Himalayas : Its rocks, tectonics and orogeny. *Rec. Geol. Surv. India.* **45**, 89.

Wynne, A.B. 1887 Notes on the tertiary zone and the underlying rocks in the northwest Punjab. *Rec. Geol. Surv. India* **10**, 113.

TABLE 2

Micrometric analyses of some specimens of the older group of granitic rocks.

Mineral	1 (7464)	2 (7353)	3 (7463)	4 (7557)	5 (6817)	6 (7522)	7 (6451)	8 (6738)	9 (7457)
Quartz ..	46.7	41.5	31.3	40.2	23.1	38.3	40.9	45.0	26.7
Pot. feldspar. ..	16.3	26.6	26.6	9.4	31.2	3.0	6.2	4.4	36.3
Plagioclase. ..	15.4	15.4	20.2	22.7	20.3	26.0	23.5	26.9	21.2
Biotite* ..	13.8	10.6	12.1	14.8	10.4	14.7	11.8	16.5	5.9
Muscovite ..	6.6	3.8	7.6	11.5	14.3	16.0	16.9	5.7	8.6
Accessories.** ..	1.6	2.1	2.2	1.4	0.6	2.0	0.9	1.5	1.3
Total counts ..	2222	2244	2900	2670	2570	2520	2750	2200	2830
Pot. fels/ (Pot. fels + plag.) ..	0.53	0.64	0.57	0.29	0.61	0.11	0.21	0.14	0.63
Recalculated to percentage									
Pot. feldspar. ..	21	32	34	13	42	5	9	6	43
Plagioclase. ..	19	18	26	32	27	38	33	35	25
Quartz. ..	60	50	40	55	31	57	58	59	32

*includes minor chlorite and partially chloritized biotite.

**include ore, garnet, apatite, tourmaline, zircon, monazite, epidote ; and andalusite in case of andalusite granites.

TABLE 2 (*conti.*)

Mineral	10 (6332)	11 (6275)	12 (7455)	13 (6553-A)	14 (6553-B)	15 (7338)	16 (6817)	17 (6394)	18 (7065)
Quartz ..	40.0	19.6	37.3	32.7	39.6	27.2	27.9	37.8	23.4
Pof. feldspar. ..	32.2	27.7	19.8	35.9	27.5	30.4	26.4	18.2	41.3
Plagioclase. ..	25.3	12.2	18.0	19.3	17.7	22.4	20.2	22.7	19.6
Biotite* ..	1.1	33.3	10.3	5.7	7.9	10.2	10.8	14.2	12.1
Muscovite ..	1.3	6.4	13.5	5.1	5.8	7.8	13.4	5.8	2.3
Accessories.** ..	0.3	1.1	1.1	1.3	1.5	1.9	1.3	1.3	1.3
Total counts. ..	2145	3690	1880	1860	1930	2200	1970	2850	1820
Pot. fels./ (Pot. fels + plag.)	0.56	0.69	0.51	0.65	0.61	0.57	0.57	0.45	0.68
Recalculated to percentage									
Pot. feldspar. ..	33	46	26	41	32	38	35	23	49
Plagioclase. ..	26	21	25	22	21	28	27	29	23
Quartz. ..	41	33	49	37	47	34	38	48	28

*includes minor chlorite and partially chloritized biotite.

**include ore, garnet, apatite, tourmaline, zircon, monazite, epidote, and andalusite in case of andalusite granites.

AN IMPROVED SCHEME FOR CHROMITE ANALYSIS

BY

SHAFEEQ AHMAD

Department of Geology, University of the Punjab, Lahore, West Pakistan

Abstract : *Chromite sample* (80-120 *mesh*), *purified with the help of a magnetic separator and heavy liquids, is decomposed by heating with a mixture of* HNO_3 *and* $HClO_4$ (60-70%) *in a beaker.* SiO_2 *is determined by volatilization with HF.* Cr_2O_3 *is determined titrimetrically with* $K_2Cr_2O_7$ *in two parts, one in* R_2O_3 *precipitate and the other in the filtrate of the phosphates of Mg, Mn, Ca and Ni. Total iron is determined titrimetrically with* $K_2Cr_2O_7$. TiO_2, MnO, V_2O_5 *are determined with a spectrophotometer and CaO with flame-photometer.* MgO, Al_2O_3, NiO *are determined gravimetrically and FeO by Seil's method.*

INTRODUCTION

The exact analysis of chrome ore is a matter of some difficulty (Furman, 1966). The writer has been confronted with this problem while investigating the geochemistry of chromites of West Pakistan. For this purpose a large number of chemical analyses of chromites from different localities were required. The author consulted various schemes of chemical analysis produced by Bilgrami and Ingamells (1960), Dinnin (1959), Furman (1966), Malhotra (1956) and Vogel (1964). The writer noticed certain difficulties inherent in these schemes and therefore developed an improved scheme of chromite analysis. Portions of a purified chromite sample were analysed separately by these schemes as well as by the scheme developed by the writer. The results obtained are given in Table No. 1.

DISCUSSION OF EARLIER SCHEMES

The possible sources of error in the schemes of the above mentioned workers are discussed below.

1. Separation and Estimation of Chromium:

(*a*) Bilgrami and Ingamells (op. cit. p. 588) recommend that Cr should be completely separated in the R_2O_3 precipitate after its reduction from hexavalent to trivalent form with H_2O_2. However, the writer has noted that in practice it is very difficult to achieve complete reduction by this method and this may result in an incomplete separation of Cr in R_2O_3.

(*b*) For the estimation of Cr, these workers recommend colorimetric or KI-thiosulphate method. While the colorimetric methods are generally suitable for substances present in quantities of less than 2 percent (Vogel, op. cit. p. 738) the KI-thiosulphate method is subject to a number of errors (Vogel, op. cit., p. 350), such as:—

(*i*) the reaction is not instantaneous.

(*ii*) there is a loss of iodine owing to its appreciable volatility.

(*iii*) the hydroiodic acid (produced by the reaction of excess iodide and H_2SO_4) is readily oxidized by air, especially in the presence of chromic salts.

(*iv*) The chromic salt produced in the reaction has a sky blue colour and the change to light green colour at the end point is rather difficult to judge.

(*c*) After decomposition of sample with Na_2O_2, Furman (op. cit. p. 362) recommends to dissolve the decomposed mass in H_2SO_4 and HNO_3. He boils the solution first with $AgNO_3$, $KMnO_4$ and $(NH_4)_2S_2O_8$, and afterwards with HCl. He recommends this

step in order to oxidize chromium and to discharge the violet colour produced by manganese. The scheme by Dinnin (op. cit , p. 45) is almost the same except that he uses $KMnO_4$ instead of $AgNO_3$ and $(NH_4)_2 S_2O_8$. The writer has noted that, by applying either of these schemes, $Cr_2 O_3$ upto 2% escapes estimation.

2. Separation of Iron and Titanium :

The methods given by Bilgrami and Ingamells (op. cit., p. 589) and by Furman (op. cit., p. 363) are quite satisfactory. However, the writer has noted that equally effective but more rapid separation can be achieved by using Na_2O_2 and therefore prefers this method of separation.

3. Estimation of Aluminium :

Bilgrami and Ingamells (op. cit., p. 589) estimate $Al_2 O_3$ simply by substracting the combined weight of oxides of Fe, Ti and Cr from the total weight of precipitate of $R_2 O_3$. According to Vogel (op. cit., p. 472) for converting $Al(OH)_3$ to Al_2O_3, the R_2O_3 precipitate is requiried to be ignited at a minimum temperature of 1200° C for atleast 10-15 minutes. At this raised temperature, the $Fe_2 O_3$ produced by the ignition of $Fe(OH)_3$ at a lower temperature, may get atleast partially changed to $Fe_3 O_4$ (Vogel op. cit., p. 470).

Malhotra (op. cit., p. 464) separates Al, Fe and Ti from Mg, Ca and Mn by adding $NH_4 OH$. This results into co-precipitation of Mg and Mn with Al, Fe and Ti (Vogel, op. cit., p. 472). He estimates $Al_2 O_3$ by substracting the combined weights of Fe, Ti from the weight of $R_2 O_3$ composed of only Fe, Ti oxides and Al oxide. This method has the same temperature-effect as that of Bilgrami and Ingamells (op. cit., p. 589).

4. Estimation of Calcium :

Bilgrami and Ingamells (op. cit. p. 589) and Furman (op. cit. p. 365) precipitate calcium as $CaSO_4$ in alcoholic medium before the estimation of Mn. After precipitation, they estimate Ca by volumetric or by gravimetric methods. Since the amount of Ca in chromites is very small, both volumetric and gravimetric methods are expected to give inaccurate results.

5. Estimation of Manganese :

Bilgrami and Ingamells (op. cit. pp. 587, 589) estimate Mn by two methods. In the first they determine Mn on a separate chromite sample after its decomposition with Na_2O_2. While in the second they determine Mn that is precipitated along with the phosphates of Mg, Mn, Ca and Ni. The writer noted that Mn determined by the second method was 0.21% less than the first method. This amount, actually got precipitated in $R_2 O_3$, escaped estimation in the second method and calculated as $Al_2 O_3$, which adds another error in the $Al_2 O_3$ estimation.

Similar is the case with the methods of Furman (op. cit. p. 365) and Malhotra (op. cit. p. 464) in which manganese estimated is less than the actual amount due to its partial precipitation in $R_2 O_3$ and in $(Fe_2 O_3 + Al_2 O_3 + TiO_2)$ respectively.

THE IMPROVED SCHEME

Keeping various sources of error and complications in view the writer has put forward the following scheme of chromite analysis, the accuracy of which has been checked on standard elements.

(1) H_2O

Water is determined by Penfield method.

(2) SiO_2

Take 0.5gm of sample (80-120 mesh), dried at 110°C in a 500 ml beaker. Add about 5 ml HNO_3 and 40 ml of $HCLO_4$ (60-70%). Place a stirring rod in the beaker, cover it with a watch glass and place it on a hot plate. Heat gently first, then strongly till the whole sample gets decomposed completely. Cool and dilute with water to about 200 ml. Filter through Whatman No. 41 filter paper. Wash filter paper thoroughly with distilled water about 10-12 times. Dry the filter paper and ignite it in a platinum crucible to a constant weight. Determine SiO_2 by volatilization with HF. Fuse the residue with 2-3 gms. of $Na_2 CO_3$ and wash the crucible thoroughly with water in the main solution.

(3) R_2O_3.

Add about 5 gms. of $NH_4 Cl$, heat to boil, cool and add filtered (1:1) $NH_4 (OH)$ to get a pH value between 6.5-7.5 Boil for one or two minutes and filter through Whatman No. 41 filter paper. Wash the precipitate with hot 2% $NH_4 NO_3$ 3-4 times. Dissolve the precipitate in dilute $H_2 SO_4$, repeat precipitation, filtration and washing as before. Dissolve the precipitate in water containing about 5 ml $H_2 SO_4$.

(4) Fe, TiO_2, MnO.

Add $Na_2 O_2$ to the above solution till precipitation of Fe, Ti and Mn starts, add 1-2 gms more and boil for 1-2 minutes to destroy peroxide completely. Filter the precipitate through Whatman

No. 41 filter paper. Wash the precipitate with 2% NaOH to a colourless filtrate. Dissolve the precipitate in water containing 5 ml H_2SO_4. Filter, wash thoroughly with water and reduce the volume to 100 ml.

(*i*) Fe (as total iron).

Take 25 ml. from the above solution, add 1-2 ml HCl and boil for 2-3 minutes. Add freshly prepared dilute $SnCl_2$ solution till a colourless solution is obtained and add 1-2 drops in excess. Cool rapidly under tap, dilute with water to about 100 ml and add saturated solution of $HgCl_2$ to neutralize excess of $SnCl_2$. A whitish precipitate of mercurous cholride must appear. (Discard the solution if it turns black, which is due to excess of $SnCl_2$). Add 5 ml of H_3PO_4 and 6-7 drops of 0.2% sodium diphenylamine sulphonate solution. Titrate against N/10 $K_2Cr_2O_7$ to a violet end point.

(*ii*) TiO_2

Add 5 ml H_3PO_4 and 3 ml of 3% H_2O_2 to 50 ml. of the above solution and determine TiO_2 spectrophotometrically at 410 mu. (Snell and Snell, op. cit.).

(*iii*) MnO

Add 5 ml H_3PO_4 to the remaining 25 ml of the above solution. Heat to boil and add 0.5 gms KIO_4. Boil for 1-2 minutes, allow to cool slowly and estimate MnO spectrophotometrically at 550 mu. (Snell and Snell, op. cit).

4. Al_2O_3

Acidify the filtrate from iron, titanium and manganese with H_2SO_4 and precipitate Al as $Al(OH)_3$ by filtered 1:1 $NH_4(OH)$ at pH 6.5-7.0. Boil for 1-2 minutes and allow to settle. Filter through Whatman No. 42 filter paper, and wash the precipitate with hot 2% NH_4NO_3 to a colourless filtrate. Dissolve the precipitate in H_2SO_4 and carry out precipitation, filtration and washing as before. Transfer the dried precipitate along with filter paper to a weighed platinum crucible and ignite first at a low heat and finally at about 1200°C for 10-15 minutes. Weigh and calculate percentage of Al_2O_3.

5. Cr_2O_3 precipitated in R_2O_3

Adjust the above filtrate to 250 ml. Take 10 ml of this, add NaOH till solution turns green due to the formation of Na_2CrO_4. Add dilute HCl till solution is acidic. Add known excess of approximately N/10 $FeSO_4(NH_4)_2SO_4.6H_2O$ (with an excess of ferrous salt the solution turns green.) Add 5 ml H_3PO_4, 7-8 drops of 0.2% solution of sodium diphenylamine sulphonate as an indicator and titrate against N/10 $K_2Cr_2O_7$ to a violet end point. Titrate the same amount of $FeSO_4(NH_4)_2SO_4.6H_2O$ under similar conditions of acidity as used in the estimation of Cr_2O_3. From this calculate the amount of Cr_2O_3 precipitated in R_2O_3.

6. V_2O_5

Precipitate vanadium from the remaining solution with cupferron as described by Schoeller and Powell (1955). Add filter pulp and filter through Whatman No. 41 filter paper. Wash precipitate with cold N.HCl containing a little cupferron. Burn off the paper and precipitate at low temperature and then at red heat. Fuse the residue with $KHSO_4$ or pyrosulphate, dissolve the fused mass in water and determine V_2O_5 with a spectrophotometer as peroxyvanadate at 450 mu. (Snell and Snell op. cit.)

7. MgO, MnO, CaO, NiO, Cr_2O_3

Add 5 gms of $(NH_4)_3PO_4$ to R_2O_3 filtrate. Heat to boil, cool to room temperature. Add filtered (1:1) $NH_4(OH)$ till precipitation starts. Add 15 ml more while stirring vigorously and allow to stand for about 12 hours. Filter through Whatman No. 40 filter paper, wash the precipitate with 2% $NH_4(OH)$ to a colourless filtrate. Repeat precipitation, filtration and washing after dissolving the precipitate in water containing H_2SO_4. Reserve the filtrat and washing for the estimation of Cr that escaped precipitation in R_2O_3. Ignite the precipitates of Mg, Mn, Ca, and Ni at 1000-1100°C and weigh as $Mg_2P_2O_7 + Mn_2P_2O_7 + Ca_3(PO_4)_2 + Ni_2P_2O_7$.

(*i*) MnO

Dissolve the above ignited precipitate of Mg, Mn, Ca and Ni in dilute HNO_3. Boil off HNO_3 and add 5 ml H_3PO_4. Heat to boil and add 0.5 gms of KIO_4. Boil for 1-2 minutes, cool slowly and estimate MnO spectrophotometrically at 550 mu. Add this to MnO already determined.

(*ii*) CaO

Add 10 ml H_2SO_4 to the above solution, evaporate to fumes of sulphur trioxide, cool and add 100 ml of 95% ethyl alcohol. Stir vigorously and allow to stand for about 12 hours. Filter the percipitate of $CaSO_4$ through Whatman No. 40 filter paper. Wash 10-15 times with 80% alcohol containing 2 ml H_2SO_4 per litre for complete removal of all phosphoric acid. Ignite the precipitate and dissolve in dilute HCl. Boil for 1-2 minutes and determine CaO by flame photometer.

(*iii*) NiO

Reduce the above filtrate from Ca precipitate to about 100 ml. Neutralize the solution with NaOH, add 5-10 ml acetic acid and 5 ml of 1% solution of dimethyl-glyoxime in alcohol. Filter the precipitate through weighed sintered glass crucible previously heated to 110-120°C. Wash the precipitate with cold water and dry at 110°-120°C for 40-45 minutes. Cool in a desiccator and weigh as Ni $(C_4H_7O_2N_2)_2$ which contains 20.32% of Ni.

Calculate Mn, Ca, Ni as $Mn_2P_2O_7$, $Ca_2(PO_4)_2$ $Ni_2P_2O_7$ respectively and deduct from the combined weight of their ignited precipitate to get $Mg_2P_2O_7$. Convert $Mg_2P_2O_7$ to MgO.

(*iv*) Cr_2O_3

Adjust the volume of filtrate from precipitate of Mg, Mn, Ca and Ni to 250 ml. Take 10 ml and determine Cr_2O_3 as before. Add this amount of Cr_2O_3 to that already determined.

(8) FeO

FeO has been determined by Seil's (1943) indirect method. The method has been slightly modified by Bilgrami and Ingamells (op. cit. p. 586.). Instead of KI-$Na_2S_2O_3$ titration, as recommended by Bilgrami and Ingamells, the author has preferred the use of ferrous ammonium sulphate-dichromate titration. The reasons for which are given in introduction. The apparatus is illustrated in Fig. 1.

Add about 10 ml H_2O in the reaction flask. Add 0.5 gm of chromite sample (80-120 mesh) dried at 110°-120°C in the reaction flask. Add 25 ml (4:1) mixture of $H_3PO_4+H_2SO_4$ previously boiled for about 30 minutes, to the reaction flask. Stir the flask well. Add 15 ml of $K_2Cr_2O_7$ in (*c*) and 5 ml in (d). Dilute with water. Place hot plate below the reaction flask. Pass CO_2 at the rate of 1-2 bubbles per second as observed in (a). Maintain hot plate at a temperature of 220°C. At first reaction will be very slow until all the water has been evaporated from acid mixture. Then the ore will dissolve fairly rapidly. Increase flow of CO_2 when reaction starts. Continue heating for 10 minutes after the bubbles cease to form in the reaction flask. Cool the flask and increase rate of flow of gas in order to avoid sucking back of the liquids from the absorption flasks (c, d). Disconnect the absorption flasks and collect the solution in a titration flask. Determine the change in normality caused by the reduction of $K_2Cr_2O_7$ by SO_2 and Ph_3 evolved from reaction flask and calculate amount of FeO present in the sample.

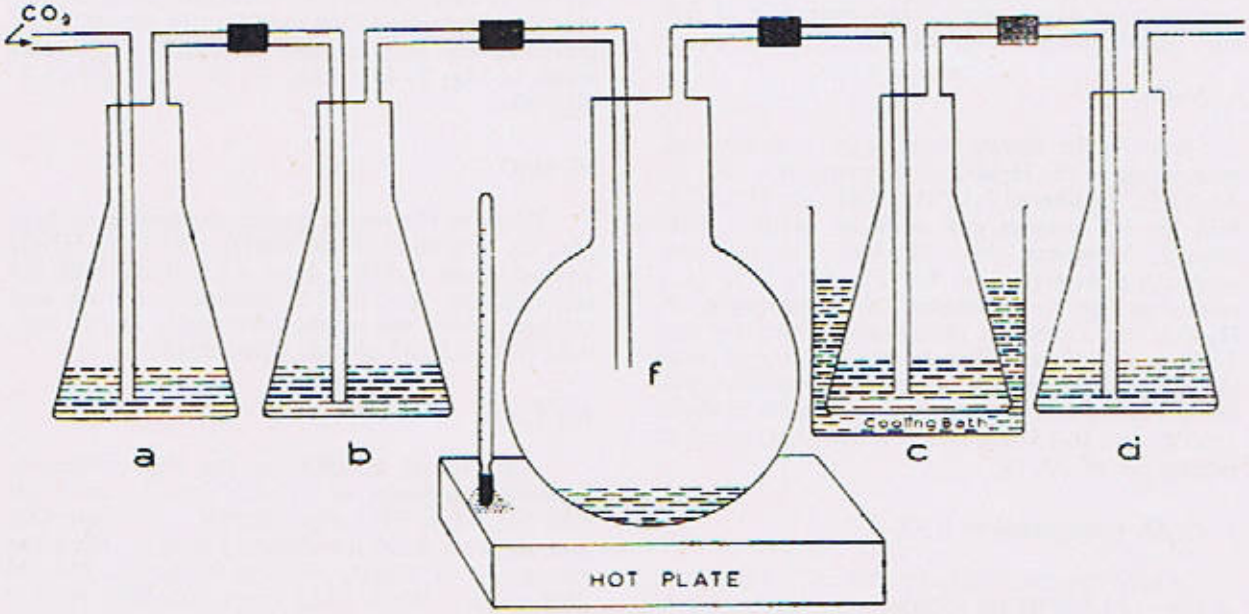

Fig. 1. (f) 250 ml round bottom flask (a) bubbler containing 6 % NaHCO3 to which has been added an equivalent amount of ferrous ammonium sulphate to remove O_2 and H_2S from the CO_2. (b) washing bubbler containing water. (c,d) bubblers containing N/10 $K_2Cr_2O_7$ in 5 % H_2SO_4.

ACKNOWLEDGEMENT

The writer thanks Prof. F. A. Shams, Geology Department, Punjab University, Lahore for his constant encouragement, helpful advice and for critically reading the manuscript.

TABLE No. 1

Elements as oxides		Weight percentage by different methods						Cations on basis of 32(O)	
		Shafeeq	Bilgrami, et al.	Vogel	Dinnin (*a*)	Furman	Malhotra	Shafeeq	Malhotra
(1)	Cr_2O_3	56.99	49.38	56.95	55.12	55.69	55.58	11.9864	11.5530
(2)	Al_2O_3	10.32	12.33	—	—	10.58	13.00	3.2364	4.0290
(3)	Fe_2O_3	3.78	3.91	—	—	—	4.61	0.7547	0.9100
(4)	TiO_2	0.38	0.37	—	—	0.38	0.36	15.9775	16.4920
(5)	V_2O_5	Nil	Nil	—	—	—(*b*)	—	—	—
(6)	FeO	17.06	16.82	—	—	18.98	16.23	3.7209	3.4965
(7)	MgO	11.00	11.40	—	—	10.96	9.92 (*c*)	4.2534	3.7635
(8)	CaO	0.06	0.15 (*d*)	—	—	0.12	0.06	0.0159	0.0158
(9)	MnO	0.26	0.26 (*e*)	—	—	—	traces	0.0575	—
			0.05		—	—	—	8.0477	7.2758
(10)	NiO	Nil	Nil	—	—	—	—	—	—
(11)	SiO_2	0.21	0.22	—	—	—	0.24	—	—
(12)	H_2O	0.01	0.01	—	—	—	—	—	—
		100.07	94.85				100.00	24.0252	23.7678

(*a*) Due to non-availability of certain reagents complete analysis by the scheme of Dinnin could not be carried out.

(*b*) Total iron determined as FeO

(*c*) CaO determined by flame—photometer.

(*d*) MnO by first method

(*e*) ,, second ,,

REFERENCES

Vogel, A. I. 1964, QUANTITATIVE INORGANIC ANALYSIS. Longmans, Green and Co. Ltd. London.

Bilgrami, S. A., and Ingamells C. O. 1960 Chemical composition of Zhob valley chromites, West Pakistan. *Amer. Mineral.* **45**, pp. 576-590.

Dinnin, J. I. 1959, Rapid analysis of chromite and chrome ore *U. S. Geol. Survey, Bull.* 1084-B, pp. 31—68.

Furman, N. H. 1966, STANDARD METHODS OF CHEMICAL ANALYSIS. 350—371. D. Van Nostrand Company, Inc. Princeton, New Jersey.

Hamilton, L.F. and Simpson, S. G. 1964. QUANTITATIVE CHEMICAL ANALYSIS,244—247. Macmillan Company, New York.

Malhotra, P. D. and Prasada Rao, G. H. S. V. 1956, On the composition of some Indian Chromites: *Amer. Mineral*, **41**, 464.

Schoeller, W. R. and Powell, A. R. 1955. ANALYSIS OF MINERALS AND ORES OF THE RARE ELEMENTS. Charles Greffin and Company Ltd. London.

Seil, Gilbert 1943, Determination of ferrous iron in difficulty soluble materials : *Indus. and Chem. Anal.* Ed. V, **15**, 189.

Snell, F. D. and Snell, C.T. 1959, 1961 COLORIMETRIC METHODS OF ANALYSIS Vol. IIA, II. D. Van Nostrand Company Inc. Princeton, New Jersey.

LITHOLOGICAL DATA FOR DIVISIONS OF MIOCENE ROCKS FROM BARA INANI KHAL SECTION IN CHITTAGONG HILL TRACTS, EAST PAKISTAN

BY

Y. A. MIKHAILOV, ABDUS SAMAD AND SAYED AZHAR ALI
Oil and Gas Development Corporation, Karachi

Abstract : *The lithological investigations of rocks of Miocene age from Bara Inani Khal section of Chittagong Hill Tracts formed part of a detailed project which was undertaken with a view to find uniform basis or litho-stratigraphic divisions and correlation of these deposits.*

The data, obtained from field and petrological investigations make it possible to define, on the basis of stability of sedimentation and rate of accumulation of sediments, three distinct members, namely, Clay-Silt, Silt-Sand and Clay. The Silt-Sand member can be correlated with the Tipam Sandstone. The other two members are partially exposed in this section and their correlation is not distinct.

INTRODUCTION

This paper deals with the results of field and petrological investigations of rock samples collected from Bara Inani Khal section in the Chittagong Hill Tracts, East Pakistan. These investigations formed part of a detailed project which also included field and laboratory investigtions of Jaldi, Bandar Ban and Sitakund structures. The work was undertaken with a view to find uniform basis for lithostratigraphic division and correlation of Miocene deposits.

The importance of the project lies in the fact that sofar four wells have been drilled by Oil & Gas Development Corporation and still the division and correlation are based on individual interpretation.

The investigations carried out consist of grain size, heavy mineral and spectrographic analyses for determination of trace elements ; for the purpose of correlation spectrographic analyses can be used in a similar way as the heavy mineral analyses. As the data has been obtained from one section only the estimation of correlative value of different lithological divisions, discussed in the present paper is tentative. We hope that similar investigations on material from other areas will result in establishing firm basis for the subdivision and correlation of Miocene deposits of East Pakistan.

The results of the study of granulometric composition of the rocks are given in Table 1* and plotted in a triangular composition diagram (Fig. 1). The composition diagram was drawn after the method adopted by Krysanov and Sementovsky (1955). In this triangular diagram, values of granulometric composition were computed; the closely ranging values falling in the same field were grouped, thus forming 5 fields. Each of the field defined different types of rocks according to their granulometric composition. An effort has been made to classify the rock types thus obtained, according to preponderance of a size fraction, clastic component-cement-matrix ratio and the degree of sorting. The ratio of clastic component and cement-matrix was determined considering the carbonate content as part of the cement ; the results are shown in Table 2.* Five types of rocks have been defined according to degree of sorting (Table 3).

TABLE 3

Showing classification of rock types on the basis of degree of sorting

Rock type No.	Predominant Fraction in Percent	Degree of Sorting
I	Above 70 (or 65)	Well
II	From 70 (65) to 55 (50)	Medium
III	From 55 (50) to 45 (40)	Poor
IV	Less than 45 (40)	Unsorted
V	Predominent fraction not defined	

*These tables are given at the end.

The rock types thus defined are described below:

1. Rock Type-1-SILTY CLAY :—It is represented by sample No. 1 and is composed of 75% of pelite fraction, 17.8% of silt and 7.2% of sand fraction. Total content of cement-matrix comprises 77.8% including carbonate content of 11.2%. Clastic part comprises 22.2% of the whole rock, which is well sorted.

2. Rock Type II—SAND SILT:—It is characterised by 9 samples and is composed of silt fraction (53.8 to 91.5%;) sand fraction (4.6 to 40.5%) and a small quantity (2.7—8.9%) of pelitic fraction. This type of rock is characterised by predominance of clastic material, content of which is never below 85.6% and sometimes reaches 93%. The content of cement varies, accordingly, from 7.0 to 14.4% while the carbonate ranges from 4.4 to 7.0%. The rock is mostly well sorted but occasionally sorting is of medium grade.

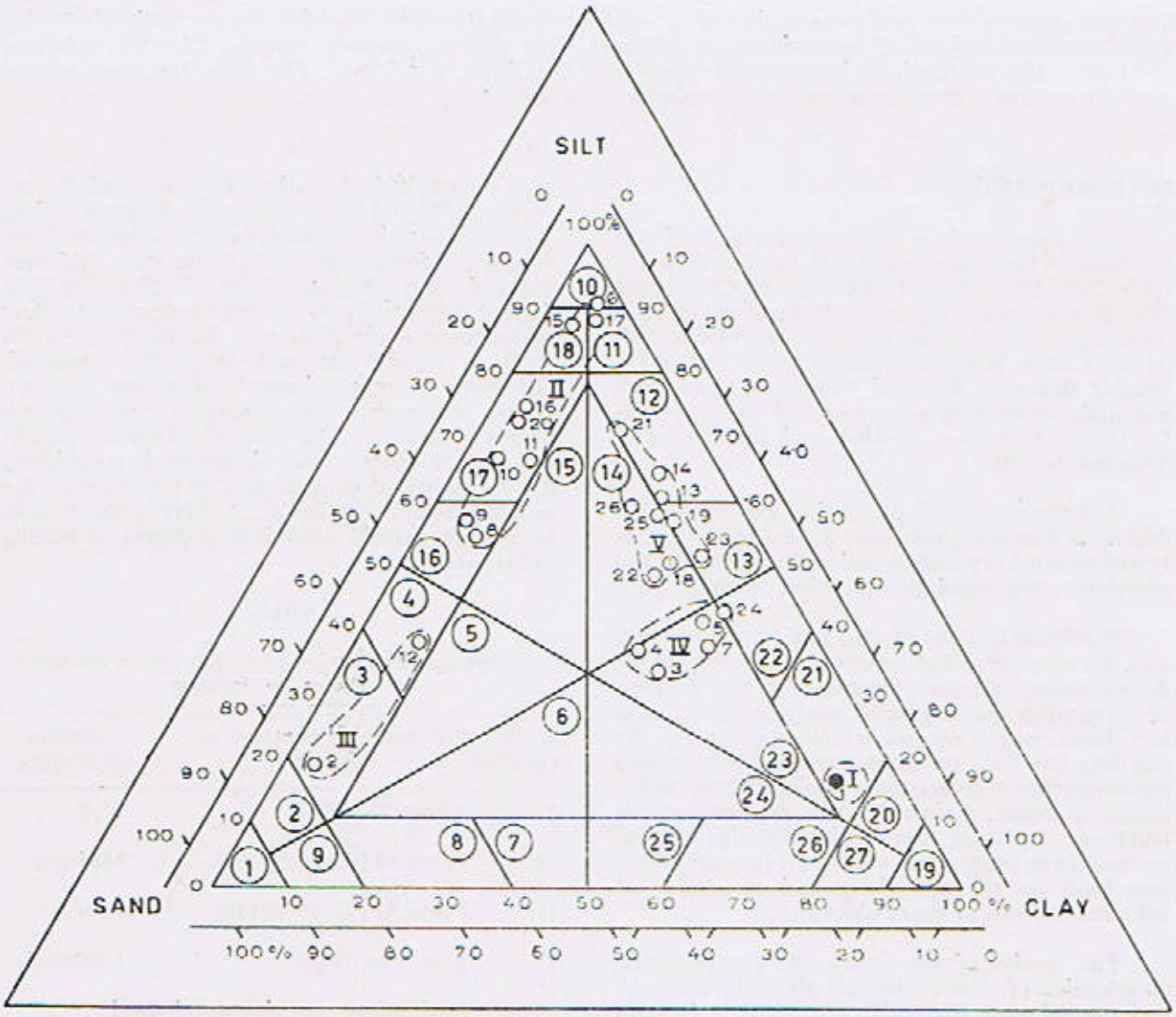

Fig. 1 Granulometric composition : Miocene rocks from Bara Inani Khal Section.
According to N.V. Kyrsanow and Y.V. Sementovsky (1955)

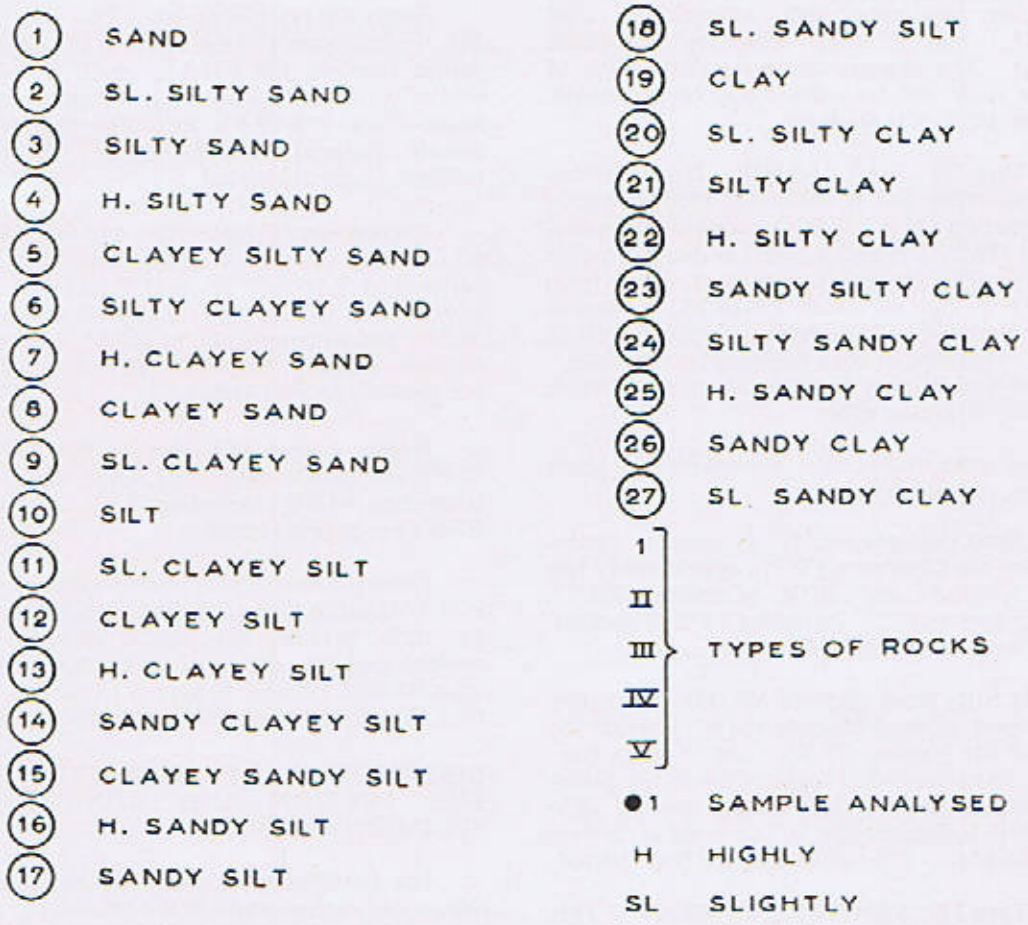

Explanation of Fig. 1

The varieties of this class, alongwith their short descriptions, are given below :—

Silt (Sample No. 6)—It is represented almost entirely by silt fraction (91.5%) and contains very little sand (4.6%) and pelitic fraction (3.9%). The cement-matrix contains 4.4% carbonate. The rock is very well sorted.

Slightly Sandy Silt (Samples No. 15, 17)—It also contains high percentage (83-88%) of silt, slightly higher than in the foregoing variety. Sand fraction is 7.9—12% and pelite fraction is 3.6-4.4% Cement-matrix comprises 9.2-10.4%, including 5.0-7.0% carbonate content. The rock is well sorted.

Sandy Silt (Samples No. 10, 11, 16, 20) is composed of predominantly silt fraction (65.9-74.8%) with a noticeably higher content of sand fraction (22.7-31.4%). The content of pelite is very low (2.3-3.3%) and in only one sample (No. 11) it

increases upto 8.9%. Cement-matrix comprises 7.0-14.4% out of which 4.4-6.6% is carbonate. The rock is well sorted.

Highly Sandy Silt (Samples No. 8, 9). Silt constitutes more than half of this rock (53.8-57.1%) and contains relatively high amount of sand (38.5-40.5%) and a small quantity of pelite (4.3-5.6%). The cement comprises 9.6-11.0% of the whole rock and includes 5.6% of carbonate. The sorting of rock is medium.

3. Rock Type III—SILTY SAND:—It is represented by 2 samples and is composed predominantly of sand fraction (54.9—78.0%), subordinate quantity of silt (19.5-38.7) and a small amount of pelite (2.4-6.3%). The content of cement varies from 4.2 to 19.6%, out of which 1.8-14.2% comprises carbonate material. The sorting of rock is well to medium. This type of rock includes two varieties : Silty Sand and Highly Silty Sand, one differing substantially from the other.

The varieties of this class, alongwith their short desaiptions, are given below :—

Silty Sand (Sample No. 2) It consists predominantly of sand fraction (78%), considerably less silt (19.5%) and very little of pelite (2.4%). Cement comprises 4.2%, including 1.8% of carbonate. The rock is well sorted.

Highly Silty Sand (Sample No. 12). It is only half composed of sand fraction (54.9%), while the contents of silt fraction (38.7%) and of pelite fraction (6.3%) are somewhat higher than in the preceding variety. Quantity of cement ranges upto 19.6%, which is due, mainly, to increased carbonate content (14.2%). The rocks are medium sorted.

4. Rock Type IV—SANDY SILTY CLAY:—This group is represented by 5 samples. It is composed of more or less equal quantities of pelitie (37.2-49.2%) and silt (32.2-43.5%) fractions. The sand fraction is also comparatively high (10.1-25.9%). Cement constitutes half of rock's contents (49.2-50.2%), in which the carbonate content varies from 1.6-10.6% The rock is practically unsorted. Almost all samples (3, 4, 5, 7) are of very similarg ranulometric composition and only sample No. 24 is bordering between Sandy Silty Clay and Highly Silty Clay, due to the increased content of silt fraction (43.5%).

5. Rock Type V—CLAYEY SILT :—It is characterised by 9 samples. Typically, its content of silt fraction varies from 49.2 to 74.2%, while the pelitic fraction comes second in order and its content varies from 16.0 to 38.6%; content of sand fraction is much lower (9.2-17.3%). The cement comprises, on the whole, 33-39%, out of which 8-9% consists of carbonates. The rocks are medium to poorly sorted except for the sample No. 21 which is well sorted. This type of rock consists of the following varieties : Sandy Clayey Silt, Clayey Silt, Highly Clayey Silt.

Sandy Clayey Silt (Sample Nos. 18, 19, 22, 25, 26) consists mainly of silt fraction (49.2-60.2%) and pelitic fraction (26.1-35.1%) with a subordinate quantity of sand (7.5-9.8%). Content of cement varies from 32.8-39.6% including that of the carbonate material from 6.0-9.0%. The rocks are medium to poorly sorted.

Clayey Silt (Sample Nos. 13, 14, 21) contains 60.7-74.2%, of silt fraction with 16.0-30.1% of pelite and 7.5-9.8% of sand fractions. Quantity of cement in sample Nos. 13 and 14 comprises 35.2-36.8%, and in sample No. 21 -22.4% with carbonate content ranging between 7.2-11.2%. The rocks are medium to well sorted.

Highly Clayey Silt (Sample No. 23) contains 52.0% silt, 38.6% pelite and 9.4% sand. Cement comprises 44.0% including 8.8% of carbonate. Rocks are poorly sorted.

From the description of rock types given above, it is noticeable that according to the main indices-*i.e.* ratio between the clastic material and the cement, and the sorting of rocks, type II is close to type III and type IV to type V; type I is a unique rock that does not resemble any other rock type.

DISTRIBUTION OF ROCK TYPES ALONG THE SECTION AND CONDITIONS OF SEDIMENTATION

The distribution of rock types along the section shows that various parts of the section are represented either by rock of one type only, or by an association of rocks of different types. The structural features and thickness of different parts of the section are shown along with a correlation chart. (Fig. 2). Study of rocks from various parts of section has shown that the conditions of sedimentation during their formation did not remain constant. The two main indicators of sedimentation conditions *i.e.* stability of the sedimentation and the rate of sediment accumulation, were determined.

Stability of sedimentation was determined from the nature of rock alternation, while the rate of sedimentation was determined from sorting of the rocks.

From distribution of rock type upwards from base of the section, the following lithological beds were defined : Clay—Silt, Silt, Clayey Silt, Sand,

42/95

GROUP	FORMATION	MEMBER	BED	THICKNESS (M)	COLUMN	LOCALITY AND SAMPLE Nos.	LITHOLOGICAL DESCRIPTION
TIPAM	GIRUJAN CLAY	CLAY	CLAY	100		1	Silty Clay
	TIPAM SANDSTONE	SILT - SAND	SILT-CLAY	135		2	Silty Sandstone
			SAND	160		3	Sandy Silty Clay
						5	
						6	Alternation of Sandy Silty Clays and Sandy Silts, with Fossils Fragments at the top
						7	
						8	
						9	
						10	
						11	Silty Sandstone with Beds of Sandy Silt & Fossil Fragments at the Base
						12	
			CLAYEY SILT	45		13	
						14	Clayey Siltstone
						15	
			SILT	90		16	Sandy Silt with Sparse Bed of Clayey Siltstone
						17	
SURMA	BOKA BIL	CLAY - SILT	CLAY - SILT	310		20	
						18	Alternation: Sandy Clayey Silt and Sandy Silty Clay
						19	
						21	
						22	With Subordinate Beds of Sandy Siltstone
						23	
						24	
						25	
						26	

GRANULOMETRIC COMPOSITION — SAND, SILT, CLAY — 0 50 100

CARBONATE CONTENT % — 0% 10 20%

HEAVY MINERALS

TERRIGNIC: Zircon, Rutile, Tourmaline, Andalusite Kyanite, Hornblende, Actinolite Tremolite, Staurolite, Garnet, Enstatite, Diopside, Epidote, Biotite, Muscovite, Chlorite, Chloritoid, Ilmenite, Magnetite, Leucoxene

AUTHIGENIC: Limonite, Glauconite, Pyrite

Fig. 2. Lithological Characteristics of Rocks From Bara Inani Khal Section

Silt-Clay and Clay. These are described below :—

(*i*) **Clay-Silt Bed**—This partly exposed bed is approximately 310 m. thick and is represented mainly by an alternation of Sandy Clayey Silt (rock-type V) and Sandy Silty Clay (rock-type IV) with subordinate layers of Sandy Silt (rock-type II). The alternation indicates the unstable conditions of sedimentation. On the other hand it should be noted, that rock-types V and IV are very close to each other as regards the granulometric composition as well as the degree of sedimentation. The poor sorting of the rocks shows that the rate of sedimentation was high. At the top of the bed sparse layers of rock-type II are present which show substantially different granulometric composition and degree of sorting. These layers may probably be taken to be the first indication of the subsequent changes in sedimentation conditions.

(*ii*) **Silt Bed**—This bed with a thickness of 90 m. is composed of Sandy Silt (rock type-II) with intercalations of Clayey Silt (rock type V). As compared with the underlying bed, the rocks are better sorted, due to relative retardation of sedimentation rate, and contain a considerably greater quantity of clastic material. Moreover, the Silt bed does not show any alternation of rocks which is a characteristic of the Clay-Silt bed. It is represented by a single type of rock, which indicates stability of sedimentation conditions, while the sparse layers of type V rocks indicate periodic returns to previous conditions that existed during formation of the underlaying bed.

(*iii*) **Clayey Silt Bed**—This bed has a thickness of 45 m. and is represented by Clayey Silt, the rock type V. The same type of rocks compose the Clayey Silt Bed, occurring at the base of the section. These beds are distinct by their uniform composition, and absence of interlayers due to retardation of the sedimentation rate. Thus, although sedimentation conditions of Clayey Silt bed are similar to those of Clay-Silt bed, the difference between them indicates the irreversible development of the sedimentation basin.

(*iv*) **Sand Bed**—This bed has a thickness of 160 m. and is composed of Highly Silty Sand, the rock-type III, with layers of Sandy Silt, the rock type II. As regards its granulometric composition and sorting, this bed is comparable with the Silt Bed. Sedimentation conditions of both these beds were apparently similar. The main distinction is that the Sand Bed contains a layer with remains of marine fauna at the base of the bed. This indicates, firstly, that the sedimentation occurred under conditions of marine environments and secondly, that the rate of sedimentation was retarded. The remains of fauna represent fragments of thick-walled shells (pelecypod ?), characteristic of the coastal conditions of sedimentation.

(*v*) **Silt-Clay Bed**—This bed has a thickness of 135 m. and is represented by Sandy Silty Clay, the rock-type IV, alternating with Sandy Silt, the rock-type II. The alternation of different types of rocks with various degrees of sorting indicates that the conditions of sedimentation were unstable as compared to those of the preceding bed although they resemble to a certain extent those of the above described Clay-Silt bed, occurring at the base of the section. However, the main difference in this bed is the alternation of layers of Sandy Silty Clay and sandy silt and the presence, at the top of the bed, of a layer with remains of marine fauna. The remains are similar to those of the Sand Bed. It is evident from the predominance of sorted rocks in the bed, that the sedimentation rate was retarded.

(*vi*) **Clay Bed**—This partly exposed bed has a thickness of approximately 100 m. and is composed predominantly of Sandy Silty Clay, the rock-type IV, with layers composed of Silty Sand, the rock-type III, and Silty Clay the rock-type I at the top of the bed. It is possible, that the top of this bed belongs to the overlying bed. However, as the section is not fully exposed at the top, it is difficult to define, reliably, the boundaries of the overlying bed. Almost throughout its thickness, the Clay Bed is composed, of practically unsorted rocks, which indicate an extremely high rate of sedimentation peculiar to deltaic deposits. The sorting of rock, however, improves towards top of the bed.

From the above description of various beds it is evident, that each bed corresponds to a certain stage in the development of the sedimentation basin with characteristic sedimentation conditions.

Development stage, such as defined by the bed in the section, is considered to be of IInd order, lower type. In the same way it is possible to consider every layer inside each bed, represented by an alternation of various types of rocks, as a sedimentation stage of a still lower type (order III). However, a sufficiently detailed description of the section is not available for such infinitesimal division of beds. Therefore, the bed, corresponding to development stage of the order II, is taken as a subdivision of the section.

The larger subdivisions of section-members are separated on the basis of the nearest conditions of sedimentation as regards the rate of deposition and the stability of its process. As a rule, the member corresponding to order I (higher type) of the basin's development stage, represents several development stages of the order II.

TABLE NO. 4

Development stages of the order II				Development stages of the order I				
No.	BEDS	Sedimentation Conditions		No.	MEMBERS	Sedimentation conditions		FORMATIONS
		Rate of Deposition	Stability—			Rate of Deposition	Stability	
1.	CLAY-SILT	High	Unstable	1	CLAY-SILT	High	Unstable	BOKA BIL
2.	SILT	Low	Stable					
3.	CLAYEY SILT	Retarded	Stable	2	SILT-SAND	Predominantly Low	Predominantly Stable	TIPAM SANDSTONE
4.	SAND	Low	Stable					
5.	SILT CLAY	Retarded	Unstable	3	CLAY	Very High	Unstable	GIRUJAN CLAY
6.	CLAY	Very high	Unstable					

When this subdivision is compared with the existing lithostratigraphic subdivision for East Pakistan, it is noticable that the various members correspond to various formations approximately. Thus, the Silt-Sand member in the investigation section however is not fully exposed.

As a result, it seems possible to tie-in the lithostratigraphic formations of the section with subdivisions on the basis of natural development stages of the sedimentation basin. The advantages of the latter method lie in the possibility to subdivide the sections not only on the basis of changes in rock composition, but also by other indications relating to nature of alternation and the degree of sorting. On the basis of latter two indications it is possible to compare rocks of various compositions. Relationship between the beds (development stage of IInd order), members (development stage of Ist order) and lithostratigraphic formations is shown in Table 4.

HEAVY MINERALS AND THEIR DISTRIBUTION IN THE SECTION

Distribution of heavy minerals (sp. gr. over 2.7) along the section is shown in Fig. 2. Heavy minerals are divided into two genetic types : terrigenic and authigenic minerals.

(*a*) Terrigenic minerals.

The investigated section is characterised by the following complex of heavy minerals : zircon, rutile, tourmaline, minerals of group andalusite-kyanite, hornblende, minerals of group actinolite-tremolite, staurolite, garnet, enstatite, diopside, epidote, biotite, muscovite, chlorite, chloritoid ilmenite and leucoxene.

Among the widespread minerals the most common are of the mica group: biotite, muscovite and chlorite. Equally widespread and somewhat less abundant are the ore minerals : ilmenite, magnetite and leucoxene ; the last mineral is the product of ilmenite's alteration. Diopside is distributed uniformly along the section in quantities comparable to those of the mica and ore minerals. Epidote and enstatite are also uniformly distributed, but in lesser quantities. A number of minerals, such as zircon, tourmaline and staurolite, were encountered in rocks of all the defined lithological beds, although they are not uniformly distributed.

In the group of minerals, characterising particular parts of the section, the most interesting is the distribution of hornblende. This mineral is characteristic for the rocks of the Silt-Sand member, where it is contained in considerable quantities and is of stable distribution.

Comparable quantities of hornblende are contained in the rocks of the overlying Clay member as well. In the underlying Clay-Silt member, this mineral is encountered only at the top of the section, where there is an alternation of rocks, and is characteristic for both the Clay-Silt and the Silt-Sand members.

Similar conformity of distribution is characteristic also for minerals garnet and chloritoid, and minerals of group andalusite-kyanite. However, these minerals were encountered also in smaller quantities in rocks of Clay-Silt member also at the base of the section.

Minerals of group actinolite-tremolite are of restricted distribution and are confined only to Silt-Sand member.

(*b*) **Authigenic minerals.**

Authigenic minerals contained in the investigated rock-samples are pyrite, limonite and glauconite. Pyrite is present in rocks of Silt-Sand member, in rocks of transition type at the top of Clay-Silt member and in a single rock sample of the Clay member. It is interesting to note, that the maximum quantity of pyrite is encountered in rocks at the base of layer containing the remains of marine fauna. Glauconite was found in lesser quantities in deposits of Silt-Sand member and only in one sample among the rocks of Clay bed. This mineral was not encountered in rocks of Clay-Silt bed and in the one rock sample of Clay bed.

The studied authigenic minerals are the indicators of geochemical conditions of rock formation. Limonite indicates oxidising conditions, while the presence of pyrite and glauconite show predominance of reducing conditions of formation. Distribution of these mineral indicators is an evidence of the presence of oxidising conditions during the formation of rocks of the Clay-Silt bed; at the top of this bed there is a transition zone that represents alternation of oxidising and reducing facies. The Silt-Sand bed was formed in stable reducing conditions. In the overlying Clay Bed alternation of oxidising and reducing conditions is again observed.

Thus, in the investigated section, there are two clearly defined complexes of minerals, each of which is characteristic for a particular part of the section. At the base of the section, within the range of Clay-Silt bed (Boka Bil Formation), following heavy minerals are present :

Biotite	Tourmaline
Muscovite	Enstatite
Chlorite	Epidote
Ilmenite	Staurolite
Magnetite	Zircon
Leucoxene	Limonite
Diopside	

At the top of the section, represented by the Silt-Sand bed and partially by Clay bed (Tipam Formation), the mineral complex is distinct from the one given and includes the following minerals :

Biotite	*Andalusite-Kyanite*
Muscovite	Actinolite-Tremolite
Chlorite	Diopside
Ilmenite	Enstatite
Magnetite	Zircon
Leucoxene	Tourmaline
Hornblende	Staurolite
Garnet	Epidote
Rutile	*Pyrite*
Chloritoid	*Glauconite*

The minerals in italics are either not encountered in the basal part of the section or are present in negligible quantities.

The investigated heavy mineral assemblages include minerals that belong to different stability groups as regards their capacity to withstand intrastratal solution effects of appreciable quantities and weathering. It may be inferred from the presence in the rocks of medium and low stability minerals such as mica, amphibole and pyroxene, that the sedimentation rate during the formation of Boka Bil and Tipam deposits was rather high.

The nature of these minerals indicates that most probably they were derived from metamorphic rocks.

TRACE ELEMENTS IN THE ROCKS

To determine the nature of trace elements and their distribution in the section, the rocks were subjected to spectrographic analysis ; the results are given in Table 5.* It can be seen from the table that, on the basis of ratio of certain elements, the section can be divided into parts—upper part, corresponding to the Tipam Sandstone and the lower part corresponding to the Boka Bil deposits. The difference between the contents of certain elements in these two parts of the section is shown in Table 6.

The nature of the elements is such that they are thought to belong to the heavy mineral fraction of rocks. It is obvious that, for subsequent investigations of rocks from other sections it would be expedient to use spectrographic analyses separately for the heavy mineral fraction as this may provide additional data for the division of sections.

Besides difference in the quantitative ratio of elements, the qualitative variation is also a characteristic of different parts of the section.

*This table is given at the end.

TABLE 6

Elements	Tipam	Boka Bil Formation
Mn	0.006-0.01	0.01-0.03
Ni	0.001-0.06	0.006-0.01
Ti	0. 1	0.003-0.006
V	0.01	0.01-0.03
Cu	0.003-0.006	0.006-0.01
Zn	0.006	0.01
Pb	0.003	0.006

This is shown by the constant presence, in Tipam Sandstone, of the element yttrium while in Boka Bil Formation this element is not present at all.

The subdivisions of section defined from the results of spectrographic analysis coincide with those defined on the basis of data from petrographic and mineralogical investigations, described elsewhere.

ACKNOWLEDGEMENT

The authors owe their thanks to Dr. M. H. Khan, Head of Geological and Analytical Laboratories, O.G.D.C., for his kind help and advice during preparation of this paper.

REFERENCES

Dana, E.S. and Ford, W. E. 1932. A Textbook of Mineralogy. John Willy and Sons, Inc., New York.

Kerr, P. F. 1959. Optical Mineralogy. McGraw-Hill Book Company, Inc., New York.

Krishanan, M. S. 1960. Geology of India and Burma. 4th Ed. Higgmbothamas Ltd., Madras.

Krumbein, W. C. and Garrels R. M. 1952 Origin and classification of the chemical sediments in terms of PH and Eh. *Journ. Geol.* **60**, 26.

Krumbein, W. C. and Pettijohn, F. J. 1938. Manual of Sedimentary Petrography. Appleton—Century-Crafts Inc., New York.

Krysanov. N. V. and Sementovsky, Y. A. 1955. Classification of terrigenic rocks, *Academy of Science, U.S.S.R.*, **5**.

Pettijohn, F. H. 1956. Sedimentary Rocks.. *2nd Ed.* Harper and Brothers, New York.

TABLE 1

GRANULOMETRIC COMPOSITION OF ROCKS FROM BARA INNANI KHAL SECTION

S. No.	Sample No.	Type of Rocks	Carbonate Content	Name of Rocks	Fractions Contents					
					Pl (—0.01 mm)		Al (0.01—0.1)		Ps (0.1—1.0 mm)	
					Gm	%	Gm	%	Gm	%
1.	IN-- 1	I	5.6	Silty Clay	33.283	75.0	7.899	17.8	3.196	7.02
2.	6	II	2.2	Silt	1.831	3.82	43.826	91.53	2.226	4.65
3.	8	..	2.8	Highly Sandy Silt	2.665	5.65	25.398	53.83	19.120	40.52
4.	9	..	2.7	..	2.044	4.32	27.031	57.13	18.238	38.55
5.	10	..	2.3	Sandy Silt	1.279	2.68	31.483	65.92	14.982	31.40
6.	11	..	3.0	..	4.176	8.88	30.985	65.92	11.846	25.20
7.	15	..	2.5	Slightly Sandy Silt	2.069	4.36	39.611	83.35	5.842	12.29
8.	16	..	2.8	Sandy Silt	1.112	2.35	35.333	74.83	10.775	22.82
9.	17	..	3.5	Slightly Sandy Silt	1.698	3.65	41.137	88.48	3.659	7.87
10.	20	..	3.3	Sandy Silt	1.543	3.29	34.603	73.82	10.637	22.73
11.	2	III	0.9	Silty Sand	1.191	2.43	9.586	19.52	38.319	78.05
12.	12	..	7.1	Highly Silty Sand	2.724	6.35	16.596	38.71	23.555	54.94
13.	3	IV	5.3	Sandy Silty Clay	19.435	43.48	14.382	32.19	10.875	24.33
14.	4	..	3.7	..	17.237	37.23	17.069	36.91	11.973	25.86
15.	5	..	3.4	..	21.138	45.36	18.820	40.37	6.650	14.27
16.	7	..	0.8	..	24.246	49.19	18.155	36.84	6.880	13.97
17.	24	..	3.6	..	21.513	46.37	20.199	43.53	4.688	10.11
18.	13	V	3.6	Clayey Silt	13.982	30.10	28.210	60.72	4.264	9.18
19.	14	..	5.6	..	12.815	28.85	28.239	63.57	3.362	7.58
20.	18	..	3.0	Sandy Clayey Silt	16.493	35.15	24.561	52.33	5.878	12.53
21.	19	..	4.5	..	14.908	32.78	26.394	58.03	4.177	9.19
22.	21	..	3.8	Clayey Silt	7.376	15.96	34.297	74.22	4.529	9.82
23.	22	..	4.6	Sandy Clayey Silt	15.212	33.47	22.256	49.19	7.882	17.34
24.	23	..	4.4	Highly Clayey Silt	17.593	38.57	23.720	52.06	4.297	9.42
25.	25	..	4.3	Sandy Clayey Silt	13.985	34.57	26.948	58.91	4.811	10.52
26.	26	..	4.5	..	11.868	26.1	27.364	60.18	6.236	13.72

TABLE 1

CLASSIC COMPONENT—CEMENT MATRIX RELATIONSHIP OF ROCKS FROM BARA INANI KHAL SECTION

Samples No.	Type of Rocks	Name of Rocks	Clastic Component					Cement Matrix				
			Al		Ps		Total	Carbonate		Pl		Total
			Gm	%	Gm	%	%	Gm	%	Gm	%	%
IN— 1	I	Silty Clay	7.9	15.8	3.2	6.4	22.2	5.6	11.2	33.3	66.6	77.8
6	II	Silt	43.8	87.6	2.2	4.4	92.0	2.5	4.4	1.8	3.6	8.0
15	,,	Slightly Sandy Silt	39.6	79.2	5.8	11.6	90.6	2.5	5.0	2.1	4.2	9.2
17	,,	—do—	41.1	82.2	3.7	7.4	89.6	3.5	7.0	1.7	3.4	10.4
10	,,	Sandy Silt	31.5	63.0	15.0	30.0	93.0	2.2	4.4	1.3	2.6	7.0
11	,,	,,	31.0	62.0	11.8	23.6	85.6	3.0	6.0	4.2	8.4	14.4
16	,,	,,	35.3	70.6	10.8	21.6	92.2	2.8	5.6	1.1	2.2	7.8
20	,,	,,	34.6	69.2	10.6	21.2	90.4	3.3	6.6	1.5	3.0	9.6
8	,,	Highly Sandy Silt	25.4	50.8	19.1	38.2	89.0	2.8	5.6	2.7	5.4	11.0
9	,,	,,	27.0	54.0	18.2	36.4	90.4	2.8	5.6	2.0	4.0	9.6
2	III	Silty Sand	9.6	19.2	38.3	76.6	95.8	0.9	1.8	1.2	2.4	4.2
12	,,	Highly Silty Sand	16.6	33.2	23.6	47.2	80.4	7.1	14.2	2.7	5.4	19.6
3	IV	Sandy Silty Clay	14.4	28.8	10.9	21.8	50.6	5.3	10.6	19.4	38.8	49.4
4	,,	,,	17.1	34.2	12.0	24.0	58.2	3.7	7.4	17.2	34.4	41.8
5	,,	,,	18.8	37.6	6.6	13.2	50.8	3.4	6.8	21.2	42.4	49.2
7	,,	,,	18.1	36.2	6.9	13.8	50.0	0.8	1.6	24.2	48.4	50.0
24	,,	,,	20.2	40.4	4.7	9.4	49.8	3.6	7.2	21.5	43.0	50.2
198	V	Sandy Clayey Silt	24.6	49.2	5.9	11.8	61.0	3.0	6.0	16.5	33.0	39.0
19	,,	,,	26.4	52.8	4.2	8.4	61.2	4.5	9.0	14.9	29.8	38.8
22	,,	,,	22.3	44.6	7.9	15.8	60.4	4.6	9.2	15.2	30.4	39.6
25	,,	,,	26.9	53.8	4.8	9.6	63.4	4.3	8.6	14.0	28.0	36.6
26	,,	,,	27.4	54.8	6.2	12.4	67.2	4.5	9.0	11.9	23.8	32.8
13	,,	Clayey Silt	28.2	56.4	4.2	8.4	64.8	3.6	7.2	14.0	28.0	35.2
14	,,	,,	28.2	56.4	3.4	6.8	63.2	5.6	11.2	12.8	25.6	36.8
21	,,	,,	34.3	68.6	4.5	9.0	77.6	3.8	7.6	7.4	14.8	22.4
23	,,	Highly Clayey Silt	23.7	47.4	4.3	8.6	56.0	4.4	8.8	77.6	35.2	44.0

TABLE 5

RESULT OF SPECTROGRAPHIC ANALYSIS OF ROCKS FROM BARA INANI KHAL SECTION

No.	CONTENT OF TRACE ELEMENTS %															
	Mn	Ni	Co	Ti	V	Cr	Mo	W	Zr	Nb	Ta	La	Cu	Zn	Pb	Sn
1.	0.01–3	0.006	0.001	0.1	0.006	0.006	—	—	0.006	—	—	—	0.003	0.006	0.001	0.001
2.	0.006	0.001	—	0.1	0.003	0.003	—	—	0.003	—	—	—	0.001	—	0.001	—
3.	0.006	0.003	0.003	.0 1	0.01	0.006	—	—	0.006	—	—	—	0.003	0.006	0.003	Tr
4.	0.006	0.006	0.001	0.1	0.01	0.006	—	—	0.006	—	—	—	0.003	0.006	0.003	Tr
5.	0.006	0.006	0.003	0.1	0.01	0.01	—	—	0.006	—	—	—	0.006	0.01	0.006	Tr
6.	0.006	0.003	0.003	0.1	0.01	0.03	—	—	0.01	—	—	—	0.003	0.006	0.003	0.001
7.	0.01	0.006	0.003	0.1	0.01	0.01	—	—	0.006	—	—	—	0.006	0.01	0.003	0.001
8.	0.01	0.006	0.003	0.1	0.01	0.01	—	—	0.006	—	—	—	0.003	0.006	0.003	0.001
9.	0.006	0.006	0.003	0.1	0.01	0.01	—	—	0.006	—	—	—	0.003	0.006	0.003	Tr
10.	0.006	0.003	0.003	0.1	0.01	0.006	—	—	0.01	—	—	—	0.003	0.006	0.003	Tr
11.	0.01	0.006	0.003	0.1	0.006	0.006	—	—	0.006	—	—	—	0.003	0.003	0.003	Tr
12.	0.1—03	0.006	0.003	0.1	0.006	0.006	—	—	0.006	—	—	—	0.003	0.003	0.003	Tr
13.	0.01	0.006	0.003	0.1	0.01	0.01	—	—	0.006	—	—	—	0.003	0.006	0.003	Tr
14.	0.03	0.006	0.003	0.1	0.01	0.01	—	—	0.003	—	—	—	0.003	0.006	0.003	0.001
15.	0.01	0.01	0.003	0.1	0.01	0.01	—	—	0.006	—	—	—	0.006	0.006	0.003	0.001
16.	0.006	0.003	0.003	0.1	0.01	0.006	—	—	0.006	—	—	—	0.003	0.006	0.003	—
17.	0.01	0.006	0.003	0.1	0.01	0.006	—	—	0.006	—	—	—	0.003	0.006	0.003	Tr
18.	0.01	0.006	0.003	0.06	0.01	0.006	—	—	0.003	—	—	—	0.006	0.006	0.003	0.001
19.	0.01	0.01	0.003	0.06	0.001	0.01	—	—	0.001	—	—	—	0.01	0.006	0.006	0.001
20.	0.01	0.003	0.003	0 .1	0.01	0.006	—	—	0.006	—	—	—	0.003	0.006	0.003	Tr
21.	0.01	0.006	0.003	0.1	0.01	0.006	—	—	0.003	—	—	—	0.006	0.006	0.006	—
22.	0.01	0.01	0.003	0.05	0.01	0.01	—	—	0.003	—	—	—	0.01	0.01	0.006	0.100
23.	0.03	0.01	0.003	0.3	0.03	0.01	—	—	0.006	—	—	—	0.01	0.01	0.006	0.001
24.	0.03	0.01	0.003	0.03	0.01	0.01	—	—	0.001	—	—	—	0.01	0.01	0.006	0.001
25.	001—3	0.006	0.003	0.03	0.03	0.01	—	—	0.003	—	—	—	0.01	0.01	0.006	0.001
26.	0.03	0.006	0.003	0.03	0.03	0.01	—	—	0.003	—	—	—	0.01	0.006	0.006	0.001

TABLE 5

REPULTS OF SPECTROGRAPHIC ANALYSIS

	CONTENTS OF TRACE ELEMENTS % by wt.																	
No:	Be	Ba	Sr	Cd	P	Y	Yb	Sb	As	Bi	Hg	Ge	Ga	Hf	Ca	Mg	Al	Si	Fe
1.	0.0003	0.01	0.006	—	—	0.001	0.0001	—	—	—	—	—	0.001	—	3	10	10	10	6—10
2.	0.0003	0.01	0.006	—	—	—	—	—	—	—	—	—	0.001	—	3	6	10	10	1—3
3.	0.0003	0.01	—	—	—	—	0.0001	—	—	—	—	—	0.001	—	1—3	10	10	10	6
4.	0.0003	0.01	—	—	—	0.001	0.0001	—	—	—	—	—	0.001	—	3	10	10	10	6
5.	0.0003	0.01	—	—	—	0.001	0.0001	—	—	—	—	—	0.001	—	3—6	10	10	10	6
6.	0.0001	0.01	—	—	—	0.001	0.0001	—	—	—	—	—	0.001	—	1—3	6	6	10	6
7.	0.0003	0.001	—	—	—	0.001	0.0001	—	—	—	—	—	0.001	—	3	10	10	10	6—10
8.	0.0003	0.01	0.006	—	—	0.001	0.0001	—	—	—	—	—	0.001	—	6	10	10	10	6
9.	0.0003	0.01	—	—	—	0.001	0.0001	—	—	—	—	—	0.001	—	6	10	10	10	6
10.	0.0003	0.01	—	—	—	0.001	0.0001	—	—	—	—	—	0.001	—	3	6	6	10	6
11.	0.0003	0.01	0.006	—	—	0.001	0.0001	—	—	—	—	—	0.001	—	6	10	10	10	6
12.	0.006	0.01	0.006	—	—	0.001	0.0001	—	—	—	—	—	0.001	—	10	10	10	10	6
13.	0.006	0.01	0.006	—	—	0.001	0.0001	—	—	—	—	—	0.001	—	3	10	10	10	6
14.	0.006	0.01	—	—	—	0.001	0.0001	—	—	—	—	—	0.001	—	3	10	10	10	6
15.	0.006	0.03	0.006	—	—	—	0.0001	—	—	—	—	—	0.001	—	3	10	10	10	6
16.	0.0003	0.01	0.006	—	—	0.001	0.0001	—	—	—	—	—	0.001	—	1—3	6	6—10	10	3
17.	0.0006	0.01	0.006	—	—	0.001	0.0001	—	—	—	—	—	0.001	—	3	10	6	10	3
18.	0.0006	0.01	—	—	—	—	0.0001	—	—	—	—	—	0.001	—	3	10	6—10	10	6
19.	0.0006	0.01	—	—	—	—	0.0001	—	—	—	—	—	0.001	—	3	10	10	10	6
20.	0.0006	0.01	0.006	—	—	0.001	0.0001	—	—	—	—	—	0.001	—	3	10	10	10	6—10
21.	0.0006	0.01	0.006	—	—	0.001	0.0001	—	—	—	—	—	0.001	—	3—6	10	10	10	6
22.	0.0006	0.01	—	—	—	—	0.0001	—	—	—	—	—	0.001	—	3—6	10	10	10	6—10
23.	0.0006	0.01	0.006	—	—	0.001	0.0001	—	—	—	—	—	0.001	—	3—6	10	10	10	6—10
24.	0.0003	0.01	0.006	—	—	—	0.0001	—	—	—	—	—	0.001	—	3—6	10	10	10	6—10
25.	0.0006	0.01	0.006	—	—	—	0.0001	—	—	—	—	—	0.001	—	3—6	10	10	10	6
26.	0.0003	0.01	—	—	—	—	0.0001	—	—	—	—	—	0.001	—	3—6	10	10	10	6

GRAVITATIONAL FORCES AND CONTINENTAL DRIFT

BY

G.T.P. TARRANT*

Physics Department, Chiengmai University, Thailand

Abstract : *Many physicists disbelieve the considerable geological evidence that continents have drifted long distances into their present positions, primarily because they believe that the three possible mechanisms should produce movements in the wrong directions. Unwarranted assumptions have however been made in the mathematical treatment of all three of the postulated mechanisms. The present paper deals with the treatment of the gravitational force between floating masses and shows that, on revision, this force is one of repulsion and not of attraction. It also indicates that mountain ranges near a coast should have near and parallel to them depressions in the ocean floor similar to the Peru trench.*

INTRODUCTION

Many of the mountain masses of the world appear to behave somewhat as if they were the tops of immense icebergs floating in a denser sea which is covered with a layer of ice. Such systems might move under the action of horizontal forces if the ice layer was elasticoviscous, able to sustain shears of short duration but flowing as a liquid of great viscosity under forces of long duration. They might also move in sudden catastrophic jumps if the ice layer was a brittle solid and not elasticoviscous, because then there would come a time when, as a result of denudation, excess upthrusts would cause the ice layer to break up.

Floating masses of this kind should be under the influence of three different forces which may exist separately or together. If motion does occur it will be in the direction of the resultant force only if this happens to be along a line of latitude because of the profound effects of the rotation of the earth.

The first two of these forces are accelerative in character-which could be important if the viscosity of the "liquid" were not too high and if the motion proceeded by 'catastrophic jumps'. This is because, when the solid surface film broke up, the floating mass would accelerate forward and might possibly reach such a velocity that it could break further amounts of solid surface film and thus move great distances in a comparatively short time. These two accelerative forces are a rather small one produced by direct gravitational effects and a second, normally thought to be a thousand times larger, produced by the difference of gravity between the poles and the equator. We will call this the Eötvos force.

The third force, first considered by Pekeris depends on whether the convection currents in the earth are 'cellular' or normal and even whether they can occur at all in view of the density variations in the interior. If these currents do occur and reach near to the surface they should move horizontally just under the surface before descending and should drag floating continents with them. According to the calculations given in Jeffreys book 'The Earth' this force should carry continents from the equator to the poles with speeds of the order of 1 cm per year. Since the continents are not clustered at the two poles and since this force should be the largest of the three (if it occurs at all), Jeffreys (1959) believes that the motion must be stopped by the strength of the solid skin of the earth so that continental drift cannot occur. He is confirmed in this view by the knowledge that continents are not spread uniformly round the equator as is thought to be a consequence of the Eötvos force.

The arguments concerning all three mechanisms appear, however, to the writer to be based on simplifying assumptions which are quite unwarranted and which, when put right, completely alter the con-

*Formerly at the Mathematics Department, University of the Punjab, Lahore.

clusions. The final result appears to be that, until we have further knowledge of the physical properties of the crust of the earth and the material underneath it, we cannot rule out, on grounds of physics, the possibility that continents have drifted.

In this paper, we consider only the gravitational forces which though small, are of interest, (*a*) because they are tolerably independent of assumptions as to the values of quantities of which we have no certain knowledge, (*b*) because they suggest an explanation for the deep ocean trenches lying near to mountain ranges.

GRAVITATIONAL FORCES

It is easy to see in a general way that the direct gravitational attraction of two floating masses could become changed into a repulsive one if the effect of the distortion of the fluid surface is taken into account.

To see how this could happen, we will regard the icebergs as being made up of a multitude of pairs of very small spheres placed above or below each other on light radial rods and of sizes such that the downwards force of gravity on the upper member, C, is exactly balanced by the corresponding Archimedean upthrust on the partner bottom sphere, B. (Fig. 1)

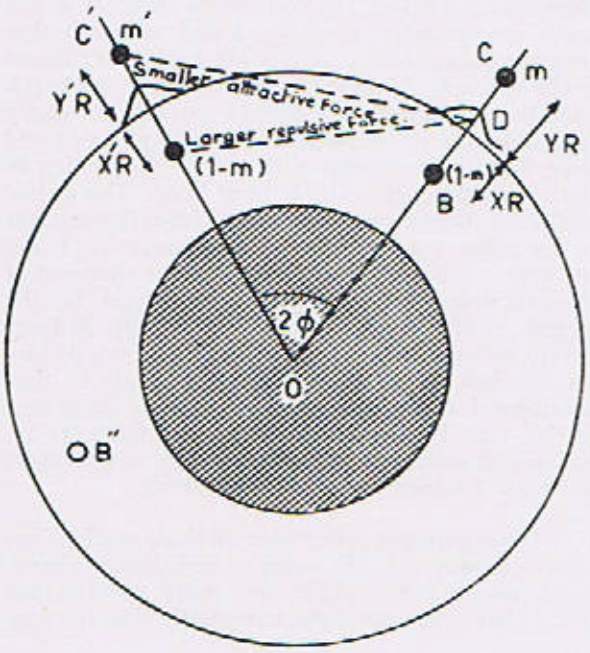

Fig. 1

Then the mass m at C will attract water in the region near to D, taking it from more remote regions. This effect will be enhanced by the fact that the mass at B is less by m than it would had been completely uniform. (By analogy with electrostatics where a charge of e just outside a conducting sphere attracts a nearly identical charge close to it, the total bump of water at D should be roughly equal to the mass m as a result of the outside attraction and a second m from the inside repulsion.)

The extra water near to D will produce an acceleration on matter placed at C' which will have an attractive component perpendicular to OC' of

$$\frac{G\,m}{(C'D)^2}\,\frac{D}{}\,\sin \widehat{DC'O} = \frac{G\,m}{(C'D)^3}\,\frac{D}{}\,(OD)\sin 2\phi,$$

since $\dfrac{\sin 2\phi}{C'D} = \dfrac{\sin \widehat{DC'O}}{OD}$

The gravitational acceleration at B' will be a little larger than this because, if 2ϕ is tolerably large, B'D is less than C'D. But at B'we have a mass which is m' less than the mass of the same volume of water and the Archimedean upthrust make such bodies move in a direction opposite to that of gravity. There will therefore be a repulsive force on B' which is rather greater than the attractive one on C'.

It is this force which is now believed to account for the mutual drifting apart of the continents although the matter is not quite as simple as we have suggested. We will examine it by evaluating (*a*) the direct attraction between the pair of masses at B and C and the pair at B' and C' (*b*) the magnitude of the repulsive forces caused by the bunching of the liquid at D and will show that the latter exceeds the former at reasonably large values of 2ϕ.

THE DIRECT ATTRACTIVE FORCE BETWEEN PAIRS OF SPHERES

In this phase of the work we ignore completely the distortion of the liquid surface and assume it is compelled by some form of rigid skin to remain a true sphere.

$$\text{Now } (C'C)^2 = R^2(1+Y')^2 + R^2(1+Y)^2 - 2R^2(1+Y')(1+Y)\cos 2\phi$$

$$= R^2\{2(1+Y')(1+Y)(1-\cos 2\phi) + (1+Y')^2 + (1+Y)^2 - 2(1+Y')(1+Y)\}$$

$$= 4\sin^2\phi\, R^2 \left\{1+Y'+Y+YY' + \frac{(Y'-Y)^2}{4\sin^2\phi}\right\}$$

So the component of the gravitational acceleration produced by the mass at C at the point C' and which is perpendicular to OC is, TOWARDS OC.

$$= Gm\,\frac{\sin \widehat{OC'C}}{(OC')^2} = \frac{Gm\,(OC)\sin 2\phi}{(OC')^3} -$$

$$= \frac{Gm\,R\,(1+Y)\,2\sin\phi\cos\phi}{8\sin^3\phi\,R^3}\left[1+\left\{Y'+Y+YY' + \frac{(Y'-Y)^2}{4\sin^2\phi}\right\}\right]^{-\frac{3}{2}}$$

$$= \frac{Gm\cos\phi}{4R^2\sin^2\phi}(1+Y)\left[1-3/2\left\{Y'+Y+YY' + \frac{(Y-Y')^2}{4\sin^2\phi}\right\} + 15/8\,(Y'+Y)^2\right]$$

$$= \frac{Gm\cos\phi}{4R^2\sin^2\phi}\left[1-3/2\left\{Y'+Y+YY' + \frac{(Y'-Y)^2}{4\sin^2\phi}\right\} + \frac{15}{8}(Y'+Y)^2 + Y - \frac{3}{2}Y(Y'+Y)\right]$$

$$= \frac{Gm\cos\phi}{4R^2\sin^2\phi}\left[1-\frac{3}{2}Y' - \tfrac{1}{2}Y + \tfrac{3}{4}YY' + \frac{15}{8}Y'^2 + \frac{3}{8}Y'^2 - \frac{3(Y'-Y)^2}{8\sin^2\phi}\right] \quad \ldots\ldots\ldots(1)$$

The special feature of the mass at B is that it is m less than the symmetrically placed identical volume at B''. This means that, in determining the components of the gravitational acceleration which are perpendicular to OC' we can account for the combined effect of B and B'' by pretending we have a negative mass at B which produces accelerations away from B. In consequence, remembering that—X replaces Y in the above expression, we can write the component of the acceleration produced at C' by B as :—

$$-\frac{Gm\cos\phi}{4R^2\sin^2\phi}\left[1-\frac{3}{2}Y'+\tfrac{1}{2}\times-\frac{3}{4}XY'+\frac{15}{8}Y'^2 + \frac{3}{8}X^2 - \frac{3(Y'+X)^2}{8\sin^2\phi}\right]$$

The total component of acceleration TOWARDS OC produced by B and C together at C' will then be :—

$$\frac{Gm\cos\phi}{4R^2\sin^2\phi}\left[-\tfrac{1}{2}(X+Y)+\tfrac{3}{4}Y'(X+Y)+ \frac{3}{8}(Y^2-X^2)+\frac{3(X^2+2Y'X-Y^2+2Y'Y}{8\sin^2\phi}\right]$$

$$= -\frac{Gm\cos\phi}{8R^2\sin^2\phi}(X+Y)\left\{1-\frac{3}{2}Y'+\tfrac{3}{4}(X-Y) - \frac{3(X-Y+2Y')}{4\sin^2\phi}\right\}$$

In a similar manner the total component of acceleration towards OC produced by B and C together at B' will be :—

$$-\frac{Gm\cos\phi}{8R^2\sin^2\phi}(X+Y)\left\{1+\frac{3}{2}X'+\tfrac{3}{4}(X-Y) - \frac{3(X-Y-2X')}{4\sin^2\phi}\right\}$$

In writing down the force this produces we must remember that light objects which are completely immersed in denser liquids have forces on them opposite in direction to the acceleration and equal to that acceleration times the difference between the masses of the same volume of liquid and solid. The sum of the forces on B' and C' towards OC will therefore be :—

$$-\frac{Gmm'\cos\phi}{8R^2\sin^2\phi}(X+Y)\left\{-\frac{3}{2}Y'-\frac{3}{2}X' - \frac{3(2Y'+2X')}{4\sin^2\phi}\right\}$$

$$= \frac{3\,Gmm'\cos\phi\,(X+Y)(X'+Y')}{16R^2\sin^2\phi}\left(1+\frac{1}{\sin^2\phi}\right)$$

This means that the force is an attractive one.

FORCES PRODUCED BY SURFACE DEFORMATIONS

A direct calculation of the magnitude of the bump of liquid give only the first term of a series since the first bump of liquid thus calculated attracts a second and so on.

An indirect approach proves shorter. We will compare two ways in which a world surface could be kept in equilibrium when a small speherical mass has been taken from the inside and put outside. These are, (*a*) that we do nothing to the surface so that surface deformations occur producing some sort of 'bump' near to the external mass, and (*b*) that we spray the surface with a film of positive or negative masses of infinite density and so of zero thickness in such a manner that the equilibrium state is a true sphere. We then argue that accelerations or forces produced at remote points by the bump must be almost identical with those produced by the surface mass film—which

can be calculated by the method of images developed for electrostatics.

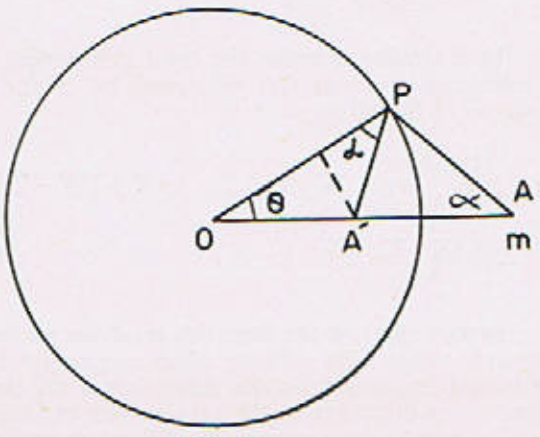

Fig. 2

According to this method we notice that if two points A and A' are selected as shown (Fig. 2) so that (OA) (OA')=R², then, independent of the position of P,

$$\text{Tan } \alpha = \frac{(OA')\sin\theta}{R-(OA')\cos\theta} = \frac{R^2(OA)^{-1}\sin\theta}{R-R^2(OA)^{-1}\cos\theta}$$

$$= \frac{R\sin\theta}{(OA)-R\cos\theta} = \tan\beta$$

The two triangles containing O are therefore similar, so that $\frac{OA}{AP} = \frac{OP}{A'P}$. This means that a mass m placed at A will produce a potential at P of $\frac{m}{AP}$, which is exactly opposite to that of a mass of $\left(-m\frac{OP}{OA}\right)$ placed at A', which is $-m\frac{(OP)}{(OA)}\cdot\frac{1}{(A'P)} = -\frac{m}{(AP)}$.

Now the theory of zonal harmonics shows that axially symmetrical potentials which tend to zero at infinity can be expanded in a power series in q the distance from the origin and that $V=V_0+K\frac{R}{q}+\Sigma A_n\left(\frac{R}{q}\right)^{n+1}P_n$. This will apply both to the series coming from (1) the surface distribution and (2) the mass at A'. Consequently, since the potential is by definition zero when R=q, it follows that the coefficients A_n must all be identical so that the fields produced outside of the sphere by (1) and (2) must be indistinguishable.

Inside the sphere the total potential coming from the external mass and from the mass distributed on the sphere must be of the form $V=V_0+\Sigma A'_n\left(\frac{q}{R}\right)^n P_n$ since it cannot be infinity when q=O. Therefore at q=R it must be $V_0+\Sigma A'_n P_n$. This can be zero for all angles only if there is zero gravitational field inside.

It thus appears that the surface distribution of mass which produces a constant potential over the surface of the sphere, in the presence of a mass m OUTSIDE at RY from the surface, must be such that there is zero field inside while outside the fields correspond to m at YR from the surface together with a mass of $-\frac{m}{1+Y}$ at a depth below the surface of (R-OA') $= R\left(1-\frac{1}{(1+Y)}\right)=\frac{RY}{1+Y}$.

An exactly similar argument shows that if a mass of −m is placed inside the sphere at a distance (XR) BELOW the surface the field will correspond to this mass and to an image mass of $+\frac{m}{1-X}$ at a distance $\frac{RX}{1-X}$ ABOVE the surface. Outside the field will be zero.

These conclusions can now be used. A comparison with equation (1) shows that the sideways acceleration at C' which is produced by a mass of $-\frac{m}{1-Y}$ at a height of (Y^2-Y) will be :—

$$= -\frac{Gm\cos\phi}{4R^2\sin^2\phi}(1-Y+Y^2) - \left[1-\tfrac{3}{2}Y' - \tfrac{1}{2}(Y^2-Y) + \tfrac{3}{4}(-Y)Y' + \tfrac{15}{8}Y'^2 + \tfrac{3}{8}Y^2 - \frac{3(Y'+Y)^2}{8\sin^2\phi}\right]$$

$$= -\frac{Gm\cos\phi}{4R^2\sin^2\phi}\left[(1-Y+Y^2) - \tfrac{3}{2}Y'(1-Y) + \tfrac{1}{2}Y(1-Y) - \tfrac{1}{8}Y^2 - \tfrac{3}{4}YY' + \tfrac{15}{8}Y'^2 - \frac{3(Y'+Y)^2}{8\sin^2\phi}\right]$$

$$= -\frac{Gm\cos\phi}{4R^2\sin^2\phi}\left[1-\tfrac{1}{2}Y + \tfrac{3}{8}Y^2 - \tfrac{3}{2}Y' + \tfrac{7}{4}YY' + \tfrac{15}{8}Y'^2 - \frac{3(Y'+Y)^2}{8\sin^2\phi}\right]$$

Since this is numerically exactly the same as the acceleration produced by the external mass m alone but is of opposite sign, we see that the total acceleration on a particle at C' will be zero.

The same will also apply to the mass—m' at B'. Since the total acceleration components produced at B' and C' by the masses at B and C and the surface layer at D is zero, it follows that the 'bump' of liquid at D must produce on masses M'

and—M′ at B′ and C′ a repulsive component of force which is exactly equal to the attractive component coming from B and C (equation 2).

This is, however, only part of the story because the 'bump' of liquid at D′ will also be exercising a replusive force on the masses at B and C. This bump at D′ will therefore move slightly to the left away from BC until this replusive force is completely compensated by components of attraction coming from B′ and C′. We thus have three forces acting on B′ and C′ all numerically equal. The first, produced by B and C, is attractive and is given by equation (2) ; the second comes from the 'bump' at D and is repulsive ; the third comes from the displacement of the 'bump' at D′ is an attraction to the left which counts as a repulsive force.

The final result is therefore that a repulsive force acts on B′ and C′ of magnitude

$$= \frac{3\,Gmm'\cos\phi\,(X+Y)\,(X'+Y')}{16\,R^2\sin^2\phi}\left(1+\frac{1}{\sin^2\phi}\right)$$

THE FORCE BETWEEN CONTINENTS

Consider a uniform narrow rod of area dA which is floating vertically in the region of BC and

Fig. 3

whose bottom part is made up of a multitude of little spheres such as that at B (Fig. 3).

Then the top part can also be formed of the partner spheres similar to that at C providing :— (*a*) x is selected to be $\left(\frac{s}{D_w - D_s}\right)$ y which will produce equilibrium, if we ignore the slight variation of gravity, with $h_y/h_x = (D_w - D_s)/D_s$, if D_s and D_w are the densities of the solid and of the water respectively. (*b*) the upper spheres are moved about sideways a little, keeping y constant, to fill the space completely – a procedure which will produce no effect on the forces since the movement necessary is very small as the cylinder considered is very narrow.

Then the force between the cylinder and the two spheres at B′ and C′ will be $\frac{3\,Gm'\cos\phi}{16R^2\sin^2\phi}$.

$$(X'+Y')\left(1+\frac{1}{\sin^2\phi}\right)\int(X+Y)\,dm$$

But $\int(X+Y)\,dm = \int\left(\frac{(x+y}{R}\right)D_s\,dAdy = \frac{D_s dA}{R}$

$$\int\left(\frac{D_s}{D_w - D_s}+1\right)ydy = \frac{D_s D_w\,dA}{R(D_w - D_s)}\quad\frac{h^2y}{2}$$

Now repeat the process by carrying out a similar integration in the region of B′C′ to find the force between the two floating tubes. The result is

$$\text{Force} = \frac{3G\cos\phi}{64R^4\sin^2\phi}\left(1+\frac{1}{\sin^2\phi}\right)\left(\frac{D_s D_w}{D_w - D_s}\right)^2 \cdot (h'_y\,h_y)^2\,dA'\,dA$$

Further integration to find the total forces between two floating masses the size of continents is complicated by the awkward function of ϕ and by the fact that the forces will not all lie in the same straight line. To estimate the order of magnitude, however, we can assume that the whole masses are concentrated in points separated by $2\phi = 90°$ so that $\frac{\cos\phi}{\sin^2\phi}\left(1+\frac{1}{\sin^2\phi}\right) = 4$ and that obliquity effects will reduce this to about 2. Then, the total force between two continents of radius 2000 km, average density 2.7 gm/cc which is floating in liquid of density 3.3 gm/cc. at a height of 6×10^5 cm above the liquid line (which is 4 kms below sea level), should be

$$\frac{3\,(6.6\times10^{-8})}{64\,(6.4\times10^8)^4}\cdot\ 2.\ \left(\frac{2.7\times2.3}{0.6}\right)^2(6\times10^5)^4.$$
$$(4\times10^{16}\,\pi)^2 = 1.65\times10^{16}\ \text{dynes.}$$

Since Jeffreys expresses his forces in units of dynes per cm² we will divide this by $\pi(2\times10^8)^2$ and thus find repulsive forces of the order of 0.13 dyne/cm².

SURFACE DEFORMATIONS.

It is shown in Ferraro (1962, page 163), that a charge +e placed outside an equipotential sphere at a distance R(1 + Y) from the centre attracts a surface charge density of

$$-\frac{e}{4\pi R\,r_1^3}\cdot\left\{R^2(1+Y)^2 - R^2\right\}$$, where r_1 is the distance from the charge to any point P on the surface of the sphere. Consequently any distortions of the equipotential produce by an external mass m placed at (YR) from the surface of a spherical world will be annulled completely by a surface mass density of $\sigma_e = +\frac{mR}{4\pi r_1^3}(2Y+Y^2)$ where the change of sign occurs because similar masses attract instead of repelling.

We have already shown that if a mass of (−m)

is placed inside a spherical equipotential at a distance RX beneath the surface then the sphere will remain an equipotential if we also placed a mass of $+\frac{m}{1-X}$ outside the surface at a distance of $\frac{RX}{1-X}$.

Combining the last two paragraphs we see that the distortions produced by a mass of $(-m)$ inside and XR beneath the surface will be annulled completely by a surface mass density of

$$\sigma_i = -\frac{\left(\frac{m}{1-X}\right)R}{4\pi r_2^3}\left\{\frac{2X}{1-X}+\frac{X^2}{(1-X)^2}\right\}$$

$$= \frac{m\,R}{4\pi r_2^3}(2X+5X^2)$$

Now, if 2ϕ is the angle at the earth's centre subtended by r_1,

$$r_1^2 = R^2+R^2(1+Y)^2-2R^2(1+Y)\cos 2\phi$$

$$= R^2\left\{1+(1+Y)^2-2(1+Y)(1-2\sin^2\phi)\right\}$$

$$= R^2\left[\left\{1-(1+Y)\right\}^2+4(1+Y)\sin^2\phi\right]$$

$$= R^2\left\{Y^2+4(1+Y)\sin^2\phi\right\}$$

The total surface mass density $\sigma = \sigma_0+\sigma_i$ is therefore :—

$$\sigma = \frac{m\,R}{4\pi R^3}\left[\frac{(2Y+Y^2)}{\{Y^2+4(1+Y)\sin^2\phi\}^{3/2}}\right.$$

$$\left.-\frac{(2X+5X^2)}{\left\{\left(\frac{X}{1-X}\right)^2+4\left(1+\frac{X}{1-X}\right)\sin^2\phi\right\}^{3/2}}\right]$$

The total mass of the surface film is therefore

$$\int\sigma(2\pi R\sin 2\phi)\,R\,d(2\phi) = 2\pi R^2\int\sigma(2\sin\phi\cos\phi)(2d\phi) = 4\pi R^2\int\sigma\,d(\sin^2\phi)$$

$$= m\left[\frac{(2Y+Y^2)(-2)}{4(1+Y)\{Y^2+4(1+Y)\sin^2\phi\}^{\frac{1}{2}}}\right.$$

$$\left.-\frac{(2X+5X^2)(-2)}{4(1+X)\{X^2+4(1+X)\sin^2\phi\}^{\frac{1}{2}}}\right]$$

If the limits are taken as $\sin\phi = 1$ and 0, the total surface mass is $m\left[\frac{1}{1+Y}-\frac{1}{1+X}\right]$.

Of greater immediate importance is the amount of surface mass contained between the limits of $\sin\phi'$, though small, is large compared with X or Y ($\sim \frac{30\text{ kms}}{6000\text{ kms}} = \frac{1}{200}$). This is because, as far as forces between continents 1000 kms apart are concerned, this mass will act effectively as if it were a point. It is :—

$$-\tfrac{1}{2}m\left[\frac{2Y(1+\frac{1}{2}Y-Y)}{\sqrt{4(1+Y)}\left\{1+\frac{Y^2}{4(1+Y)\sin^2\phi'}\right\}^{\frac{1}{2}}}\right.$$

$$-\frac{2Y(1+\frac{1}{2}Y-Y)}{Y}-\frac{2X(1+\frac{5}{2}X-X)}{\sqrt{4(1+X)}\left\{1+\frac{X^2}{4(1+X)\sin^2\phi'}\right\}^{\frac{1}{2}}}$$

$$\left.+\frac{2X(1+\frac{5}{2}X-X)}{X}\right]$$

$$= -\tfrac{1}{2}m\left[Y(1-Y)\left\{1-\frac{Y^2}{8\sin^2\phi'}\right\}\right.$$

$$\left.-2(1-\tfrac{1}{2}Y)-X(1+X)\left\{1-\frac{X^2}{8\sin^2\phi'}\right\}-2(1+\tfrac{3}{2}X)\right]$$

$$= -\tfrac{1}{2}m\left[2Y-Y^2+2X-X^2-\frac{Y^3-X^3}{8\sin^2\phi'}\right]$$

$$= m(X+Y)\text{ approximately,}$$

As this result is affected but very slightly indeed by an alteration in the angle ϕ' selected, providing only that it is larger than $\frac{1}{200}$ radian, we come to the important conclusion that almost all the surface mass is concentrated in such a narrow region round the axis that it can be considered to be a point.

Another interesting conclusion can be drawn by referring again to the equation for the surface mass density σ. This should pass through a minimum when its differential with respect to ϕ is zero. This occurs when $\sin\phi$ is given by

$$\frac{(-1\frac{1}{2})(2Y+Y^2)(1+Y)\,8\sin\phi\cos\phi}{\{Y^2+4(1+Y)\sin^2\phi\}\,2\frac{1}{2}}$$

$$= \frac{(-1\frac{1}{2})(2X+5X^2)(1+X)\,8\sin\phi\cos\phi}{\{X^2+4(1+X)\sin^2\phi\}\,2\frac{1}{2}}$$

$$\left\{X^2+4(1+X)\sin^2\phi\right\}^{2/5}\left\{Y^2+4(1+Y)\sin^2\phi\right\}^{2/5}$$

$$= X^{2/5}Y^{2/5}\left(Y^{-4/5}-X^{-4/5}\right)$$

$$4\sin^2\phi\,Y\left(Y^{2/5}-X^{2/5}\right) = Y^2X^{2/5}-X^2Y^{2/5}$$

$$\sin\phi = \tfrac{1}{2}(XY)^{1/5}\sqrt{Y^{2/5}+X^{2/5}} = \frac{1.35}{2}Y^{2/5}\sqrt{Y^{2/5}+1.82Y^{2/5}}$$

Since, $X = \frac{YD_s}{(D_w - D_s)}$

$= 2.7\ Y/0.6 = 4.5\ Y.$

It, therefore, follows that this minimum value of the depression in the surface of the liquid will occur at a distance out from a pair of shpheres of: $R(2\frac{1}{2}) = 2.28\ R\ Y^{0.4} = 230$ kilometres. It is natural to try to identify these depressions in the surface of the liquid with observed depressions in the floor of oceans in the vicinity of steep, high mountain ranges. An analogy may be drawn with the case of the Peru Trench, about 200 miles from the Andean Range.

CONCLUSION

The numerical value of the gravitational repulsions between continents, as obtained above ($\simeq$ 0.13 dynes/cm^2.) is much smaller than the values usually accepted for the Eötvos forces ($\simeq$ 4000 dynes/cm.^{2}) or the Pekeris forces (10^8 dynes/cm.^{2}). The calculation thus tends to confirm the natural feeling of many physicists. However, such feelings are not completely reliable and need to be confirmed mathematically. The simplifying assumptions employed by Jeffreys were so great that one can hardly regard his work as providing the necessary confirmation.

Certain unpublished reflections indicate that neither the Eötvos nor the Pekeris forces are so simply calculated as is normally assumed and that these forces may well, under certain circumstances, be so greatly reduced in value that gravitational forces may perhaps still play a minor part in causing continental movements.

REFERENCES

Ferrero, V.C. 1962 ELECTROMAGNETIC THEORY, 3rd Edition., Athlone Press, University of London (Constable).

Jeffreys, H. 1959. THE EARTH, 6th Edition, Cambridge University Press,

59/60.

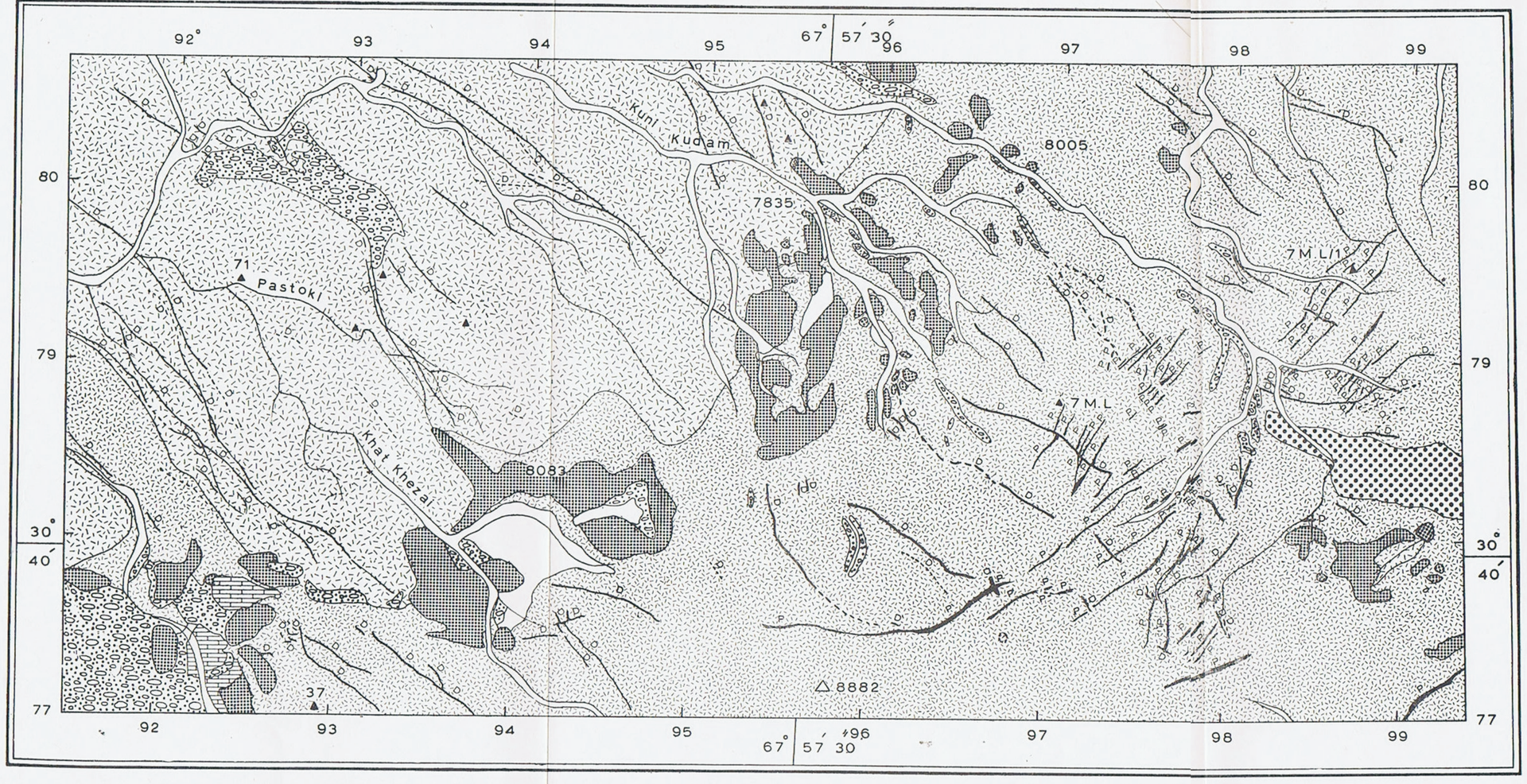

LEGEND

- Sedimentary Rocks
- Dunite
- Harzbergit - Dunite Complex
- Pyroxenite
- Dolerite Dyke
- Dolerite
- ▲ Chromite Mine
- Laterite
- Conglomerate
- Recent Alluvium
- Nala

N

Scale

Furlongs 2 0 1 Mile

Fig. 1 Geological map of the Palaklara area.

GEOLOGY OF THE PALAK LARA AREA SPLAITORGARH, HINDUBAGH, ZHOB DISTRICT, WEST PAKISTAN

BY

ZULFIQAR AHMED and M. NAWAZ CHAUDHRY

Department of Geology, University of the Punjab, Lahore.

Abstract : *A geological map on a scale of 4 inches to a mile of the Palak Lara area is presented. Most of the area comprises of serpentinized dunite and serpentinized dunite-harzburgite complex ; the latter is considered to be younger than the former. Some workable concentrations of chromite in dunite are described. Pyroxenites and dolerites occur as the minor intrusives of the area. Petrography, chemistry and origin of ultramafics is discussed. The pyroxenite veins, which consist wholly of diopside, are thought to have arisen by the action of silica and lime-rich fluids on the dunite. Textural, structural and chemical evidence for this origin is presented. A Cretaceous age is proposed for a small outcrop of calcareous and argillaceous sedimentary rocks, based on the study of their faunal assemblage. A conglomerate bed of Recent age is also present at some places.*

A total of 2,600 joints were measured. Their synthesis reveals that the first compressive stress acting along N40° E direction was followed by a second compressive stress acting along N50° W direction. The ultramafics at some places have a zoned laterite cap. Chemistry, mineralogy and origin of zoned laterite is discussed. A fairly mild subtropical rather than a tropical climate is proposed during the course of formation of these laterites.

INTRODUCTION

The Palak Lara area lies about 25 miles southeast of Hindubagh and is connected with it by a dirt road. The mapped area is a rectangle of about 9.5 square miles. It lies between latitudes 30°41.5′ N to 30°39.5′ N and longitudes 67° 55′ E. to 67°59.6′ E. The area has a fairly high altitude lying between 7,550 feet to 8,882 feet, and is devoid of vegetation. The exposures are excellent.

According to Colombo Plan Reconnaissance Report (1960), the area is a part of Hindubagh Igneous Complex of a probable Cretaceous and early Palaeocene age. This complex is emplaced in a basin, slightly lenticular in plan, formed by calcareous, argillaceous, siliceous and arenaceous geosynclinal sediments.

The southeastern part of the area (Fig. 1) comprises of strongly serpentinized dunite, followed in the northwestern part by an equally serpentinized mixed dunite-harzburgite complex. A small area in the southwestern corner is occupied by a fossiliferous sedimentary sequence of limestones and shales. The dunite in the southeast is cut by subparallel pyroxenite veins that trend N.E.-S.W. Dolerite dykes cut across pyroxenite veins and trend NW-SE. Distinctly zoned laterites have developed along the contact between dunite and dunite-harzburgite complex. Recent to subrecent conglomerates overlie all other rock-types, including the laterites.

METHODS OF MAPPING AND STUDY

The mapping of the Palak Lara area was carried out on photographic enlargements (4 inches to 1 mile) of the 1 inch to 1 mile topographic sheet No. 34, 9/14 (published by the Survey of Pakistan). The contacts were followed throughout their exposed extent.

In the laboratory, petrographic work was supplemented by optical study of major mineral constituents. For this purpose, olivine and pyroxene minerals were separated from different rock samples by heavy liquids and centrifugal methods. The refractive indices were determined by the liquid immersion method using white light. The accuracy of these determinations is considered to be $\pm .002$. The optical axial angles were determined on a four axes Leitz universal stage. The accuracy of these determination is $\pm 1.0°$ for the angles below and $\pm$ 2.0° for the optical angles above 80°.

For the chemical analyses of rocks, the

contents of SiO_2, CaO, MgO and total R_2O_3 were determined gravimetrically. Colorimetric methods of Riley (1955) were used to determine total Fe_2O_3, MnO and TiO_2. The alkalies were determined by the flame photometric methods. Combined water was determined by the Penfield method.

Strike-dip readings were taken on well-developed joints, and joint-orientation diagrams were prepared and contoured following routine methods (Billings, 1942). The plots were obtained on Schmidt equal-area net, using lower hemisphere. The strike-frequency and dip-frequency diagrams were also used for interpretation.

DESCRIPTION OF THE IGNEOUS COMPLEX

1. The Serpentinized Dunite

Located in the southeastern part of the area, serpentinized dunite covers the largest areal extent of the mapped area. It is a fairly brittle rock and weathers to a rusty brownish colour. The weathered surfaces show sooty grey to black magnetite and chromite grains ; the former readily alters to rusty brown limonite. The dunite is massive and devoid of any internal structures, except for certain early magmatic structures present in the associated chromite concentrations ; that are dealt with separately.

The content of serpentine minerals almost always exceeds 75% of the rock, and may even reach a maximum of 95%. The degree of serpentinization does not show any definite pattern in space. Sparse olivine relicts (1-15%) are frequently found replaced by serpentine along cracks and grain boundaries. Pseudomorphs of serpentine always exhibit mesh texture consisting of two serpentine minerals, antigorite and chrysotile. In this texture, small irregularly rectangular areas are occupied by antigorite commonly showing anomalous blue interference colours. Antigorite grains are surrounded by veinlets of fine grained, fibrous chrysotile. Olivine, separated from three samples of dunite from different locations, gave the following optical data :—

	1	2	3
	(8101)	(8124)	(8692)
α	1.655	1.655	1.654
β	1.673	1.673	1.673
γ	1.685	1.684	1.684
2 Vz	89°	88°	88°
Estimated composition	Fo 90 Fa 10	Fo 91.5 Fa 9.5	Fo 91.5 Fa 9.5

The above data for the olivines indicate that their composition is more or less uniform.

Magnetite forms about 3% to 5% of the rock and occurs as small subhedral grains as well as very fine specks scattered throughout serpentine. It also occurs as thin lining around chromite grains. Chromite is generally less than 2% and occurs as subhedral to euhedral octahedra.

2. The Serpentinized Dunite-Harzburgite Complex.

The northwestern part of the area comprises of a "Serpentinized Dunite-Harzburgite Complex" ——so called because of a complex intermixed occurrence of the two rock types in it. Small layers and lensoid bodies of different sizes of one rock type occur inside the other. The two components of this complex can be easily distinguished in the field by the following criteria :—

(*a*) Fresh dunite is light green and weathers to a rusty brown colour, whereas the fresh harzburgite is olive-green and weathers to a lighter brown colour with olive green tints.

(*b*) Weathered surfaces of dunite are compact, even grained and smooth ; while those of the harzburgite are pitted, uneven and fairly rough.

(*c*) In hand specimen, harzburgite shows small shining crystals of pyroxene set in serpentine, while in dunite such shining crystals are lacking.

The dunite of this complex is similar to the main dunite, except probably for the slightly higher fayalitic content of their olivines (see below). The harzburgite has been serpentinized to a lesser degree than dunite. Nevertheless, the serpentine minerals, antigorite and chrysotile, showing mesh texture of fine fibres, constitute approximately from 60% to about 85% of the harzburgite. The relicts of olivine and pyroxene crystals show strong replacement by serpentine along cleavage cracks and grain boundaries. An olivine relict separated from a harzburgite sample (No. 8698) furnished the following optical data :—

$\alpha = 1.622, \beta = 1.675, \gamma = 1.692$ and $2Vz = 91°$

This indicates a composition of Fo_{85} Fa_{15} for the olivine and is therefore distinctly richer in iron content than the olivines from the main dunite. Orthopyroxene constitutes 5% to 20% of the harzburgite and occurs as subhedral crystals that are

sometime partly altered. In some cases it shows zoning and may become host to exsolution lamellae of clinopyroxene occuring parallel to (010) or inclined to this plane within 10° to 15°. An orthopyroxene from harzburgite gave the following optical data :—

$\alpha = 1.665$, $\beta = 1.669$, $\gamma = 1.674$ and $2Vz = 74°$

This indicates a composition within enstatite range.

Magnetite and chromite are ubiquitous accessories in harzburgite. Chromite is much less in amount (always < 1%) than in dunites while magnetite has the same mode of occurrence as in dunites.

3. The Chromitites

Chromitites are those parts of dunite which contain chromite in sufficient amounts to set them apart from the normal dunite. These bodies exhibit a variety of shape and size, mode of aggregation and relative proportion of chromite and serpentine. The bodies of sufficient size and containing more than 50% chromite are being mined. Four of such mines namely 7 M.L., 7 M.L./1, 71 and 37, lie within the area mapped and are described below :—

(*i*) Mine 7 M.L. is located on a linear zone of vertical to subvertical lenses that widen downwards. Shearing and slickensiding effects are notable at the contact of chromitite body with the host rock, and also along certain other planes. Hydromagnesite has crystallized to fill fracture and crack openings. Chromite ore is of low-grade type, with chromite content varying from 50% to 75%. Schlieren banded variety of chromite is most common. It consists mostly of linear bands alternatively rich in chromite and serpentine, but sometime these bands may acquire spindle-shaped, lensoid or very rarely even curved forms. Another common variety is lenticular banded, consisting of small lenticles of chromite set in a groundmass of serpentine ; this variety trends parallel to the associated schlieren bands.

(*ii*) Mine 7 M.L./1 occurs in a geological setting similar to the mine 7 M.L. The chromite content of this mine varies from 50% to 75%.

(*iii*) The mine 71 is the most productive at present and its chromite content is always more than 90% ; most of the chromite is of massive variety. Exact shape of this chromite body is not known, but digging shows it to be a vein widening rapidly downwards.

(*iv*) Mine 37 contains massive chromite of a medium grade ; its production has declined.

(*v*) The "grapeshot ore" variety of chromite is found in an abandoned mine (Grid reference 932795). It is composed of rounded to subrounded chromite nodules in a groundmass of serpentine and *vice versa*. The individual nodules range from 0.2 inches to over 2 inches across. Sometimes the nodules are elongated with their longer axes roughly parallel to one another. The nodular chromite is restricted to specific bands that alternate with those rich in serpentine. The ore is low-grade due to high serpentine content.

Partial chemical analyses of chromite from different mines of the area show that the Cr : Fe ratio varies from 2.91 : 1 to 3.52 : 1 (Bilgrami, 1964). Under the microscope, euhedral to subhedral chromite grains generally have abundant shatter cracks occupied by fine-grained serpentine which is similar in optics to that found in the serpentinized dunites. A thin lining of magnetite is present along the chromite grain boundaries. Very fine, dusty magnetite is generally found scattered in serpentine.

4. The Pyroxenites

Monomineralic pyroxenites occur in the form of vertical to subvertical veins and dykes in dunite in the southeastern part of the area ; they are totally absent from the area covered by dunite-harzburgite complex. In thickness, they range from veins, only 6 inches across to dykes upto about 100 feet across, while their length ranges from about 6 feet to over half a mile. Generally their strike direction is NE-SW. The pyroxenites resist weathering better than the enclosing dunite, and therefore, they stand out as subparallel ridges. There is no evidence of chilling at the margins, rather gradational relation to dunite is shown. Blocks of serpentinized dunite sometimes occur partly or wholly enclosed in pyroxenites. The main rock is composed almost entirely of a dark green to light green prismatic clinopyroxene that can be seen with unaided eye. Under the microscope, they show hypidiomorphic granular pyroxene crystals with variable size and orientation. Material separated from a typical specimen gave the following optical data, suggesting the clinopyroxene to be a diopside :

$\alpha = 1.672$, $\beta = 1.679$, $\gamma = 1.698$, $2Vz = 54°$, $c \wedge Z = 42°$.

5. The Dolerites

The dolerite intrusions represent the final phase of igneous activity in the area. They occur as four main dyke swarms (Fig. 1) that cut the ultramafic as well as the sedimentary rocks. They are subparallel and vary in attitude from

NW-SE to WNW-ESE. Their thickness ranges from about 15 feet to 100 feet. Generally the margins show effects of chilling and all varieties of texture from ophitic to intersertal type are seen. Plagioclase makes up from 45 to 60 percent of the rock and ranges in composition from An_{40} to An_{65}. Diopsidic augite constitutes from 30% to 40% of the rock. Magnetite and picotite are the common accessories. Leucoxene is a common alteration product probably of ilmenite. Olivine as well as quartz are both absent.

Saussuritization effects of varying intensity are seen in some dolerites. In such rocks primary plagioclase is altered and cloudy but its ophitic relationship with the associated pyroxene is intact. The composition of this plagioclase ranges from An_{28} to An_{40}. Another crop of recrystallized plagioclase occurs as thin veinlets and fracture-fillings. It is fresh and its composition varies between An_{20} and An_{25}. Both generations of plagioclase form about 62% of the altered dolerites. Pyroxene, forming approximately 20% to 25% of the altered dolerites, shows alteration to bluish green hornblende and chlorite (3-8%) towards the grain margins. Epidote grains (5%) occur in clusters in the hornblende-free areas. Coarse-grained secondary calcite (5%) occurs in small veinlets and is commonly associated with the recrystallized plagioclase. Subhedral magnetite forms about 3% of the rock.

Some dolerites show small veins of pure white colour that occupy the release joints and consist of albite (55-60%) and lawsonite (40-45%). Albite (An_3) occurs as fresh, euhedral and spindle-shaped crystals that are rarely twinned. The lawsonite occurs in heaps of long and thin, radiating needles and project into the margins of the associated albite crystals. It's optical data is $\alpha = 1.665$, $\beta = 1.673$, $\gamma = 1.685$ $2Vz = 80°$. It appears to have crystallized slightly later than the albite, and perhaps was generated from the anorthite component of the plagioclase feldspar during the saussuritization stage.

6. Chemistry of Ultramafic Rocks

Two samples of dunite, one of harzburgite and one of pyroxenite from the area were chemically analysed (Table 1). This shows that harzburgite represents a phase richer in SiO_2, CaO and total iron, and poorer in MgO as compared to the dunites. The pyroxenite, on the other hand, contains much higher SiO_2 and CaO and much lower MgO and total iron as compared to the other rock types.

Petrogenesis

The present investigation shows that chromite was most probably the earliest mineral to crystallize and formed different types of magmatic concentrations. It continued to crystallize as disseminated crystals during solidification stages of the liquid that later on formed dunite and harzburgite. The latter conclusion is based on the fact that disseminated crystals of chromite have been found in these rocks, although much rare and not exceeding 1%. There are many a varieties of chromite concentrations. The schlieren banded variety forming the main

TABLE 1

Chemical Analyses of Ultramafic Rocks

Sample No.	8693	8101	8699	8700
Rock Name	Serpentinized Dunite	Serpentinized Dunite	Serpentinized Harzburgite	Pyroxenite
SiO_2	37.51	37.64	42.74	49.82
TiO_2	0.06	0.07	0.20	0.25
Al_2O_3	0.98	0.85	0.69	3.20
Fe_2O_3	3.87	3.79	1.68	0.80
FeO	3.65	3.60	6.99	4.63
MnO	0.01	0.03	0.02	0.00
MgO	40.86	41.04	36.25	16.92
CaO	0.13	0.08	3.01	23.16
Na_2O	0.08	0.07	0.20	0.45
K_2O	0.04	0.03	0.10	0.10
Cr_2O_3	0.61	0.57	0.40	0.00
CO_2	0.00	0.00	0.00	0.00
H_2O^+	11.59	11.84	7.50	0.89
H_2O^-	0.38	0.31	0.38	0.06
Total ..	99.77	99.92	100.16	100.28

Analyst : M. Nawaz Chaudhry

ore-body at mine 7 M.L., formed during early crystallization and gravitative accumulation of chromite that now is met with as bands alternating with olivine-rich bands (now serpentinized) of comparable dimensions. Such a crystallization is thought to be responsible for lenticular banded varieties of chromite as well. The chromite occupies its present position by virtue of later tectonic movements within the dunite mass. The slickensides at their mutual contacts show variation of trend and plunge over very small distances, thus indicating the past activity of many a small scale independent movements.

Massive chromite ore, with accessory serpentine, is found in the form of segregated and intrusive veins. Another variety is the "grapeshot ore" which has nodules of chromite embedded in serpentine "eyes" and *vice versa*. Shams (1964) explained this structure by proposing that at some stage during the cooling history of the magma, two immiscible liquids were co-existing, one chromite-rich and the other olivine-rich. Furthermore, the grapeshot ore shows distinct bands formed by joining together of chromite globules. This suggests that differentiation of the magma was still active at the time of liquid immiscibility.

Dunite crystallization is believed to have followed the chromite concentration. Initial composition of the ultramafic magma was highly magnesian, as indicated by the composition of olivine relicts in serpentinized dunite and by the chemical analyses as well. In the northern portion of the area, harzburgite is thought to have invaded the still hot dunite mass resulting in the intermixed dunite-harzburgite complex. At the time of harzburgite crystallization the iron content of the liquid had increased and Mg content decreased to some extent, but the main effects of differentiation were enrichment in silica and lime.

Both the dunite and harzburgite are now met with as serpentinized masses and this brings us to the problem of serpentinization and various effects resulting from it. Many workers have advocated significant volume increase during serpentinization. Hostetler et . al (1966) suggested that volume increases of 35 to 40 percent take place during serpentinization of peridotites, while Hess (1955) proposed a 25 percent increase in volume. Contrary to this, Thayer (1966) does not believe in volume increase and claims (p. 695) that :—

"Volume increases . . . . . should be easily detectible in rocks under suitable conditions."

In the area investigated, there does not appear to be any significant evidence of volume increase except for the shatter-cracks developed on microscopic scale in the chromite grains and the enstatite of the harzburgite. However, the freshness of the enstatite crystals suggests a limited action of solutions, so that shatter-cracks could have been produced either by slight expansion or by diastrophic movements. Near the mine 7 M.L. an exposure of strongly sheared and powdered serpentine and hydromagnesite is present ; this, however, may not be caused by expansion during serpentinization but is considered to have been an effect of rather unstable tectonic environments, that are characteristic of the Alpine-type ultramafics. Volume for volume replacement is evidenced by the dunite-harzburgite complex wherein layers and lenses of completely serpentinized dunite alternate with those of less serpentinized harzburgite. Also primary magmatic structures of chromite, e.g., schlieren banding, "grapeshot ore", presence of segregated and intrusive chromite veins, etc., are well-preserved and are continuous over long distances. These fragile chromite structures would have been completely disrupted in case of any significant expansion. All these features suggest that serpentinization, at least in the area investigated, is essentially a constant volume metasomatic process.

So far as the chemical changes during serpentinzation are concerned, the serpentines in thin sections show pseudomorphous habit, and the chemical changes involved can be explained by addition of silica-rich aqueous fluids. There is no evidence of Mg—or Si—metasomatism in the older sediments lying in the area or in those described by Bilgrami (1956) lying just outside the intrusion. The chemical reactions may be represented by the equations described by Thayer (1966, p. 698). Connate waters available during geosynclinal phase of the orogeny might be responsible for the removal of about 30 percent material as required by these equations, and solutions from other sources may also be effective ; this reduction may counterbalance any expansion during serpentinization. The end product in every case includes the same serpentine minerals and magnetite dust from either harzburgite or dunite. Therefore, there seems to have occurred no major chemical fluctuation in the process of serpentinization or physical conditions prevailing during the process.

Pyroxenites crystallized after the formation of harzburgite and are restricted to serpentinized dunites only. They show gradational contacts and sometimes enclose blocks of dunite. Some of the blocks are found surrounded by pyroxenite from three sides, the fourth side being continuous with the host dunite. These features show their origin by replacement, and not by normal crystallization

from a peridotite magma. Their formation is thought to have been controlled by the tectonic conditions prevailing at that time with the axis of maxmimum stress trending N40°E and producing tension joints. These joints were filled by highly siliceous and lime-rich solutions that ascended from depths and formed pyroxenite veins by replacement of the dunite.

Post-ultramafic dolerite dykes were intruded after a tension was developed trending N50°W. The rocks crystallized previously, were pushed aside elastically and tension cracks developed in a NW-SE direction. The dolerites show chilled margins, and sometimes are extensively saussuritized. They are relatively insignificant in the total bulk. Bilgrami (1956) concludes that dolerite magma represented the residual liquid of intermediate composition left after normal crystallization of basic magma. However, the lack of basic rocks in significant amounts and distinctly later intrusive relationships of the dolerites suggest it to be an independent intrusion.

SEDIMENTARY ROCKS

An outcrop of argillaceous and calcareous fossiliferous rocks is found in the southwestern part, generally having a strike of N80°W and dip of 19°SSW. For most of the part, these rocks are covered by a thin layer of Recent to sub-Recent conglomerate. The sequence is conformable and structurally not much disturbed. A measured section is subdivided into the following horizons (Fig. 2) from top downwards :—

Horizon	Description	Thickness
L	Cream-yellow, well-bedded limestone very rich in gastropod, pelecypod and brachiopod fauna.	20′
K	Carbonaceous shales with coal bands and plant fossils, also with limestone and gypsum at places : succeeded downwards by a 4 to 5 feet thick bed of yellowish creamy-white limestone very rich in oyster shells : further downwards having a 10 feet thick shale bed without coaly layers.	30′
J	Oyster limestone, about 80% composed of fossil shells of *Ostrea* and other pelecypoda. The fossils are bounded by a clayey calcareous matrix.	5′
I	Light green slaty coloured shales with thin laminations of carbonaceous matter.	10′
H	Yellow coloured coquina limestone, composed chiefly of the fossils of the genus *Ostrea*, Turitella, etc. The fossils are set in a mixed calcareous and argillaceous matrix.	5′
G	Carbonaceous and gypsiferous shales containing thin coal laminations rich in leaf-impressions. This horizon also contains a yellow coloured fossiliferous limestone.	30′
F	Light grey marl with small gastropod fossils.	10′
E	Yellow coloured limestone with some gypsum crystals and pyrite nodules.	3′
D	Whitish limestone with very small gastropods and pelecypods. These fossils range in size from 0.05 inches to more than 0.3 inches.	10′
C	Black coloured shales.	10′
B	Cream yellow Ostrea-bearing limestone.	3′
A	Light greenish grey shales, unfossiliferous, splintry and rather poorly consolidated.	10′

The following molluscan genera have been recognized from this sedimentary sequence :—

Ficus, Voluta, Pagodea ; Turitella, Corthium, Carramites ; Neritaria ; Rapbispira; Spondylus, Arctica, Crassatellites, Ostrea.

The fossils indicate an Upper Cretaceous age. The environments of deposition were shallow water marine with abundance and variety of fauna and flora.

A conglomerate bed of Recent age occurs as small outcrops on the sides of the present-day streams ; except in some cases, when this bed extends for long distances in length and breadth. This well-consolidated and structurally undisturbed rock exhibts a good development of cross-bedding, graded-bedding and rock-benches ; and shows that present day streams have eroded below the level of previous plain, after a rejuvenation phase. At some places, shallow and broad caves are developed below the conglomerate bed.

Pebbles are predominant (65-80%) over the cement and are angular to subangular rock fragments from less than 1 inch to 10 feet or more across. Source of these pebble lies very near, usually at a distance of less than 50 feet. Pebbles are broken pieces of serpentinized dunite, harzburgite, pyroxenite, dolerite, calcareous sediments, laterite, etc., and their lithology and mineralogy is exactly similar

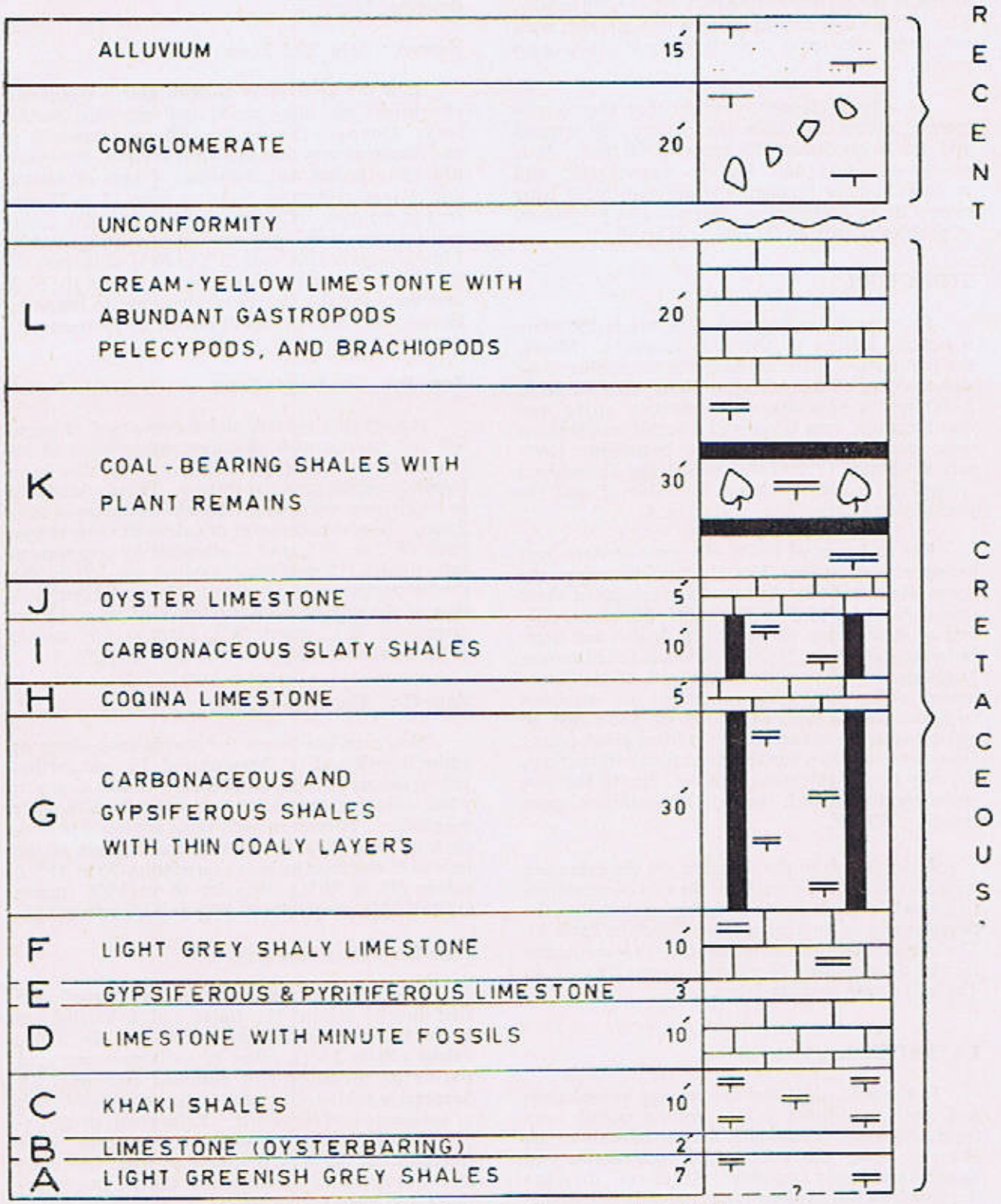

Fig. 2. Litho-stratigraphic column of sedimentary rocks in Palaklara area.

to that of the corresponding rock-types lying nearby. The pebbles are embedded in a fine-grained, well-indurated, calcareous cement, rarely of argillaceous nature.

An alluvial deposit, younger than the conglomerate, occurs alongside the present-day streams and has a maximum thickness of 50 feet. It is poorly stratified and slightly consoliated, and contains angular fragments of different rocks lying closely in an argillaceous matrix. The proportion of pebbles relative to the matrix is small.

STRUCTURE

Prominent development of joints is the main structural feature of the igneous rocks. Mostly the joints show plane surfaces but sometime poor slickensiding effects are seen along their surfaces. 2,600 joint-measurements comprising strike and dip directions were taken and orientation diagrams were prepared (Fig. 3). The prominent joint-sets developed in different rock-types as inferred from Fig. 3 are tabulated in Table 2 and the stress interpretation is given in Fig. 4

For rock-types I to III, the greatest stress axis (compressive) strikes N40°E thus bisecting the acute angle made by the two diagonal sets of shear joints (Nos. 1 and 2 in Table 2). However, only one of these is seen developed in dunites and harzburgites. Joint set No. 3 represents the extension joints developed parallel to the axis of maximum stress. After this, stress conditions are supposed to have changed so that the joint set No. 4 may be either a release joint-set due to indirect development from compression when the stress field withered out, or, may be the extension joint-set, due to the new stress conditions with the axis of maximum stress trending N50°W.

Joints (set 4) in the dolerites are the extension type that developed parallel to the axis of maximum stress; while shear joints are represented by the development of another joint set (No. 1 in Table 2). The removal of these stress conditions is evidenced by the development of release joints (No. 5 in Table 2) across dolerite dykes.

LATERITES

In the area, the laterites are quite conspicuous and show a distinct colour zoning visible even from a distance. Generally, they form peaks of the hillocks along the contact between dunite and dunite-harzburgite complex. At places, they are overlain by a bed of almost pure, massive magnesite. Field and petrographic characters of these zones are described below :—

Zone-A : The Red Zone

It is the uppermost horizon and is composed of a bright red, fine-grained and somewhat porous rock. Quartz is the chief constituent (about 50%) and occurs as very fine, anhedral crystals, often stained rusty brown with limonite. Fibres of altered and stained serpentine make up from 15 to 25 percent of the rock. Calcite occurs as very fine grains and stringers, varying in amount from 10% to 14%. Limonite makes up from 15% to 20% while magnetite and chromite each form about 1.5% of the rock and show variable degree of alteration to limonite. Occasionally a few relics of olivine or pyroxene are present.

Zone-B : The Purple Zone

It underlies zone A and is composed of purplish red laterite with abundant white veins of intergrown, coarse calcite and quartz crystals in an hypidiomorphic granular texture. These veins range in width from microscopic dimensions to more than 2 feet. Modal percentage of calcite in veins ranges from 65% to 80% and is attended by complimentary quartz. Sometimes cavities are left in the central portions of such veins. The modal composition of the laterite rock (exclusive of veins) shows serpentine 42%, quartz 8%, limonite 8%, calcite 40%, magnetite 1.5% and chromite 0.5%.

Zone C : The Yellow Zone

This zone lies below the purple zone along its entire length and is characterized by an earthy-yellow colour of the laterite rock. It also contains white calcite-quartz veins, occasionally with some magnesite. Hlowever, such veins are lesser in bulk than in zone B. The mineral constituents of the laterite of this zone include : serpentine (35 to 45%), calcite (35 to 40%), limonite (6 to 8%), quartz (12 to 15%), magnetite (0.5%) and chromite (1%).

Zone D : The Green Zone

This is the lowermost and the least altered zone that directly overlies the dunite and/or harzburgite bedrock. It contains serpentine (60 to 70%), calcite (20 to 25%), relics of orthopyroxene and olivine (9 to 10%) and chromite (0.5 to 1%). Serpentine exhibits the mesh texture composed both of antigorite and chrysotile. Relic grains of pyroxene and olivine are fractured and shattered while fractures cut the rock profusely as well. All such fractures are filled by subhedral calcite, and sometimes are lined by limonite. Pyroxene is either enstatite or a Mg-rich bronzite and shows perfect

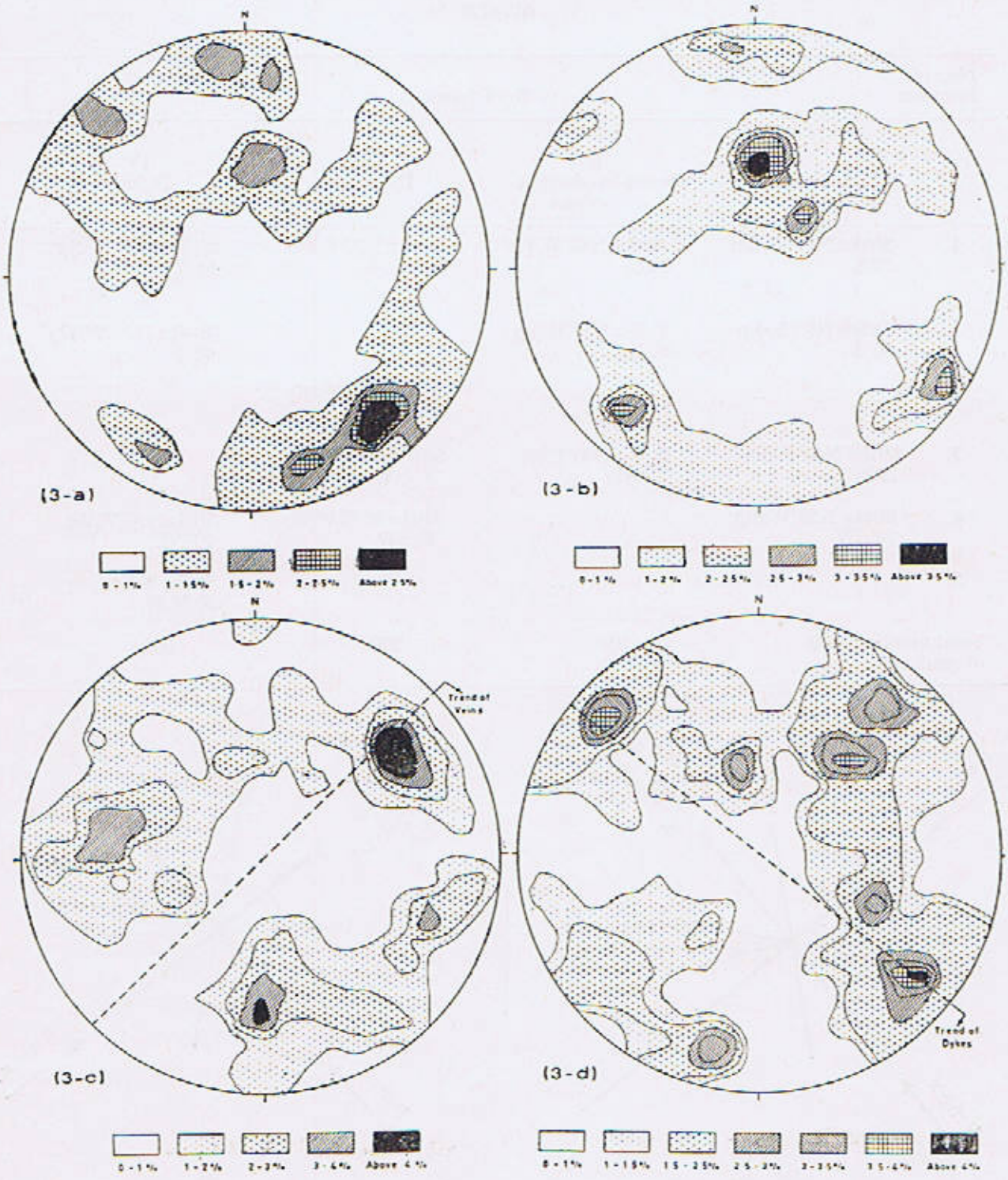

Fig. 3. Joint-orientation diagrams for :

(3-a) Serpentinized dunite ; (3-b) Dunite-harzburgite complex ; (3-c) Pyroxenite ; (3-d) Dolerite.

TABLE 2

No. of Joint-set	Rock types.			
	I Serpentinized dunite	II Dunite-harzburgite complex	III Pyroxenite	IV Dolerite
1.	Strike N85°W/dip 80°S to Strike N85°E/dip 60°S	Strike N80°W/dip 30°S to Strike N85°E/dip 80°S	Strike N80°E/dip 60°N	Strike N87°W°dip 40°S to Strike N90°W/dip 40°S
2.	..	..	Strike N10°E/dip 60°WNW	..
3.	Strike N40°E/dip 75°NE	Strike N40°E/dip 80°NW	Strike N40°E/dip 70°NW	..
4.	Strike N50°W/dip 70°SW	..	Strike N50°W/dip 80°SW	StrikeN50°W/dip 70°NE
5.	..	..	..	Strike N40°E/dip 70°N.W.
Total number of readings	900	600	500	600

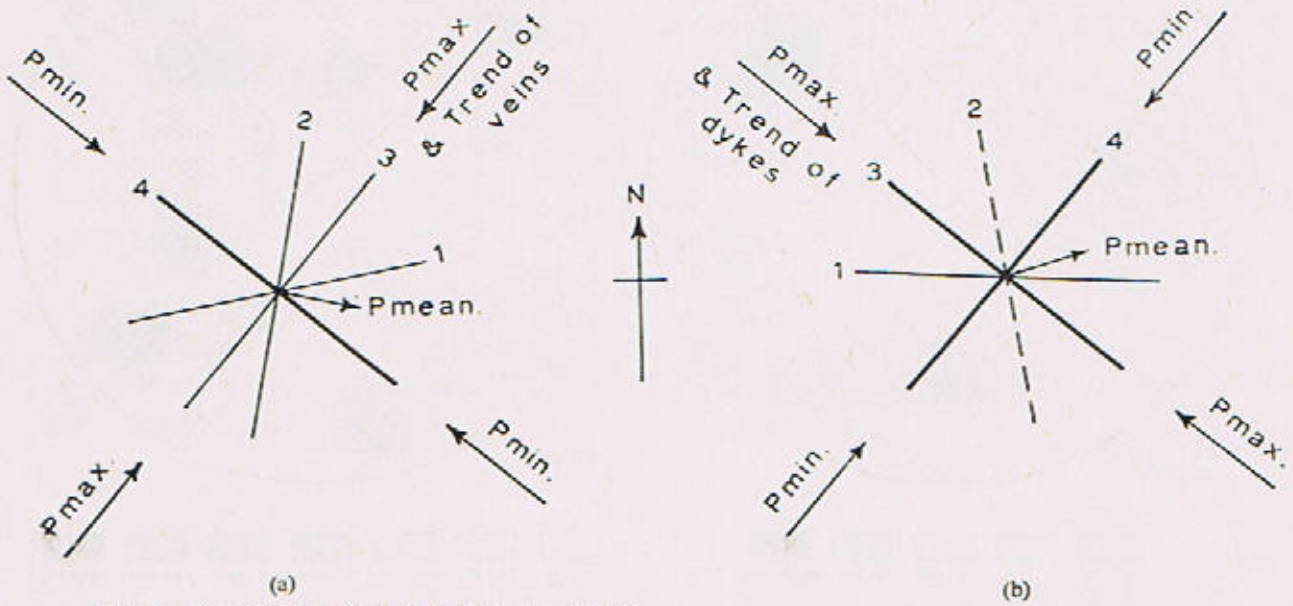

(a) (b)

Fig. 4. Stress interpretation of joint-sets measured in :
(a) Pyroxenite veins ;
(b) Dolerite dykes.

(110) cleavage. Limonite is present in accessory amounts and shows alteration to magnetite near margins. This zone passes gradually at the base into the ultramafic bed-rocks.

Chemistry of the Laterites

Chemical analyses of samples from four laterite zones are presented in Table 3. Data for zone B is not fully representative, because the sample analysed contained amount of white veins above average. The chemical data shows a decrease in silica and increase in magnesia downwards. Lime shows an initial increase and a decline afterwards whereas the content of total iron shows an increase after a gradual decrease.

Genesis of the Laterites

The laterites represent the decomposition products of dunite and harzburgite under a subtropical climate, possibly with alternating dry and wet seasons. The rain water, charged with CO_2 and having a pH more than 5.3 is known to attack the ferromagnesian minerals strongly, forming carbonates and bicarbonates of Ca, Mg, Fe and silicic acid. Magnesium concentrated at the top as magnesite, while Ca, Fe and silicic acid concentrated below the magnesite cap in the zone-A, the red zone. Silica precipitated by flocculation in the zone A, between pH 4.7 and 4.9. But this range of pH should prevent a large-scale precipitation of calcite in this zone. However, the petrographic and chemical evidence shows that larger quantities ot silica, lime and iron oxide have concentrated in this zone compared with the original dunite or harzburgite. The zone A is succeeded downwards by zone B, the purple zone ; and zone C, the yellow zone. These zones represent a moderately decomposed serpentinized dunite or harzburgite where large amounts of calcium carbonate and relatively smaller amounts of silica, hydroxides and iron have concentrated. Zone D, the lowermost zone, is the least altered and consists mostly of shattered serpentinized dunite or harzburgite with smaller amounts of calcite.

In the comparable laterites elsewhere (Percival, 1965) only three zones of regolith could be distinguished. The zone A, the uppermost zone, contains high amounts of silica as quartz, and limonite. Zone B, the middle zone is characterized by the partly decomposed rock with calcite and some quartz in veins. Zone C, the lower most, shows very little alteration.

TABLE 3

Chemical analyses of samples from different zones of laterite.

	Zone A	Zone B	Zone C	Zone D
Sample Nos.	8664	8666	8653	8649
SiO_2 ..	67.44	18.64	34.86	31.46
TiO_2 ..	0.00	0.00	0.03	0.02
Al_2O_3 ..	1.05	1.44	1.66	1.67
Fe_2O_3 ..	9.12	6.47	4.68	5.91
FeO ..	0.70	0.68	0.82	1.40
MnO ..	0.07	0.04	0.01	0.04
MgO ..	6.22	11.93	20.72	29.69
CaO ..	7.18	31.64	17.64	11.92
Na_2O ..	0.20	0.19	0.16	0.14
K_2O ..	0.25	0.08	0.15	0.11
Cr_2O_3 ..	0.68	0.48	0.46	0.31
CO_2 ..	5.33	26.02	14.29	10.51
H_2O^+ ..	1.89	1.94	3.92	6.39
H_2O^- ..	0.21	0.31	0.35	0.84
Total : ..	100.34	99.86	99.75	100.41

Analyst : M. Nawaz Chaudhry

In the Palak Lara area, the red zone and uppermost part of the purple zone correspond to the zone A described by Percival. Similarly the lower part of the purple zone and the yellow zone of this area correspond to the zone B of other areas ; and zone D of Palak Lara corresponds to the zone C in the case of other areas.

ACKNOWLEDGEMENTS

The authors are grateful to Prof. F.A. Shams Geology Department, Punjab University for his constructive criticism and guidance during writing of this paper. Thanks are also due to Mr. G. Sarwar Alam for his help during the course of field study.

REFERENCES

Bilgrami, S.A. 1956 Mineralogy and Petrology of the Central Part of the Hindubagh Igneous Complex, Hindubagh Mining District, Zhob Valley, West Pakistan, *Rec. Geol. Surv.* Pakistan, **10**, No. 2-C.

Bilgrami, S.A. 1964 The regional distribution of chemically different chromites from Zhob Valley, West Pakistan, *Geol. Bull. Punjab Univ.*, **4**, 1-16.

Hunting Survey Corporation 1960 RECONNAISSANCE OF GEOLOGY OF PART OF WEST PAKISTAN Colombo Plan Co-operative Project, Government of Canada.

Page, N.J. 1967 Serpentinization considered as a constant volume metasomatic process : A discussion. *Amer. Min.* **52,** 545-548.

Percival, F.G. 1965 The laterite iron deposits of Conakry. *Bull. Inst. Min. Met.* **74,** 429-462.

Shams, F.A. 1964 Structures in chromite bearing serpentinites, Hindubagh, Zhob Valley, West Pakistan. *Econ. Geol.* **59,** 1343-1347.

Thayer, T.P. 1966 Serpentinization considered as a constant volume metasomatic process. *Amer. Mineral.* **51,** 685-710.

Thayer, T.P. 1967 Serpentinization considered as a constant volume metasomatic process : *Reply. Amer. Mineral.* **52,** 549-552.

Turner, F.J. and Verhoogen, J. 1960 IGNEOUS AND METAMORPHIC PETROLOGY. McGraw Hill, New York.

NOTICES, ABSTRACTS AND REVIEWS

A NOTE ON THE CRETACEOUS-TERTIARY BOUNDARY IN HAZARA, WEST PAKISTAN.

Middlemiss (1896, pp. 39-40) described GREY LIMESTONE (proposed as KAWAHGAR FORMATION by the Stratigraphic Committee of Pakistan, 1969), of doubtful age, which underlies the Paleogene formations in the Hazara District of West Pakistan. Latif (1962, p. 57) pointed out that the limestone belongs to the Upper Cretaceous age because of the presence of foraminifera *Globotruncana*, *Heterohelix*, *Rugoglobigerina* and *Pseudotextularia*, which he identified by examining thin sections of the rock from certain localities, namely, Darband, Dungagali and Khan.

If we consider the lithological characteristics of the KAWAHGAR FORMATON in the district, we find that the formation is present, as a hard and very fine-grained, well-bedded, light grey limestone for which reasons the foraminifera can only be examined under thin sections. However, at some localities, for example at Changlagali (1° 43 G/5) along the Murree-Nathiagali road, which is regarded here as one of the reference sections; nearly 1½ miles east of the Jabri Forest Rest House along the Lora-Maqsood road (1° 43 G/1), this formation is predominantly represented by very thinly-bedded pale weathering marls which, on treatment with peroxide, yield loose fossil specimens. It is from the latter locality that the foraminifera, because of their better preservation, mentioned below are discussed and illustrated (Coll. Aftab, 1966, sample 9125) for the first time.

The boundary between the Kawahgar Formation and the overlying dense grey, nodular limestone, the LOCKHART LIMESTONE (name proposed by the Stratigraphic Committee of Pakistan, 1969) is marked by a laterite band of few feet in thickness. This band is very conspicuous in the field and can be used as a marker bed for the purpose of mapping.

The sampling from the marls of the Kawahgar Formation from the above mentioned localities, has shown the presence of well-preserved globotruncanids. The species/subspecies encountered are *Globotruncana linneiana*, *G. fornicata*, *G. ventricosa* and *G. concavata carinata*. Moreover, *Heterohelix globulosa*, *H. reussi* and *Rugoglobigerina rugosa* also form part of the planktonic association. *Rugoglobigerina rugosa*, recorded here as few specimens, however, has not been illustrated. This assemblage suggests that the Kawahgar Formation ranges from Coniacian upto the Campanian.

Reviewing the Cretaceous-Tertiary succession in Hazara, we find that the Kawahgar Formation marks the end of the Cretaceous period. The Paleocene begins with a new transgressive phase which is represented by nodular limestone, the Lockhart Limestone, that overlies the Kawahgar Formation. The Lockhart Limestone shows an abrupt change in lithology as well as in the faunal composition. The pelagic foraminiferal association of the Kawahgar Formation is entirely absent and the fauna is now composed of the benthonic larger foraminiferal species such as *Lockhartia haemei*, *Miscellanea miscella*, *Ranikothalia soldadensis* (=*R. sindensis*), *Daviesina khatiyahi* and *Discocyclina ranikotensis* suggesting an Upper Paleocene age.

At this stratigraphic level, similar lithologic as well as paleontologic changes have been observed by the author in the Kala Chitta and the Samana Ranges pointing towards a similar stratigraphic break. Further research is, however, in progress to discuss, in detail, the foraminiferal assemblages of these regions and their stratigraphic implications.

From the micropaleontological investigations, it appears that the laterite represents a marked unconformity between the Cretaceous and the Paleocene deposits in Hazara, whereas continuous succession between the Cretaceous and the basal Tertiary in Sind and Baluchistan has been discussed by Nagappa (1960).

Following the proposals of the Stratigraphic Committee of Pakistan made at the 9th meeting at Quetta in 1969, and applying to Hazara, Kala-Chitta and Samana, we may correlate the Upper Cretaceous and the basal Tertiary sequence as follows, as established by earlier authors in these regions.

Formation	Age	Hazara		Kala Chitta	Samana
		(Middlemiss, 1896)		(Cotter, 1933)	(Davies, 1930)
LOCKHART LIMESTONE	Paleocene	Nummulitic Series	Nummulitic* Limestone	Hill Limestone*	Lockhart Limestone and Hangu Breccia
					Hangu Shale**
			variegated sandstone and clay with coal	ferruginous pisolite	Hangu Sandstone**
				—Unconformity—	
KAWAHGAR FORMATION	Cretaceous		Grey Limestone	Shales north of Kawa Gar	Lithographic Limestone

Correlation of the Upper Cretaceous and basal Tertiary Succession.

SYSTEMATICS

Genus HETEROHELIX Ehrenberg, 1853

Heterohelix globulosa (Ehrenberg)

Plate 1, figure 5

Textularia globulosa EHRENBERG, 1840, Abh. Akad. Wiss. Berlin, p. 135, pl. 4, figs. 2, 4-5, 7-8.

Gumbelina globulosa (Ehrenberg), EGGER, 1889, Abh. Akad. Wiss. Munchen, cl.2, vol. 21, p. 32, pl. 14, fig. 43.

Heterohelix globulosa (Ehrenberg), MONTANARO GALLITELLI, 1957, U.S. Nat. Mus. Bull., no. 215, p. 137, pl. 31, figs. 12-15; SCHEIBNEROVA, 1963, Geol. Sborn., vol. 14, no. 2, p. 264, fig. 80; TAKAYANAGI, 1965, Tohoku Univ. Sci. Rep., 2nd Ser. (Geol.), vol. 36, no. 2, p. 195, pl. 20, fig. 1.

Remarks. Specimens showing initial coiling as shown by Montanaro Gallitelli (1957) of the microspheric generation, are not encountered. Our specimens resemble closely with that as figured by Scheibnerova (1963) from the Cretaceous of the Klippen belt, Czechosloakia.

Heterohelix reussi (Cushman)

Plate 1, figure 6

Gumbelina reussi CUSHMAN, 1938, Contr. Cush. Lab. Foram. Res., vol. 14, pt. 1, p. 11, pl. 2, figs. 6-9 ; 1946, U.S. Geol. Surv., Prof. paper, no. 206, p. 104, pl. 44, figs. 18-19.

Heterohelix reussi (Cushman), PESSAGNO, 1967, Paleontogr. Americana, vol. 5, no. 37, p. 263, pl. 85, figs. 1-9; pl. 86, figs. 1-2; DOUGLAS, 1969, Micropal., vol. 15, no. 2, p. 158, pl. 11, fig. 15.

Remarks. Our Specimens are sufficiently well preserved to allow specific determination.

Genus GLOBOTRUNCANA Cushman, 1927

Globotruncana linneiana (D' Orbigny)

Plate 1, figures 1a-c

Rosalina linneiana D' ORBIGNY, 1939, in Ramon de la Sagra, Hist. Phys. Pol. Nat. Cuba, Paris, vol. 8, p. 101, pl. 5, figs. 10-12.

*Part of the formation belongs to the Paleocene.

**Collectively Named as Hangu Formation by the Stratigraphic Committee and which is absent in Hazara and Kala Chitta.

Globotruncana linneiana (D' Orbigny), BRONNIMANN & BROWN, 1955, Eclog. Geol. Helvet., vol. 48, no. 2, p. 540, pl. 20, figs. 13-17 ; pl. 21, figs. 16-18 ; NAGAPPA, 1959, Micropal., vol. 5, no. 2, p. 179, pl. 6, fig. 6 ; VAN HINTE, 1965, Proc. Kon. Nederl. Akad. Wetensch., Ser. B., vol. 68, no. 1, p. 23, pl. 1, fig. 3 ; CARON, 1966, Rev. Micropal., vol. 9, no. 2, p. 83, pl. 5, fig. 3.

Globotruncana (Globotruncana) linneiana linneiana (D' Orbigny), VAN HINTE, 1965, Proc. Kon. Nederl. Akad. Wetensch., Ser. B., vol. 68, no. 2, p. 84, pl. 2, fig. 4.

Globotruncana lapparenti Brotzen, NAGAPPA, 1959, Micropal., vol. 5, no. 2, p. 179, pl. 6, fig. 8.

Remarks. Globotruncana lapparenti, as illustrated by Nagappa (1959, pl. 6, fig. 8.) from the Parh Limestone of Upper Cretaceous near Quetta (Pakistan) is regarded here to belong to *Globotruncana linneiana*.

Globotruncana fornicata Plummer

Plate 1, figures 2a-c

Globotruncana fornicata PLUMMER, 1931, Univ. Texas, Bull., no. 3101, p. 198, pl. 13, figs. 4-6 ; DALBIEZ, 1955, Micropal., vol. 1, pp. 165-166; BARR, 1962, Palaeont., vol. 4, p. 570, pl. 69, fig. 6; pl. 72, figs. 1-2 ; VAN HINTE, 1965, Proc. Kon. Nederl. Akad. Wetensch., Ser. B., vol. 68. no. 1, p. 21, pl. 1, fig. 1; pl. 2, figs. 1-2; TAKAYANAGI, 1965. Tohoku Univ. Sci. Rep., 2nd Ser. (Geol.), vol. 36, no. 2, p. 214, pl. 24, fig. 4.

Globotruncana (Globotruncana) fornicata Plummer, VAN HINTE, 1965, Proc. Kon. Nederl. Akad. Wetensch., Ser. B., vol. 68, no. 2. p. 83, pl. 1, fig. 6.

Remarks. The elongate, crescent-shaped chambers on the spiral side together with the so-called "cone in cone" arrangement of the peripheral keels—characters which have been mentioned by several authors for this commonly recorded species—can be seen in our material.

Globotruncana concavata carinata Dalbiez

Plate 1, figures 3a-c

Rotalia concavata BROTZEN, 1934, Deutsch. Ver. Palastinas, Zeitschr., Leipzig, vol. 57, p. 66, pl. 3, fig. b.

Globotruncana concavata (Brotzen), LEHMANN, 1962, Notes Serv. Géol. Maroc, vol. 21, p. 147. pl. 6, figs. 2, 4; EDGELL, 1962, Rev. Micropal., vol. 1, no. 2, p. 41, pl. 1, figs. 1-5.

Globotruncana (Globotruncana) ventricosa carinata DALBIEZ, 1955, Micropal., vol. 1, p. 168, fig. 7.

Globotruncana concavata carinata Dalbiez, SCHIEBNEROVA, 1968, Rev. Micropal., vol. 11, no. 1, p. 49, pl. 2, figs. 1-7; Acta Geol. Geogr. Univ. Comenianae, (Geol.), no. 17, p. 72, pl. 14, fig. 4; pl. 15, figs. 1-6 ; STURM, 1969, Rocznik Pol. Tow. Geol., vol. 39, no. 1-3, p. 131, pl. 11, fig. 4.

Globotruncana asymetrica SIGAL, 1952, 19th Internat. Géol. Congr., Alger, Monogr. Région., Ser. 1, no. 26, p. 34, fig. 35.

Remarks : Specimens identified as *Globotruncana concavata carinata* perfectly agree with those as described by various authors. This form has been commonly misidentified with *Globotruncana ventricosa* in the literature. In our material both the forms are distinct. *Globotruncana concavata carinata* is characterised by the presence of two closely spaced peripheral keels shifted towards the sprial side which is concave, while the umbilical side is strongly inflated and the elevated portion shows the presence of a third keel, whereas, *Globotruncana ventricosa* shows spiroconvex test and the third keel is absent.

EXPLANATION OF PLATE 1

(*a*) Spiral view ; (*b*) Apertural view ; (*c*) Umbilical view.

Figure 1 *Globotruncana linneiana* (D'Orbigny)

Figure 2 *Globotruncana fornicata* Plummer

Figure 3 *Globotruncana concavata carinata* Dalbiez

Figure 4 *Globotruncana ventricosa* White

Figure 5 *Heterohelix globulosa* (Ehrenberg)

Figure 6 *Heterohelix reussi*

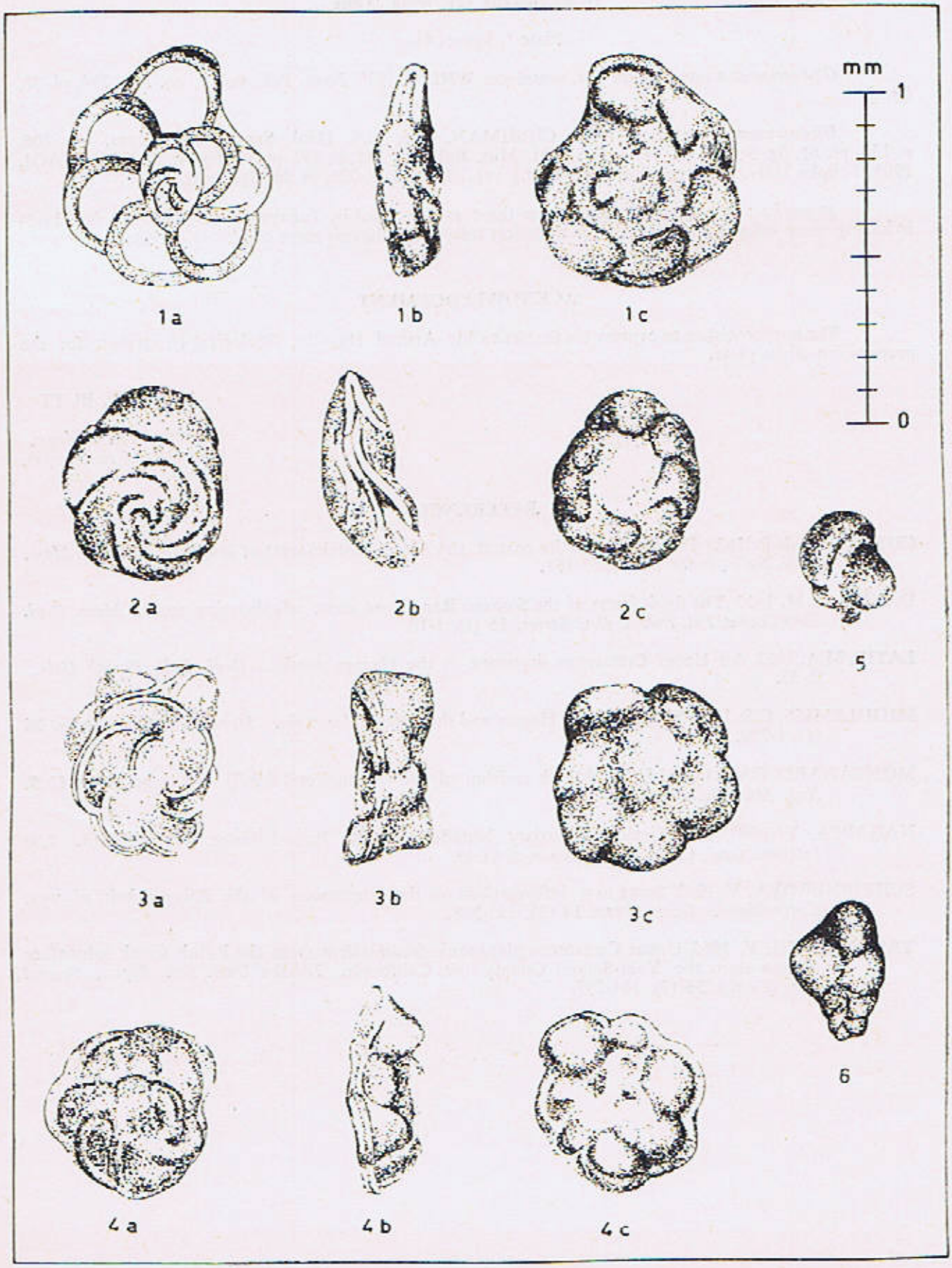

Plate 1. (a) Spiral view. (b) Apertural view. (c) Umbilical view.

Globotruncana ventricosa White

Plate 1, figures 4a-c

Globotruncana canaliculata var. *ventricosa* WHITE, 1928, Jour. Pal., vol. 2, no. 3, p. 284, pl. 38, fig. 5.

Globotruncana ventricosa White, CUSHMAN, 1946, U.S. Geol. Surv., Prof. Paper, no. 206, p. 150, pl. 62. fig. 3; BOLLI, 1957, U.S. Nat. Mus. Bull., no. 215, p. 457, pl. 13, fig. 4; TAKAYANAGI, 1965, Tohoku Univ. Sci. Rep., 2nd Ser. (Geol.), vol. 36, no. 2, p. 226, pl. 29, figs. 1a-d.

Remarks : Our specimens differ from those as illustrated by Takayanagi (1965, pl. 29, figs. 1a-d) in having more inflated chambers on the umbilical side, and in having more convex spiral side.

ACKNOWLEDGEMENT

The author wishes to express his thanks to Mr. Arshad Hussain, Geological Illustrator, for the preparation of the plate.

AFTAB A. BUTT

Department of Geology,
University of the Punjab,
Lahore.

REFERENCES

COTTER, G. de P. 1933 The geology of the part of the Attock district west of longitude 72°45′ E. *Mem. Geol. Surv., India*, **55** (2), 63-161.

DAVIES, L.M. 1930 The fossil fauna of the Samana Range and some neighbouring areas. *Mem. Geol. Surv., India, Pal. Indica, New Series*, **15** (1), 1-15.

LATIF, M.A. 1962 An Upper Cretaceous limestone in the Hazara district. *Geol. Bull. Panjab Univ.*, **2**, 57.

MIDDLEMISS, C.S. 1896 The geology of Hazara and the Black Mountain. *Mem. Geol. Surv., India*, **26** (1), 1-290.

MONTANARO GALLITELLI, E. 1957 A revision of the foraminiferal family Heterohelicidae. *U. S. Nat. Mus. Bull.*, 215.

NAGAPPA, Y. 1960 The Cretaceous-Tertiary boundary in the India-Pakistan Sub-continent. *21st Internat. Geol. Congr., Copenhagen*, 5, 41-49.

SCHEIBNEROVA, V. 1963 Some new informations on the Cretaceous of the Klippen belt of west Carpathians. *Geol. Sborn.* **14** (2), 221-268.

TAKAYANAGI, Y, 1965 Upper Cretaceous planktonic foraminifera from the Putah Creek subsurface section along the Yolo-Soland County line, California. *Tohoku Univ. Sci. Repts., Second Ser. (Geol.)*, **36** (2), 161-237.

A NOTE ON THE RELATIONSHIP BETWEEN PHYSICAL PROPERTIES AND CHEMICAL COMPOSITION OF PREHNITES AS STUDIED FROM THE CONTACT SKARNS OF THE MELDON APLITE, DEVONSHIRE, SOUTH WEST ENGLAND.

NTRODUCTION

A Na-Li aplite dyke, 60 to 80 feet thick, occurs at the Meldon quarry, Devonshire, about three quarters of a mile southwest of the Dartmoor granite (Worth, 1920). South of the main Railway Quarries, thea plite forms contact skarns with a doleritic dyke. These skarns contain prehnite as a vein mineral which had developed as a result of hydrothermal processes.

The mineral was separated from the associated diopside, hornblende, calcite, chlorite, sulphides etc. by combined heavy liquids and magnetic methods. Chemical analyses were carried out by wet techniques and the refractive indices were determined by single variation method using sodium light (accuracy ± 0.001). The cell dimensions were determined on a diffractrometer using Cu Ka radiation and silicon as internal standard. The entire data is given in Table No. 1 along with their sepcific gravities and the number of ions on the bais of 24 (0, OH). The prehnites show a variety of colour and somewhat anomalous optical properties such as wavy and bow-tie like extinction etc.

RELATIONSHIP OF PHYSICAL PROPERTIES AND CHEMICAL COMPOSITION

The chemical data show that, with increase in the total iron content, colour of the prehnites changes from white through pale and greenish yellow to light green. Furthermore, there is evidence of the replacement of silicon by aluminium in all the specimens, as was also noted by Nuffield (1943) in the case of prehnites from Ashcroft, British Coloumbia. The variation in the water content and its amount being less than required by the structural formula may be due to errors inherent in the analytical procedures (Deer *et al.*, 1962).

The variation trends of n_Y, $2V_Y$ and specific gravities in relation to $(Fe^{2+}+Fe^{3+})$ ionic contents have been studied graphically (Fig. 1) using additional data from Deer et al. (op. cit., p. 264). A direct linear variation is displayed by n_Y and and specific gravities while an inverse relationship is shown by the optic axial angles, $2V_Y$.

The cell dimension *c* increases with the increase in the (OH) content of the prehnites but the *a* and *b* dimensions show no regular relationship with ionic substitutions such as aluminium for ferric iron or silicon.

Table 1

Prehnite analyses.

	H5 White	P18 (light	M126 pale)	M18B greenish yellow	L.G.P. Light green
SiO_2	42.96	42.54	42.62	43.56	42.95
TiO_2	0.12	0.12	0.42	tr.	tr.
Al_2O_3	25.46	25.10	25.13	24.43	23.62
Fe_2O_3	0.00	0.50	0.41	0.47	2.10
FeO	0.06	0.06	0.11	0.10	0.40
MgO	0.02	0.02	0.07	0.16	0.09
CaO	26.82	26.78	26.68	27.01	26.42
Na_2O	0.16	0.28	0.19	0.12	0.02
K_2O	0.05	0.08	0.03	0.04	0.01
MnO	0.12	0.12	0.18	0.02	0.39
H_2O^+	4.11	4.15	4.03	4.36	4.17
H_2O^-	0.13	0.15	0.12	0.02	0.12
Total :	100.01	99.90	99.99	100.29	100.29
Physical Constants					
n_α	1.613	1.615	1.614	1.615	1.618
n_Y	1.634	1.636	1.634	1.637	1.651
$2V_Y$	71°	70°	72°	69°	65°
D	2.91	2.93	2.92	2.92	2.96
'*a*' A°	4.60	4.60	4.60	—	—
'*b*' A°	5.52	5.52	5.53	—	—
'*c*' A°	18.42	18.43	18.39	—	—

(Contd.)

Number of ions on the basis of 24 (9, OH)

Si	5.928	6.000	5.894	6.000	5.900	6.000	5.985	6.000	5.956	6.000
Al	0.072		0.106		0.100		0.015		0.044	
Al	4.069	4.082	3.993	4.057	4.002	4.092	3.943	3.993	3.817	4.035
Fe^{3+}	0.000		0.052		0.046		0.050		0.218	
Ti	0.013		0.012		0.044		0.000		0.000	
Fe^{2+}	0.007	4.041	0.007	4.090	0.013	4.071	0.008	4.045	0.047	4.044
Mg	0.004		0.004		0.014		0.033		0.018	
Mn^{2+}	0.014		0.014		0.021		0.002		0.046	
Ca	3.965		3.977		3.958		3.961		3.926	
Na	0.043		0.075		0.052		0.033		0.005	
K	0.008		0.013		0.013		0.008		0.002	
OH	3.783		3.827		3.722		3.990		3.858	

Analyst H5, P18 and M 125 M. Nawaz Chaudhry and M 18 B and L.G.P. R.A. Howie.

ACKNOWLEDGEMENT

The authors thank Prof. F.A. Shams for reading the manuscript and suggesting improvements.

M. NAWAZ CHAUDHARY,
Department of Geology,
University of the Punjab,
Lahore.

R.A. HOWIE,
Department of Goleogy,
King's College,
London, W.C. 2.

REFERENCES

Deer, W.A. Howie, R.A. and Zussman, J. 1962 ROCK FORMING MINERALS, Longman London Vol. 3, p. 263-266.

Nuffield, E.W. 1943 Prehnite from Ashcroft, British Columbia Univ. Toronto Stud., *Geol. Ser.* No. 48, p. 49.

Worth, R.H. 1920 The geology of the Meldon Valleys near Okehampton, on the northern verge of Dartmoor. *Quart. Journ. Geol. Soc.*, **75**, pp. 77-114.

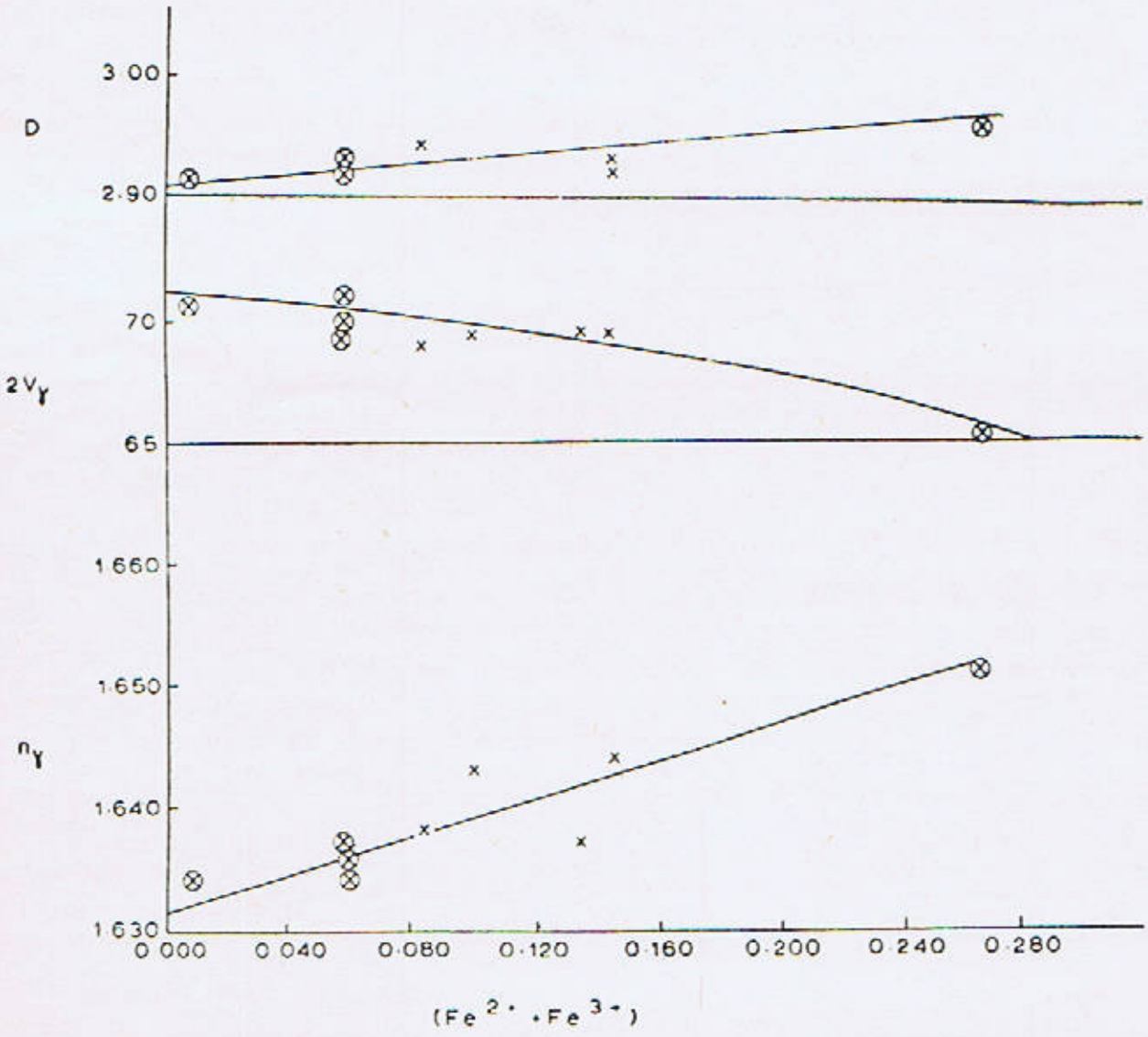

⊗ Prehnites from the Meldon aplite.

× From data on Prehnites, Deer, Howie & Zussman (1962)

Fig. 1. The relationship between the (Fe^{2+} + Fe^{3+}) and $2V_\gamma$, D and n_γ.

Name and Qualifications	*Subject*	*Appointed*
Dr. Fazal-ur-Rehman, M.Sc. (Pb.),* PH.D. (Pb.)	Geochemistry.	December, 1966.
Mr. Shafeeq Ahmad, M.Sc. (Pb.)	Geochemistry.	January, 1967.
Mr. S. Mahmood Raza, M.Sc. (Pb.)	Paleontology.	October, 1968.
Mr. Ijaz Hussain, M.Sc. (Pb.)	Mineralogy, Petrology	January, 1969.
Demonstrators :		
Mr. Ayub Asghar,	Paleontology	December, 1969.
Mr. Iftikhar Ahmad.	Mineralogy	December, 1969.
Mr. Ahmad Nawaz.	Petroleum	December, 1969.
Mr. M. Saeed Asad.	Engineering.	December, 1969.
Mr. Mubarik Ali.	Geophysics.	December, 1969.

2. Technical and Service Staff :

Mr. S.A. Kazmi, M.I.S.T. (London)	Chief Technician	March, 1963.
Mr. M. Aslam.	Junior Technician	June, 1964.
Mr. H.U. Siddiqui.	Junior Technician	June, 1965.
Mr. Arshad Hussain.	Geological Illustrator.	March, 1966.
Mr. Mahmood Ahmad.	Draftsman	January, 1967.
Mr. G.R. Bhatti.	Office Assistant	September, 1963.
Mr. K. Ahmad, B.A. (Pb.).	Library Assistant	August, 1965.
Mr. M. Riaz	Stenographer	November, 1967
Office and Library Staff	6	
Laboratory Assistants	9	
Drivers	1+1 (Summer only)	
Service Staff	3	

*On leave at Geologisk-Mineralogisk Musem, Oslo, Norway.

STAFF LIST OF THE DEPARTMENT OF GEOLOGY, UNIVERSITY OF THE PUNJAB (AT THE 31st DECEMBER 1969).

1. **Teaching Staff :**

Name and Qualifications	*Subject*	*Appointed*
Professor of Geology :		
Prof. F.A. Shams, M.Sc. (Pb.), M.A. (Cantab), Ph.D. (Pb.), Head of the Department.	Mineralogy, Petrology, X-Ray Crystallography.	November, 1956.
Readers :		
Dr. M.A. Latif, M.Sc. (Pb.), M. Sc., D.I.C., Ph.D. (London), F.P.T.C. (Vienna).	Micropaleontology, Stratigraphy.	July, 1957.
Dr. Aziz-ur-Rehman M.Sc. (Pb.), D. Rehr. Nat. (Munich).	Applied Geophysics.	February, 1960.
Mr. A.H. Gardezi, M.Sc. (Pb.), M.Sc. D.I.C. (London), D.M. (E.N.I. Roma).	Petroleum Geology,	March, 1962.
Lecturers :		
Dr. M.A. Chaudhry, M.Sc. (Pb.), Ph.D (Reading).	Sedimentology, Geomorphology.	June, 1959.
Dr. Aftab A. Butt, M.Sc. (Pb.), Ph.D. (Utrecht)	Micropaleontology, Stratigraphy.	June, 1959.
Dr. S.F.A. Siddiqui, M.Sc. (Pb.) Ph.D. (London).	Mineralogy, Petrology,	July, 1960.
Mr. Z.A. Saleem, M Sc. (Pb.)*	Geohydrology, Geophysics.	June, 1961.
Mr. Munir Ghazanfar, M.Sc. (Pb.) M.Sc. (Sheffield).	Structural Geology.	January, 1965.
Mr. M.H. Malik, M.Sc. (Pb.), M.Sc. D.I C. (London).	Engineering Geology.	March, 1965.
Mr. A. Shakoor, M.Sc. (Pb.), M.Sc. (Leads).	Petrology.	May, 1965.
Mr. Zulfiqar Ahmad, M.Sc. (Pb.).	Mineralogy, General Geology.	August, 1967.
Dr. Mohammad Nawaz, M.Sc. (Pb.), Ph.D. (London).	Mineralogy, Petrology.	January, 1968
Mr. Haroon Q.A. Khan, M.Sc. (Alig)	Paleontology, Stratigraphy.	September, 1968.
Mr. Liaquat A. Sheikh, M.Sc. (Pb.)	Paleontology, Stratigraphy.	April, 1969
Research Assistants :		
Dr. S. Taseer Hussain, M.Sc. (Pb.)	**Paleontology.	April, 1966.

*On duty leave at the Department of Hydrology, University of New Mexico, Socorro, U.S.A.
**On duty leave at the Geological Institute, Utrecht, Holland.